Susceptibility of microRNAs 145, 143 and 133b to epigenetic regulation in colorectal cancer cell lines; prediction and functional analysis of putative targets to associated microRNAs

Drishna Govan

A dissertation submitted to the Faculty of Health Sciences, University of Witwatersrand, Johannesburg in fulfilment of the requirements for the degree of Master of Science in Medicine

Supervisor:

Dr Clem Penny

Department of Internal Medicine, University of Witwatersrand, South Africa

Johannesburg, 2016

DECLARATION

I, Drishna Govan, declare that this dissertation is my own unaided work. It has being submitted for the degree of Master of Science in the Faculty of Health Sciences in the University of the Witwatersrand, Johannesburg. It has not been submitted before for any degree or examination at this or any other University.

_____

Drishna Govan

This _____ day of _____20_____

RESEARCH OUPUTS

POSTER PRESENTATIONS:

- Govan D, Penny C, Gibbon V and Ruff P (2010). Bioinformatic prediction of putative microRNA targets for further evaluation in colorectal cancer. Faculty of Health Sciences Research Day, University of the Witwatersrand, Johannesburg, Sep 22nd.

- Govan D, Penny C, Gibbon V and Ruff P (2011). Bioinformatic prediction of putative microRNA targets for further evaluation in colorectal cancer. 15th Congress of South African Society of Medical Oncology (SASMO/SASCRO) (Sun City), Aug 24th–Aug 27th.

- Govan D, Gibbon V, Ruff P and Penny C. (2012) MicroRNA target sites in colorectal cancer. South African Society of Biochemistry and Molecular Biology (SASBMB/FASBMB), Drakensberg, KwaZulu Natal, Jan 29th- Feb 1st.

ABSTRACT

Colorectal cancer (CRC) is a significant health burden maintaining its position as the third most diagnosed cancer in men and women worldwide. Despite improvements in treatments for CRC, mortality rates still remain high. Genetic instability and epigenetic deregulation of gene expression are instigators of CRC development, resulting in genotype differences which herald treatment response variability and unpredictability. Over the past decade and a half, microRNAs (miRNA) have emerged as key contributors to the perturbed proteome in cancer cells, including CRC. MiRNAs are small non-coding RNA molecules (consisting of approximately 22 nucleotides) targeted to specific mRNAs through various target recognition mechanisms to repress protein translation or to induce mRNA degradation. Three miRNAs, miR-143, -145 and -133b, are most commonly downregulated in CRC and have been proposed as potential tumour suppressors. Although downregulation of these miRNAs in CRC is to a large extent unexplained, epigenetic silencing has been postulated as a causative regulatory mechanism. Potential epigenetic modulation of miRNA expression, by means of histone acetylation and DNA methylation, was assessed in this study by treating early (SW1116) and late stage (DLD1) CRC cells with the DNA demethylating agent, 5-aza-2'-deoxycytidine (5-Aza-2'C) and the histone deacetylase (HDAC) inhibitor, Trichostatin A (TSA), respectively. Subsequently quantifying miRNA expression, using miRNA TaqMan® PCR assays for each of miR-143, -145 and -133b, revealed that while all of these miRNAs are susceptible to DNA demethylation in early and late stage CRC cells, the susceptibility to DNA demethylation is significantly pronounced in the late stage DLD1 cells. Conversely, histone acetylation moderately affected miRNA expression in early stage CRC, but with a marginal effect on the expression of miRNAs in late stage CRC cells. These associations have been argued to correlate with genotypic differences between the microsatellite stable (MSS) SW1116 cell line and the microsatellite instability (MSI) of the DLD1 cells. To further evaluate the role that these miRNAs play in CRC development, this study utilised in silico miRNA target prediction tools to identify potential miRNA gene target lists. Once generated, these

were strategically curated and filtered to allow for the election of suitable candidates for functional analysis. This approach yielded three candidates, KRAS, FZD7 and FBXW11/ß-TrCP as the most probable targets for miR-143, -145 and -133b, respectively, further supported by their inverse correlations to the associated miRNA expression in CRC. Proteomic expression of the predicted targets assessed pre- and post- transfection of HET-1A cells with anti-miR™ sequences of the associated miRNA revealed elevated protein expression with differential subcellular protein localization upon miRNA inhibition. Overall this study has provided further understanding of the contribution of epigenetics in regulation of putative tumour suppressor miRNAs in CRC. Additionally, KRAS targeting by miR-143 has been reaffirmed, while FZD7 and FBXW11/ß-TrCP expression analysis after anti-miR-145 and anti-miR-133b transfection, respectively, provides substantial evidence for their role as potential direct miRNA targets.

Keywords: *colorectal cancer (CRC), epigenetics, demethylation, histone acetylase, 5-aza-2'-deoxycytidine, Trichostatin-A, SW1116, DLD1, miR-143, miR-145, miR-133b, anti-miR, KRAS, FZD7, FBXW11/ß-TrCP*

ACKNOWLEDGEMENTS

Firstly, I would like to thank my supervisor, Dr Clem Penny, for his unwavering support, guidance and patience throughout my studies and during the development of this dissertation.

I am indebted to my family for being the support system that I needed throughout this study. Of particular mention, my sisters Aarti Moodley, Beejal Govan and Jhulan Govan and brother-in-law, Senton Moodley, are the stem of my life which keeps me standing upright and able to reach the sunshine. My parents, to whom I owe everything, are the roots to which I am firmly bound connecting me to the source of life.

To my partner, Dylan, you have provided me with the precise motivation that I had required and you have supported me without hesitation for which I am extremely grateful. Thank you for being my greatest cheerleader.

My extended family has inspired me to be the best version of myself, sincere thanks to my aunts, uncles and cousins whom have always believed in me.

I am also grateful to Dr Vicky Gibbon for being an initial source of guidance.

Additionally, I am appreciative of the following organizations and awards which have provided financial support for this research: Medical Research Council, Faculty Research Council, Post-graduate Merit Award and National Research Foundation.

TABLE OF CONTENTS

LIST OF FIGURES

LIST OF TABLES

ABBREVIATIONS & SYMBOLS

%	Percentage
°C	Degree's Celsius
µL	Microliter
µM	micromolar
18s rRNA	18s ribosomal ribonucleic acid
3'UTR	3 prime untranslated region
3p	3 prime strand
5-Aza-2'-C	5-aza-2'-deoxycytidine
5p	5 prime strand
5q32	chromosome 5 region q32
6p12.2	chromosome 6 region p12.2
AAX	AAX motif
ACS	American Chemical Society
ADP	Adenosine diphosphate
ALL	Acute lymphoblastic leukaemia
ALS	Amyotrophic lateral sclerosis
Alu	Alu repeat sequence
Anti-miR™	Anti-miRNA Oligonucleotides
APC	adenomatous polyposis coli
AT	Adenine-Thymine
ATP	Adenosine triphosphate
AU	Adenine-Uracil dinucleotide
AUC	Area under the curve
BCL	B cell lymphoma
BEBM	Bronchial Epithelial Basal Medium
BLAST	Basic Local Alignment Search Tool
BMP4	Bone Morphogenetic Protein 4
Bp	base pairs
BRAF	Proto-oncogene B-Raf
BSA	Bovine Serum Albumin
C19MC	Primate-specific microRNA gene cluster
C5	carbon ring 5 position
CAAX	CAAX motif
c-Abl	ABL1 non-receptor kinase
CDK	Cyclin Dependent Kinase
CDKN2A	Cyclin-Dependent Kinase Inhibitor 2A
cDNA	Complementary DNA
CH3	methyl group

ChIP	Chromatin immunoprecipitation
Chk1	Checkpoint Kinase 1
CIMP	CpG island Methylator Phenotype
CIN	Chromosome Instability
CML	Chronic Myeloid Leukaemia
c-Myc	Cellular homolog of the retroviral v-myc oncogene
CO_2	Carbon Dioxide
CpG	Cytosine-Guanine dinucleotide
CRC	Colorectal cancer
CSNK1G3	Casein Kinase 1, Gamma 3
Ct	Cycle Threshold
DAPI	4',6-diamidino-2-phenylindole
DCC	Deleted in Colorectal Carcinoma
DCP4	Deleted in pancreatic carcinoma 4/SMAD4
DKK1	Dickkopf WNT signalling pathway inhibitor 1
DLD1	Dukes' stage C colorectal cancer cell line
DMEM-F12	Dulbecco's Modified Eagle Medium:F-12 Nutrient mixture
DMSO	Dimethyl sulfoxide
DNA	Deoxyribonucleic acid
DNMT	DNA methyltransferase
dNTP	Deoxyribonucleotide triphosphate
dTTP	Deoxythymidine triphosphate
ECM	Extracellular Matrix
EDTA	Ethylenediaminetetraacetic acid
EGF-R	Epidermal Growth Factor receptor
ErbB	Erythroblastic Leukaemia Viral Oncogene Homolog
ERK	Extracellular signal-regulated kinases
EST	Expressed Sequence Tag
FAP	Familial adenomatous polyposis
FBS	Foetal bovine serum
FBXW11	F-Box And WD Repeat Domain Containing 11
FDA	Federal Drug Agency
FGFR1	Fibroblast Growth Factor Receptor 1
FRET	Fluorescence Resonance Energy Transfer
FZD7	Frizzled 7 (Wnt receptor)
G:U	Guanine:Uracil
G0	G zero/resting phase
G1	Gap 1 phase
G2	Gap 2 phase
G2M	G2M cell cycle checkpoint
GADD45α	The Growth Arrest and DNA Damage Protein alpha
GFP	Green Fluorescent Protein
Gli3	GLI Family Zinc Finger 3

H	Histone
H3K4me3	Histone 3 lysine 4 trimethylation
HAT	Histone acetyl transferase
HDAC	Histone deacetylase
HDACi	Histone deacetylase inhibitor
HEPA	High-efficiency particulate air
HIF	Hypoxia-inducible factors
HMM	Hidden Markov Model
HNPCC	Hereditary nonpolyposis colorectal cancer
HREC	Human Research Ethics Committee
HSRRB	Health Science Research Resources Bank
IARC	International Agency for Research on Cancer
IGF-IR	Type I insulin-like growth factor receptor
IRS1	Insulin Receptor Substrate 1
K	Lysine
Kb	Kilobase
KEGG	Kyoto Encyclopaedia of Genes and Genomes
KLF4	Krüppel-like factor
KRAS	V-Ki-ras2 Kirsten rat sarcoma viral oncogene homolog
LAQ824	Novel HDAC inhibitor
LOH	Loss of heterozygosity
m	Mean
MAPK	Mitogen-activated protein kinases
MDB	Methyl CpG binding domain proteins
MDS	Myelodysplastic syndrome
MET	Mesenchymal epithelial transition factor
MGB	TaqMan® probe
$MgCl_2$	Magnesium Chloride
Min	Minimum
miR	microRNA
miR-133b	microRNA 133b
miR-143	microRNA 143
miR-145	microRNA 145
mirBase	microRNA database
miRNA	microRNA
mL	Millilitre
MLH1	MutL homolog 1
MLL-AF4	Mixed lineage leukaemia fusion gene
mM	Millimolar
MMR	DNA mismatch repair
mRNA	messenger ribonucleic acid
MSH	MutS protein homolog
MSI	Microsatellite Instable

MSS	Microsatellite Stable
n	sample size
ND-1000	NanoDrop spectrophotometer
nM	Nanomolar
Notch	Notch signalling pathway
NSCLC	Non-small cell lung cancer
Nt	Nucleotide
NTC	No treatment control
OD	Optical density
p	Probability
p16	Cyclin-dependent kinase-4 inhibitor
p21(WAF1)	cyclin-dependent kinase inhibitor 1/CDK-interacting protein 1
p53	Tumour protein/ TP53
p68	p68 RNA Helicase
p72	p72 ATP-dependent RNA helicase
p73α	P53 related protein alpha
PAK-4	serine/threonine p21-activating protein kinase 4
PBA	Phenylbutyric acid
PBS	Phosphate Buffered Saline
PCR	Polymerase Chain Reaction
PD	Parkinsons Disease
PDGF	Platelet derived growth factor
PDGFRA	Platelet derived growth factor receptor alpha
PDGFRB	Platelet derived growth factor receptor beta
P-ERK	Phosphorylated extracellular signal-regulated kinases
pGL3	Luciferase Reporter Vectors
PI3K	Phosphoinositide 3-kinase
Pitx3	Paired-Like Homeodomain 3
Pol II	Polymerase II
Pol III	Polymerase III
PP2AC	Protein phosphatase 2A catalytic subunit
PPP2CA	Serine/threonine-protein phosphatase 2A catalytic subunit alpha
PPP2CB	Serine/threonine-protein phosphatase 2A catalytic subunit beta
PPP3CA	Protein phosphatase 3 catalytic subunit alpha
pre-miRNA	precursor miRNA
pri-miRNA	primary miRNA
PTEN	Phosphatase and tensin homolog
qPCR	quantitative polymerase chain reaction
qRT-PCR	quantitative real-time polymerase chain reaction
Ras	Ras GTPases
Rb	Retinoblastoma
Rce	Ras converting CAAX endopeptidase 1
RefSeq	Reference Sequence

RISC	RNA-induced silencing complex
RNA	Ribonucleic acid
RNase	Ribonuclease
ROC	Receiver Operating Characteristic
ROS	Reactive Oxygen Species
Rpm	Revolutions per minute
RRE	RAS-responsive element
RREB1	Ras Responsive Element Binding Protein 1
RT	reverse transcription
SAM	S-adenosyl methionine
SCF	Skp, Cullin, F-box containing complex
SD	Standard Deviation
SILAC	Stable Isotope Labelling by Amino acids in Cell culture
siPORT NeoFX	Transfection Reagent
SMAD3	Mothers against decapentaplegic homolog 3.
SMAD4	Mothers against decapentaplegic homolog 4
snRNA	Small nuclear ribonucleic acid
SP1	Sp1 Transcription Factor
SW1116	Dukes stage A colorectal cancer cell line
SWI/SNF	SWItch/Sucrose Non-Fermentable nucelosome remodeling complex
T	Thymine
TATA	Goldberg-Hogness box
TBP2	TATA-binding protein 2
TFIIB	Transcription Factor II B
TGFBR1	Transforming Growth Factor, Beta Receptor 1
TGF-ß	Transforming Growth Factor beta
Tis	Carcinoma *in situ*
TP53	Tumour protein/ p53
tRNA	transfer RNA
TSA	Trichostatin A
TSS	Transcriptional start site
UTR	Untranslated region
UV	Ultraviolet
$^{v}/_{v}$	volume per volume
VSMC	Vascular smooth muscle cells
$^{w}/_{v}$	weight per volume
Wee1	WEE1 G2 Checkpoint Kinase
Wnt	Wnt signalling pathway
wt	wild type
Xba1	XbaI restriction endonuclease
Zn^{2+}	Zinc
α	Alpha
β	Beta

ß-catenin	*Beta*-catenin
ß-TrCP	*Beta*-transducin repeat containing E3 ubiquitin protein ligase
γ	*Gamma*
δ	*Delta*
ΔCt	*Delta* Cycle threshold
ΔG	Change in free energy

Chapter 1: GENERAL INTRODUCTION

1.1 Colorectal cancer – a significant health burden

Cancer arising in the bowels or rectum, referred to as colorectal cancer (CRC), persists as a health burden, being the third most diagnosed cancer worldwide. According to the American Cancer Society the lifetime risk of developing CRC in the United States is 4.7% (1 in 21) in men and 4.4% (1 in 23) in women, with the number of new cases expected in the year 2016 to be approximately 134 490. The number of deaths expected as a result of CRC in 2016 amounts to 45 190 (American Cancer Society, 2015). In South Africa, according to the National Cancer Registry, 1 in 97 men are at risk of developing CRC in their lifetime, while 1 in 162 women are at risk of developing the disease (CANSA, 2010). Although the incidence of CRC in South Africa is low in comparison to various developed countries, such as the United States, the mortality rate in South Africa is almost equivalent to the developed world, as reported in the Globocan 2012 (IARC) analysis (Figure 1.1), a project of the World Health Organisation. The 5 year survival rate of CRC at stage I is 90%, however this survival rate rapidly decreases to 10% in stage IV metastatic colon cancer, highlighting both, the crucial importance of early detection, and improved therapies targeting CRC progression. In the developed world, although the mortality rate is said to be declining due to increased uptake of screening methods and available treatments, the burden of CRC still remains significantly high (Zauber, 2015). There are several risk factors, of which some are not changeable, that have been identified in the development of CRC; these being age, a history of adenomatous polyps, a history of inflammatory bowel disease, a family history of CRC or adenomatous polyps, or an inherited genetic risk (FAP and HNPCC). Modifiable risk factors for CRC development include diet, physical activity and obesity, cigarette smoking and heavy alcohol consumption (reviewed by Haggar & Boushey, 2009).

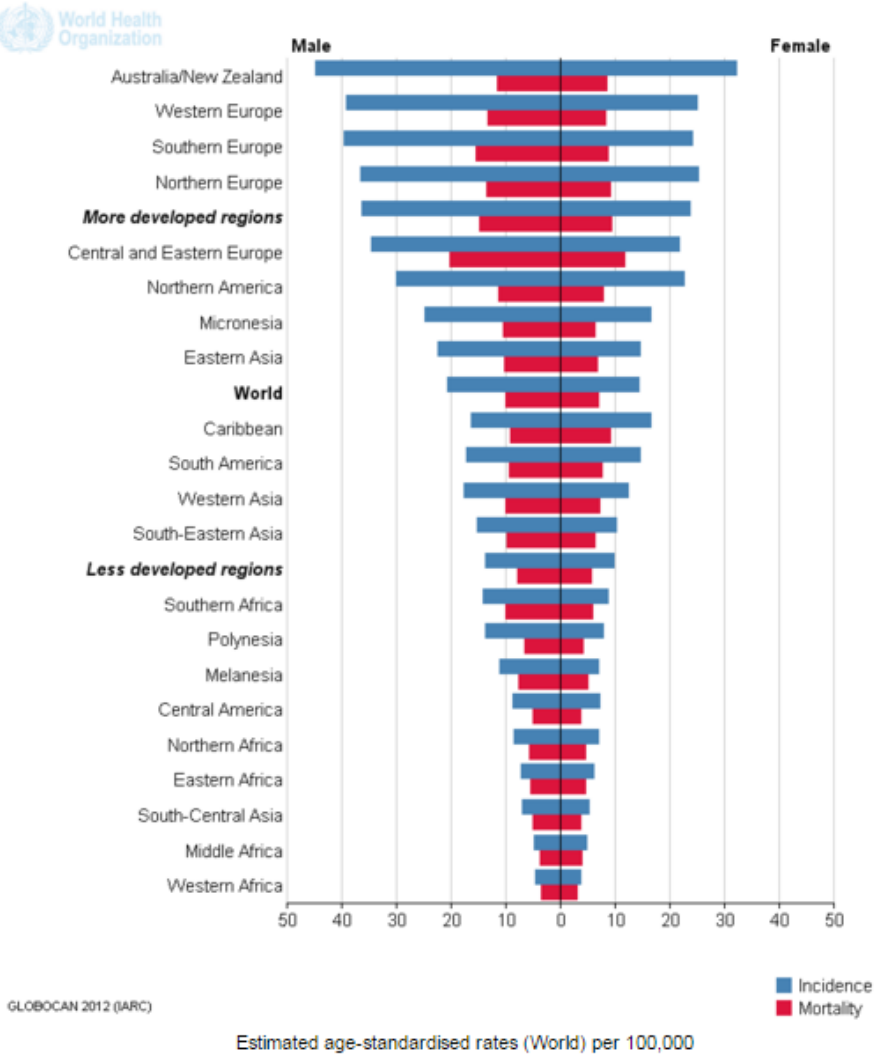

Figure 1.1: Estimated Incidence, Mortality and Prevalence of Colorectal cancer worldwide. (Globocan, 2012).

1.2 Genetic instability in CRC

CRC is known to develop in an age dependent multistep progressive manner, which is characterised by the accumulation of genetic mutations and epigenetic aberrations in response to environmental and other external factors. This process which involves the transformation of normal colorectal epithelium through progressive steps to form invasive and metastatic cancer has been termed the 'Adenoma to Carcinoma Sequence' and was proposed as a model for CRC development by Fearon and Vogelstein in 1990 (Figure 1.2). This transformation process takes approximately 15 years to progress through each step with the sequence advancing through one of

two distinct pathways, Chromosome Instability (CIN) and Microsatellite Instability (MSI).

The CIN pathway, also termed microsatellite stable (MSS), represents the development of approximately 85% of sporadic metastatic CRC tumours (Walther *et al.*, 2008). Malignant transformations occurring through the CIN pathway are associated with an initial loss of the tumour suppressor gene APC (adenomatous polyposis coli), located in chromosomal region 5q21, which is a negative regulator of the Wnt pathway, a crucial signalling pathway in CRC (Powell *et al.*, 1992). Further genetic alterations involve mutations in the KRAS oncogene, allelic loss of the 18q chromosomal region containing the DCC and DCP4/SMAD4 oncogenes and as well a late inactivation of TP53, through an allelic loss or mutation of the 17p chromosomal region (Leslie *et al.*, 2002; Vogelstein *et al.*, 1988). The prognosis of CIN CRC is poor, showing the worst survival amongst CRC stage II and III patients (Watanabe *et al.*, 2012).

MSI (microsatellite instability) refers to the epigenetic phenotype of approximately 15 percent of sporadic colon cancers (Kinzler & Vogelstein, 1996). The MSI phenotype is characterised by deficiencies in the DNA mismatch repair (MMR) pathway which is caused by mutation or hypermethylation of the MLH1, MSH2 or MSH6 genes (Peltomaki *et al.*, 2001). The MLH proteins are responsible for the integrity of the genome by correcting errors during DNA replication. Inactivation of these DNA repair proteins results in subtle adjustments in the DNA sequence by virtue of small insertions and deletions in microsatellite sequences, which are short mono- or dinucleotide repeat sequences. These changes in the DNA sequence cause frameshift mutations that ultimately alter the expression of cancer related genes (Iino & Simms, 2000). Lynch Syndrome or hereditary nonpolyposis colorectal cancer (HNPCC), a genetically inherited risk factor for CRC, develops tumours primarily through the MSI pathway in which the DNA mismatch-repair genes are altered by mutation or frameshift mutations. In contrast however, the sporadic form of MSI CRC develops through a pathway riddled with aberrations in DNA methylation, with the initial MLH1 loss attributed to silencing by CpG island promoter methylation, this

occurring in a separate MSI pathway called CIMP (CpG Island Methylator Phenotype) (Worthley & Leggett, 2010).

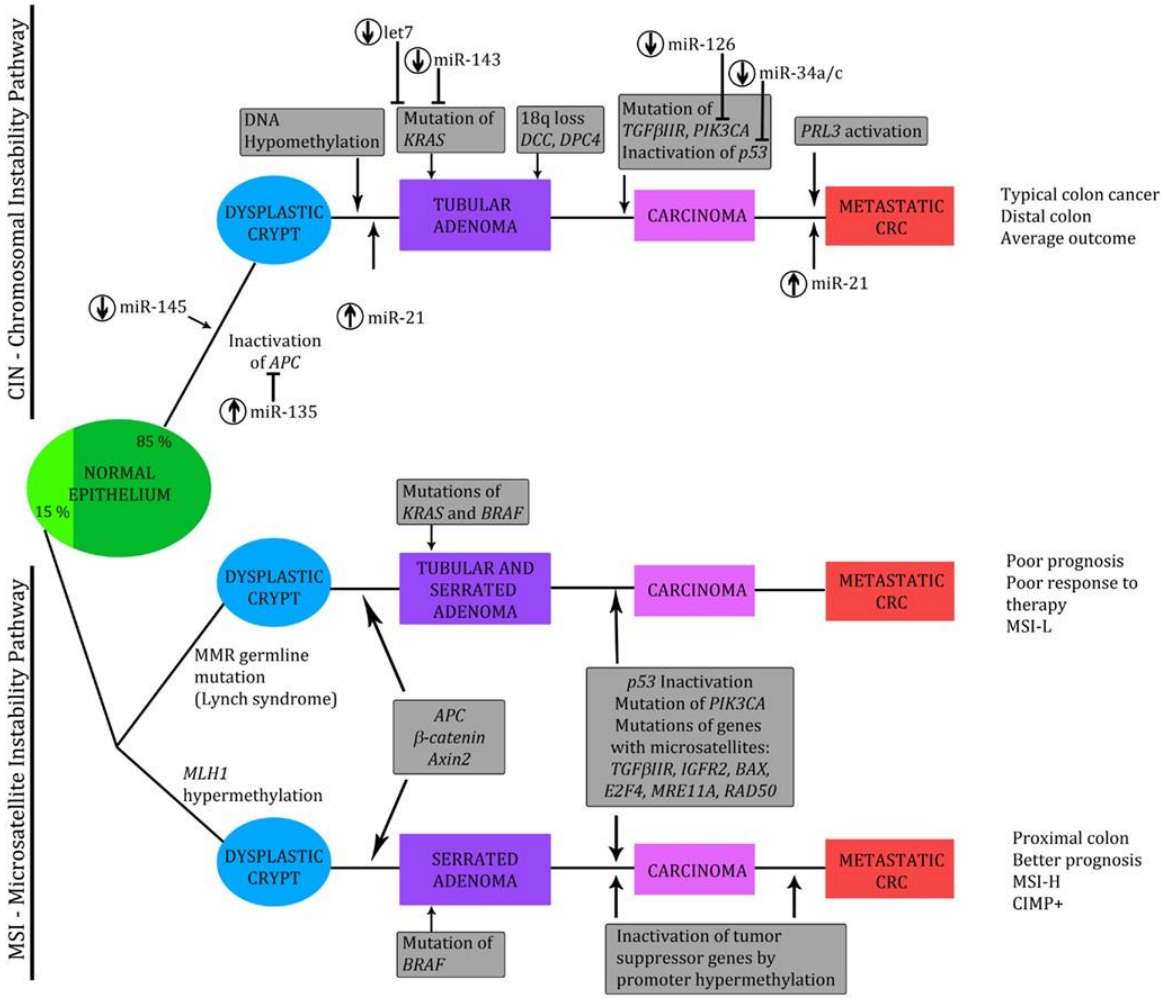

Figure 1.2: Adenoma to Carcinoma Sequence Model. CRC progresses through multiple steps from normal epithelium to metastatic CRC through two pathways, CIN and MSI. Each pathway is characterised by key genetic and epigenetic alterations at each step, ultimately resulting in varied outcomes (Adapted from Hrašovec & Glavač, 2012).

1.3 Epigenetics – the missing link

The 'Adenoma to Carcinoma' sequence is influenced by epigenetic alterations as depicted in Figure 1.2. Epigenetics provides an additional dimension of gene

regulation to the standard gene regulatory networks in a cell, demonstrating the effects of the chromatin structure and the external environment on the expression of genes, by virtue of a process known as chromatin remodelling.

Conrad Hal Waddington in 1942 first described the concept of external influences on gene expression and is responsible for the origin of the term epigenetics. He focused on epigenetics in developmental biology with the proposition that the phenotype of a cell was determined by the interpretation of the genotype to the environment and external signals, in a process termed epigenesis, thus leading to the differentiated array of cell types in the human body (Waddington, 1942). To date, however, epigenetics has evolved into a more complex and abundant field of study. A later definition of epigenetics was provided by Riggs *et al* in 1996, in which it was indicated that epigenetics is the study of heritable changes in gene expression without changes in DNA sequence (genotype). This definition is commonly cited to date and encompasses almost all epigenetic modifications studied thus far.

1.3.1 Chromatin structure

In the cell, DNA, contained in chromosomes (46 per diploid human cell), is maintained in the nucleus in the form of chromatin, an evolved formation which permits the retention of the long length of DNA within the confined dimensions of the nucleus. On a microscopic level, chromatin would reveal DNA wound around octamers of globular histone proteins to form nucleosomes (Oudet *et al*., 1975). Each octamer contains two each of four distinct core histone proteins, H2A, H2B, H3 and H4. There are also linker histones, H1 and H5, which are responsible for binding the nucleosome and locking DNA into the nucleosome structure (Van Holde, 1988). DNA weaved between nucleosomes is referred to as chromatin. Approximately 147 base pairs of DNA are weaved around one nucleosome with a 50 bp linker DNA sequence separating nucleosomes (Felsenfeld & Groudine, 2003). Refer to Figure 1.3 below for an illustration of the chromatin structure.

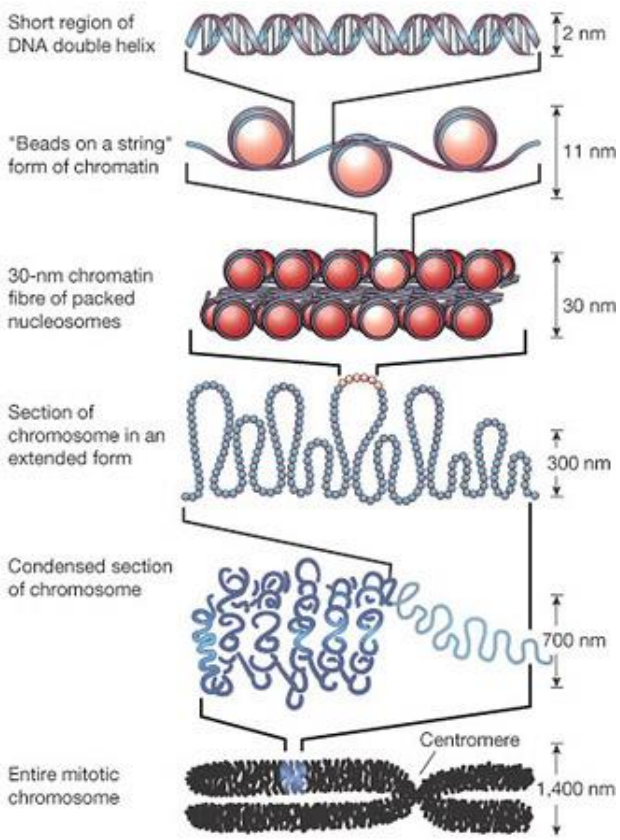

Figure 1.3: Chromatin structure within the cell: A clear indicator of the optimised packing and folding affecting the size of the length of DNA stored with the cell (Felsenfeld & Groudine, 2003).

There are two defined classifications of chromatin depending on the activity at the chromatin region. Heterochromatin, composed of condensed chromatin, is generally referred to those regions that are not required to be frequently transcriptionally active (DNA strand less accessible). In contrast, euchromatin (expanded chromatin), are those regions that have a high level of transcriptional activity and require the DNA sequence to be easily accessible to transcription initiation machinery (Eissenberg & Elgin, 2014). Open chromatin states are associated with accessibility of DNA to transcriptional machinery, as a result of DNA de-associating from the nucleosome structure. Closed chromatin states involve the folding of the DNA chromatin into its

compact form, allowing for hindrances to transcriptional machinery (Eissenberg & Elgin, 2014).

Chromatin structure is controlled in layers, of which the first level of control lies in those proteins involved in altering the topographical status of chromatin, without modifying DNA or any other components of chromatin (Phillips & Shaw, 2008). Although nucleosomes possess a degree of intrinsic mobility, eukaryotic cells have evolved a class of chromatin remodelling enzymes that are responsible for a process known as “nucleosome sliding” (Phillips & Shaw, 2008). This involves moving the nucleosome in *cis* along DNA to create accessible regions of DNA. Another mechanism involves displacing histones in *trans* within the nucleosome to allow for DNA accessibility. A key example of chromatin remodelling proteins is the SWI/SNF family of proteins. These proteins mobilise nucleosomes along DNA to allow for specific regions of DNA to be more accessible for transcription (Cairns *et al*., 1994; Tang *et al*., 2010). This function is executed by the proteins through utilizing the energy provided through ATP hydrolysis, a reaction catalysed by the enzymatic ATPase subunit contained within the chromatin remodelling proteins (Vignali *et al*., 2000). These proteins are not randomly targeted to a nucleosome, but rather found to be attracted to specific regions of chromatin depending on the cell’s transcription requirements. It is thought that transcription activating proteins bind to these chromatin remodelling enzymes and facilitate access of the DNA sequence to transcription initiation elements (Smith & Peterson, 2005).

1.3.2 Histone modifications

Histone modifications, the next layer of chromatin control, are widely studied as key epigenetic contributors to gene regulation. Histone proteins are post-translationally modified, chemically or proteomically, on their N-terminal tail (exposed) ends, resulting in changes in the dynamic states of chromatin. There are approximately eight defined types of modifications, resulting in the establishment of a histone code, whereby combinations of the modifications define chromatin state and gene expression. Acetylation, lysine and arginine methylation, phosphorylation, ubiquitination, sumoylation, ADP-ribosylation, deamination and proline isomerization

are the most current histone modifications that have been reported (Kouzarides, 2007). Histone modification functions are separated into two types of mechanisms. There are those modifications that affect the net charge of the histone resulting in decreased affinity for negatively charged DNA, therefore providing accessibility of the DNA to transcription machinery. There are also those modifications which function to recruit non-histone proteins that are necessary for the relevant transcriptional requirement for that region (Liu *et al.*, 2005).

Histone acetylation is the most widely studied modification and most relevant in this study. Historically, the concept of histone acetylation influencing transcription was proposed by Vincent Allfrey in 1964. Subsequent findings identified the preference of acetylated core histones for transcriptionally active regions (Sealy and Chalkley, 1978; Vidali *et al.*,1978; Hebbes *et al.*, 1988). It is now known that histones are acetylated at lysine (K) residues on the amino-terminal ends (tail regions) of the histones, neutralising the charge of the histone and therefore repelling negatively charged DNA, ultimately exposing the DNA to RNA polymerase to allow for transcription initiation. This reaction is possible through the action of histone acetyl transferases (HAT) which are the enzymes responsible for catalysing the transfer of an acetyl group to the amino (N)-terminals of lysine residues contained within the histones. Histone acetylation is reversible through proteins that catalyze the removal of the acetyl group, known as Histone deacetylases (HDACs) (Kouzarides, 2007). Figure 1.4 illustrates the influence of histone acetylation and deacetylation on chromatin states and the transcription switch.

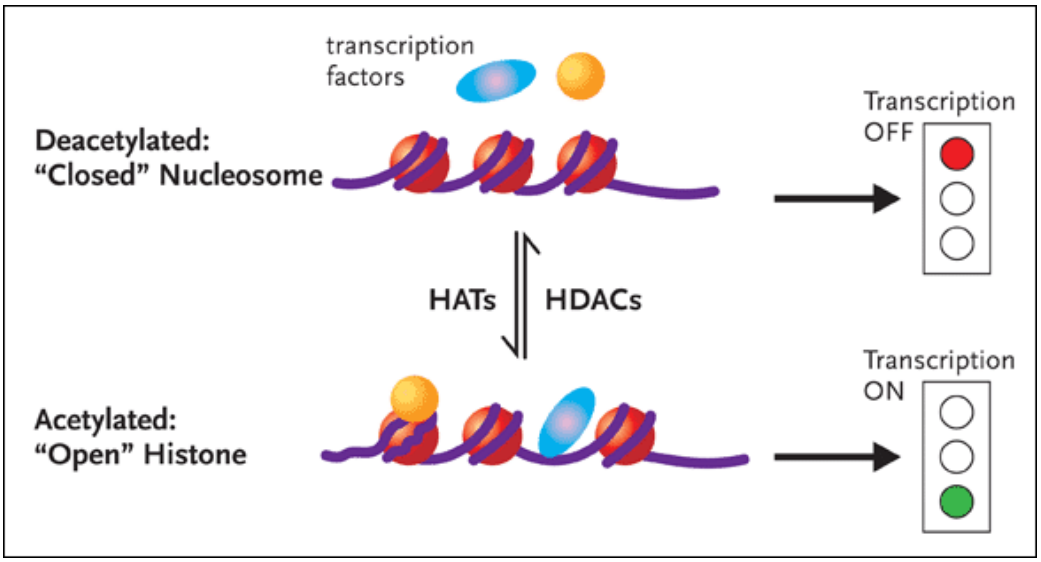

Figure 1.4: Transcriptional control of histone acetylation and deactylation. The acetylation of histones by histone acetyl transferase (HAT) changes the chromatin structure to an open state to allow for transcription to initiate. Deacetylation of histones *via* histone deacetylases (HDAC) returns the chromatin to a condensed state, halting transcription (Margolis, 2005).

1.3.3 DNA methylation

DNA methylation, first proposed by Holliday in 1979 as an epigenetic event, plays a crucial role in mammalian development. This widely studied epigenetic mechanism involves the covalent addition of a methyl (-CH3) group to the C5 position of cytosine residues occurring in large clusters of CpG dinucleotides. These CpG dinucleotides are asymmetrically scattered throughout the genome resulting in genomic areas that are either CpG-poor or CpG-rich. The latter, known as CpG-islands, are predominantly found at 5' ends (promoter regions) of approximately 60% of protein-coding genes (Kulis & Esteller, 2010). Methylation patterns are established during development and are stably propagated to progeny cells during mitosis. There are three key enzymes known as DNA methyltransferases (DNMT) that catalyse the DNA methylation process *via* methyl transfer from the methyl donor S-adenosyl-methionine (SAM) to the cytosine residue (Figure 1.5). DNMT1 is the enzyme responsible for maintenance methylation which essentially copies the methylation

patterns of the parent strand to enable stable propagation of the methylation signatures (Pradhan *et al.*, 1999). DNMT3a and DNMT3b are involved primarily in *de novo* methylation and develop the methylome during embryogenesis (Okano *et al.*, 1999). These enzymes serve important roles in development and normal cell functioning. Knockouts of either enzyme cause lethality in mice (Li *et al.*, 1992; Okano *et al.*, 1999). DNA methylation inhibits transcription by altering the confirmation of the promoter region, thereby preventing the binding of transcription factors and recruiting specific methyl-CpG binding domain proteins (MBDs) which associate with HDACs to remodel the chromosome state (Tamaru & Selker, 2001).

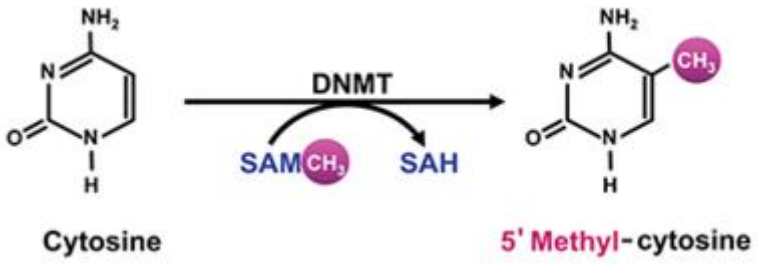

Figure 1.5: Cytosine methylation. DNA methyltransferase catalyses the transfer of a methyl group from the methyl donor SAM (S-adenosyl-methionine) to the C5 position of the cytosine residue (Adapted from Zakhari, 2013).

1.4 Cancer epigenetics

Epigenetic mechanisms are involved in fine tuning cellular processes that are critical for proper cell function. Aberrations in these mechanisms ultimately lead to cell dysfunction and are associated with diseased states, including malignant transformation. A global decrease in the load of 5-methylcytosine, or hypomethylation, is frequently recognised in cancer (Feinberg & Tycko, 2004). Alternatively, DNA methylation is found to be concentrated in large stretches of DNA in cancer cells (Frigola *et al.*, 2006). It has been thus determined that these abnormal concentrations of methylated DNA is responsible for silencing of classical tumour suppressor genes by aberrant CpG-island-promoter hypermethylation and

this phenomenon frequently occurs in different cancer types (Herman *et al.*, 1994; Merlo *et al.*, 1995). This observation is also associated with the CIMP CRC phenotype described above.

Histone modifications are another epigenetic mechanism subjected to deregulation in cancer. HDAC 1, 2, 3 and 8 are overexpressed in CRC compared to normal colon epithelium (Weichert *et al.*, 2008). Consequently, treatment of CRC cells with a histone deacetylase inhibitor (HDACi) induces anti-tumour effects by reducing proliferation signals and inducing apoptosis (Schwartz *et al.*, 1998, Miriadson, 2008). In conjunction with global increases in acetylation of H3 and H4, histone acetylation at histone 3 lysine 12 (H3K12), histone 3 lysine 13 (H3K13) and histone 3 lysine 27 (H3K27) are specifically altered in CRC (Nakazawa *et al.*, 2012; Ashktorab *et al.*, 2009; Karczmarski *et al.*, 2004).

In addition to the described epigenetic alterations, microRNAs (miRNAs), which are non-coding RNAs with an epigenetic function, are an important pathway with deregulated patterns in several cancers. The molecules are further described below.

1.5 microRNAs (miRNAs)

MiRNAs are a class of short (20-22 nt), evolutionary conserved non-coding RNAs, found to have significant roles in cellular function by post-transcriptionally regulating gene expression *via* the RNA interference pathway. Since the discovery of the first miRNA, lin-4 in the nematode *C.elegans* in 1993, substantial research has identified over a thousand miRNAs in the mammalian genome (Lee *et al.*, 1993). MiRNAs abundantly account for up to 5% of the human genome with the ability to regulate more than 30% of all mRNAs, emphasizing their immense control over gene expression (Friedman *et al.*, 2009). MiRNA biogenesis occurs through two distinct sub-cellular steps (Figure 1.4). In the nucleus miRNA genes are transcribed by Pol II and Pol III to create the primary miRNA (pri-miRNA) product, which forms a stem-loop structure with extensions at the 5' and 3' ends (Borchert *et al.*, 2006; Lee *et al.*, 2004). Processing of the pri-miRNA into precursor miRNA (pre-miR) is catalysed by

the “microprocessor” protein which consists of Drosha, an RNase III endonuclease, and the RNA binding protein DiGeorge syndrome critical region 8 (DGCR8). Pre-miRs contain the mature miRNA sequence in either the 5’ or 3’ side of the stem-loop structure (Han *et al.*, 2004). Pre-miRs are then translocated to the cytoplasm through the assistance of Exportin-5 and RanGTP, whereby cytoplasmic processing of the pre-miR to form a duplex miRNA molecule occurs *via* the RNase III nuclease Dicer (Bohnsack *et al.*, 2004; Zhang *et al.*, 2002). The miRNA duplex molecule consists of a passenger strand (denoted by miRNA* in Fig 1.6) and the mature miRNA strand. After unwinding of the duplex, the mature miRNA incorporates in the RISC (RNA-induced silencing complex) assembly unit which incorporates the four Argonaute proteins (Ago 1-4) and thereafter targets mRNA through imperfect pairing (described in chapter 3.1) to induce translation repression or mRNA degradation (Bartel, 2004).

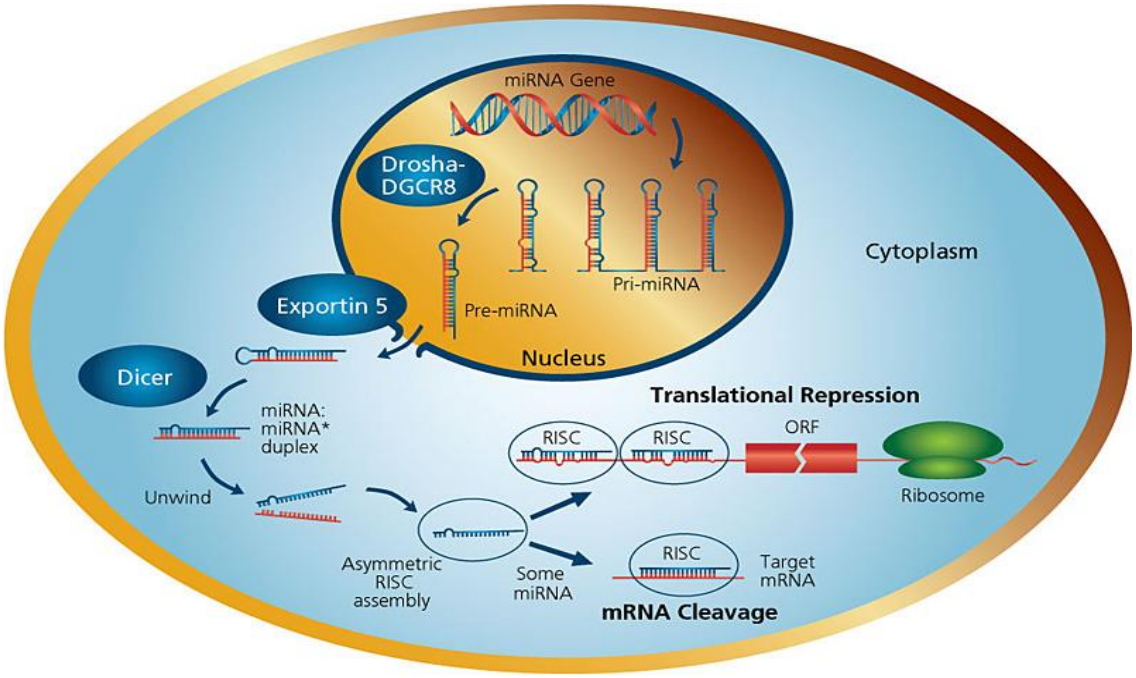

Figure 1.6: miRNA biogenesis pathway (Sigma Aldrich, 2014)

MiRNAs regulate crucial physiological processes, such as development and cellular processes, including cell differentiation, proliferation and apoptosis (Reviewed by O’Hara *et al.*, 2009). Aberrant expression of these regulators has been associated

with carcinogenesis, whereby altered miRNA expression profiles have been identified between normal tissue and derived tumour samples, demonstrating the potential of several miRNAs as putative oncogenes or tumour suppressor genes (Hammond *et al.*, 2006; Molnàr *et al.*, 2008; Wiemer, 2007; Bandres *et al.*, 2007). Tumour suppressor miRNAs are of particular interest in this study as their targets would uncover potential oncogenes of clinical significance.

1.6 CRC tumour suppressor miRNAs

MiRNA profiling of human CRCs has revealed several deregulated miRNAs. The results of these studies have identified putative tumour suppressor miRNAs that contribute to colorectal neoplasia. The focus of this study will be on putative tumour suppressor miRNAs -143, -145 and -133b. Background information is provided below on each of these miRNAs.

Michael *et al.* (2003) first identified downregulation of two miRNAs, miR-145 and miR-143, in CRC. Subsequently, Cummins *et al.* (2006) then discovered over fifty CRC-specific differentially expressed miRNAs, which also included miR-143 and miR-145. Furthermore, by utilising real time PCR, Bandres *et al.* (2006) identified thirteen miRNAs with altered expression in CRC cell lines when compared to normal colon epithelium; wherein miR-145 was also downregulated in CRC.

MiR-143 and miR-145 are cluster miRNAs possessing similar patterns of gene expression and are therefore commonly reported together, especially with regard to the tumour suppressor activity in CRC (Bauer & Hummon, 2012; Chen & Wang, 2012; Palgliuca *et al.*, 2012; Slaby *et al.*, 2007). MiR-133b has also been reported to act as a tumour suppressor and exhibits decreased expression in CRCaccording to several reports (Xiang & Li, 2014, Hu *et al.*, 2010; Lin *et al.*, 2014; Bandres *et al.*, 2006).

MiR-143 and miR-145 are closely related miRNAs and are found to have low expression levels in many cancers, thus serving as anti-oncogenic miRNA markers (Akao *et al.*, 2007; Lin *et al.*, 2009). Their genomic loci reside 1.8kb apart on chromosome 5q32 and may be transcribed together in a single primary transcript. Proliferating cells found at the base of colon membrane crypts express low levels of miR-143. Moreover, an inverse relationship between miR-143 and 145 expression and cell proliferation has been demonstrated in DLD1 colon cancer cells (Akao *et al.*, 2007). Their association with cell proliferation supports their involvement in cancer. Functionally, miR-143 regulates differentiation of adipocytes by targeting a novel mitogen of the mitogen-activated protein kinase (MAPK) family, ERK5 (Esau *et al.*, 2004). Akao *et al.* (2006) also validated ERK5 targeting by miR-143 in the colon cancer cell line, DLD1. ERK5 signalling is propagated by external stimuli such as stress and growth factors, resulting in the activation of several oncogenes which promote cell proliferation and differentiation. Translational inhibition of the oncogene KRAS by miR-143 has been elucidated and provides additional evidence for the contribution of this miRNA to the regulation of cell growth (Chen *et al.*, 2009). With regard to miR-145, a close link to carcinogenesis lies in its targeting of insulin receptor substrate-1 (IRS-1), a docking protein for Type 1 insulin-like growth factor receptor (IGF-IR), which is involved in mitogenic signalling and promoting cell survival (Shi *et al.*, 2007). Downregulation of the oncogene c-Myc by the tumour suppressor p53 has been found to be mediated by miR-145 (Sachdeva *et al.*, 2009). Interestingly, c-Myc is also a downstream target of the ERK5 signalling pathway.

The locus for miR-133b is found on chromosome 6p12.2. MiR-133b directly targets the proto-oncogene MET in CRC, consequently inducing growth inhibition (Hu *et al.*, 2010). Downregulation of miR-133b is also associated with poor survival and metastasis in CRC (Akcakaya *et al.*, 2011). Besides significant downregulation in CRC, miR-133b association with disease has been demonstrated in neurodegenerative and cardiovascular disorders (Kim *et al.*, 2007; Sucharov *et al.*, 2008). A lack of current literature available on this miRNA emphasises the necessity for its study to elucidate the mechanism by which the miRNA contributes to CRC development.

1.7 Aim

Owing to the tumour suppressor nature of miR-143, -145 and -133b coupled with the known fact that tumour suppressors are aberrantly silenced through epigenetic mechanisms in cancer, it is postulated here that these miRNAs are regulated in the same manner. Furthermore, the elucidation of miR-143, -145 and -133b gene targets could reveal potential oncogenes of therapeutic relevance. Consequentially, to understand the influence of epigenetics on the expression of potential tumour suppressor miRNAs (miR-145, miR-143 and miR-133b) and to elucidate potential miRNA targets, the following three main study objectives were derived and are described in the chapters to follow:

Objectives:

- To detect stage-specific epigenetic silencing, by means of DNA demethylation and histone acetylation, of the putative tumour suppressor miRNAs miR-143, -145 and -133b, in cell lines representing distinct stages of CRC.
- To utilise *in silico* miRNA target prediction tools to determine putative targets of miR-143, -145 and -133b. This will be accomplished using available bioinformatic resources and strategic filtering methodology.
- To conduct a functional analysis of the predicted targets for each miRNA by using anti-miR™ transfections in association with immunofluorescence technology.

Chapter 2: EVALUATION OF MIRNA REGULATION BY EPIGENETIC MODULATION

2.1 Introduction

2.1.1 Regulation of miRNAs

Chapter one outlined the aberrant epigenetic processes and some relevant de-regulated miRNA profiles that characterise transformed cells. A review of the miRNA biogenesis process and their mode of action in regulating the expression of target mRNAs were detailed. Owing to the involvement of miRNAs in crucial physiological and cellular processes such as developmental timing control, apoptosis, cell proliferation and the development of organs (Bartel, 2004), coupled with the established fact that altered patterns of miRNA expression lead to the development of diseased states (Ardekani & Naeini, 2010), one can infer that miRNAs would require finite regulation to achieve the optimal and intricate levels of expression that would drive the growth of normal and healthy cells.

Although it is known that miRNAs function to modulate the expression of various target genes by means of mRNA cleavage or translational repression, a process that is now well understood, relatively less is known of the mechanisms whereby miRNAs are themselves regulated. The key to studying the regulation of miRNAs lies in a firm understanding of the biogenesis process, previously described in chapter one, to identify the steps at which miRNAs are potentially regulated.

Firstly, when assessing the distribution of miRNA genes across the genome, it is apparent that some miRNAs exist as clusters and are transcribed as longer polycistronic primary transcripts (Kim & Nam, 2006). The vast majority of miRNA genes however are located in intergenic regions or in an antisense orientation to protein coding genes and are transcribed as independent units (Lee & Ambros, 2001; Lee *et al.*, 2002). Other miRNAs that are embedded in intronic regions of protein-coding genes are conveniently transcribed with the protein coding gene and

excised by means of splicing machinery from the longer transcript (Rodriguez *et al.*, 2004). The genomic distribution of miRNAs was identified by Calin *et al.*, in 2004 as a point of regulation, as it was found that a significant percentage (~52.5%) of miRNAs are located at fragile sites or at regions that are associated with cancer. This is of great significance when analysing the altered miRNA profiles of several cancers.

The first assumption made when approaching the mechanism of miRNA biogenesis was that these small RNAs are transcribed by RNA Polymerase III, as Pol III transcription is responsible for the transcription of small RNAs such as tRNAs and U6 snRNA. A key step in discovering the realms of miRNA regulation was the finding that these independently transcribed miRNA genes are predominantly transcribed by RNA Polymerase II (Pol II) instead and that pri-miRNAs transcribed in this manner contained a 5'cap and poly(A) tail, key characteristics of Pol II transcription. This was elucidated by Lee *et al.*, (2002) following his discovery that pri-miRNAs are several kilobases long and contain stretches of more than four Uracils, which would have terminated transcription by RNA polymerase III. This finding was validated by expressed sequence tag (EST) analyses in which chimaeric transcripts of miRNA precursor and mRNA transcripts contained poly-A tails, with the evidence of occasional splicing (Smalheiser, 2003). More direct evidence was obtained when it was shown that miR-155 and miR-172 are both poly-adenylated and spliced (Aukerman & Sakai, 2003). Furthermore, the insertion of a Pol II enhancer had induced miRNA expression as in the case of *bantem* RNA in Drosophila (Brennecke *et al.*, 2003).

Although all the advancing evidence seems to point towards miRNAs being predominantly transcribed by Pol II, there have also been studies indicating that some miRNAs are in fact transcribed by Pol III, as initially presumed. Zhou *et al.*, (2005) developed a computational program as a predictive tool to discriminate and distinguish between Pol II, Pol III and random intergenic sequences across the genomes of *C. elegans*, *H. sapiens* and *A. thaliana*. After applying their model to human miRNAs of intergenic location, it was predicted that many pre-miRNA

sequences contained Pol II promoters and only three pre-miRNA sequences contained Pol III promoters. Borchert *et al.*, (2006) validated this prediction of Pol III transcription of miRNAs in a study of the miRNA cluster on chromosome 19 (C19MC), wherein it was determined that some 43 mature miRNA sequences and in addition 52 human miRNAs were contained within repetitive elements such as Alu repeats; and only Pol III was required for transcription of these miRNAs. Although there are some miRNAs that are located within Alu repeats that are transcribed by RNA polymerase III, the reminiscence of miRNA transcription by Pol II to that of protein-coding gene transcription is eminent. This has allowed for the research direction of identifying and characterizing miRNA promoter regions.

Computational programs have aided in providing information on the regulatory elements that are located upstream of miRNA genes (Lee *et al.*, 2007). Methods to identify miRNA transcription start sites (TSS) stemmed from studies identifying chromatin signatures that were present at initiation sites. Trimethylation of lysine 4 on histone 3 (H3K4me3) is a persistent modification that signifies the TSS of many, if not all, human genes and it seems as if this modification is restricted to the sites at which transcription initiates (Guenther *et al.*, 2007; Barski *et al.*, 2007). In addition, the chromatin locations of genes that are transcriptionally active are depleted of nucleosome activity within 100-130kb surrounding the transcriptional start site (Yuan *et al.*, 2005). Using H3K4me3 as a landmark, Marson *et al.* (2008) took advantage of these findings and formulated a library of putative TSSs, revealing high confidence promoters for more than 80% of miRNAs experimentally validated in humans and the mouse. Importantly, this study allowed for the promoter regions to be mapped computationally to putative transcription factor binding sites. Saini *et al.* (2007) identified regulatory binding sites for transcription factors upstream of the pre-miRNA genomic regions and it was determined that approximately 60% of these sites were clustered within 1kb. These regulatory binding sites overlapped the predicted TSSs which were located within regions -2 and -6kb. Interestingly it was also found that miRNAs may possess more than one predicted TSS. The miRNA promoter regions were found to contain relative frequencies of several regulatory elements which include TATA box, TFIIB recognition, initiator elements, histone modifications and

CpG islands (Ozsolak *et al.*, 2008; Corcoran *et al.*, 2009). These regulatory features render miRNA promoter regions relatively indistinguishable from mRNA promoter regions.

Many relationships between known transcription factors and miRNAs have been identified since. Of particular significance to carcinogenesis, c-Myc, a proto-oncogenic transcription factor responsible for regulating genes involved in cell growth and apoptosis, has been found to modulate the transcriptional regulation of several miRNAs, most notably the oncogenic miRNA cluster miR-17-92 (O'Donnell *et al.*, 2005; Chang *et al.*, 2008). Increased expression of c-Myc in turn activates the expression of miR-17-92, forming a feedback loop. The tumour suppressor miR-34 is regulated by the p53 transcription factor (Bommer *et al.*, 2007; Chang *et al.*, 2007; Raver-Shapira *et al.*, 2007; Tarasov *et al.*, 2007; Corney *et al.*, 2007). The deactivation of p53 results in a reduced expression of miR-34 (He *et al.*, 2007). With regard to angiogenesis, miR-210 is activated upon increased expression of the heat inducible transcription factor (HIF), in response to hypoxic stress (Giannakakis *et al.*, 2007; Camps *et al.*, 2008). MiR-145, a particular focus of the present study, had induced a pro-apoptotic effect dependent upon the expression of TP53. TP53 also activates miR-145 expression demonstrating a cell death promoting loop between the two (Spizzo *et al.*, 2010). The interesting interactions between transcription factors and miRNAs were analysed using bioinformatics tools and it seems that miRNAs are inclined towards regulating transcription factors (Shalgi *et al.*, 2007). Further, autoregulation and feedback loops are evident in many instances where transcription factors that regulate the expression of miRNAs also serve as targets of the miRNAs forming an autoregulation feedback loop that controls one another's expression. Relevant examples here include Runx1 and miR-27a in megakaryopoiesis (Ben-Ami *et al.*, 2009), c-Myb and miR-15a in haematopoiesis (Zhao *et al.*, 2009) and with bearing to this study, Pitx3 and miR-133b, albeit not relevant in cancer (Kim *et al.*, 2007).

While miRNAs are involved in complicated regulatory, molecular and cellular pathways, significant gaps still exist in this field of research. What we can be certain

of is that miRNAs seem to be regulated by similar mechanisms to protein coding genes and that it can be inferred that each avenue of mRNA regulation is potentially involved in the regulation of miRNAs as well. Pursuant to this inference and coupled with the identification of CpG islands and histone modifications in miRNA promoter regions, the possibility of epigenetic regulation of miRNAs may not be dismissed.

2.1.2 Epigenetic regulation of miRNAs

The first published study targeted at investigating the effects of epigenetics on miRNA expression assessed the effect of histone acetylation on miRNA expression. The breast cancer cell line, SkBr3, was treated with the HDACi LAQ824, resulting in rapid alterations in miRNA expression, with the subsequent downregulation of 32 mature miRNAs (Scott *et al.*, 2006). Epigenetic entities (DNA methylation and histone modifications) work in a coordinate and cooperative manner to regulate gene expression and by using this premise the team of the renowned cancer epigeneticist, Prof. Peter A. Jones, conducted a study on the miRNA expression profile of the T24 human bladder cancer cell line after simultaneous treatment with the DNA demethylating agent, 5-Aza-2'-deoxycytidine (5-Aza-2'-C) and the HDACi 4-phenylbutyric acid (PBA); resulting in 17 out of 313 miRNAs being upregulated (Saito *et al.*, 2006). One of the miRNAs, miR-127, was found to be integrated within a CpG island. Since miR-127 expression is significantly reduced in cancer cells, this indicated that this miRNA and putative tumour suppressor is susceptible to epigenetic silencing. Also, a predicted target of miR-127, the proto-oncogene BCL-6, was downregulated post-treatment with 5-Aza-C and PBA. Other examples of epigenetic modulation of miRNAs include miR-1, which was upregulated in response to HDACi treatments in lung cancer cells (Nasser *et al.*, 2008). MiR-1 is encoded with the miR-133 cluster and miR-1, miR-133 and miR-206 (a miR-1 functional homologue) is significantly downregulated in several solid tumours (Hudson *et al.*, 2011). Moreover, in the context of colon cancer, in the HCT116 CRCcell line wherein the two main DNA methyltransferases DNMT1 and DNMT3b were knocked out by homologous recombination, 18 miRNAs were upregulated, including miR-124a, a

putative *bona fide* tumour suppressor (Lujambio *et al.*, 2007). The silencing of miR-124a induces the expression of the cell cycle cyclin dependent kinase 6 (CDK6) and subsequently the phosphorylation and thus regulation of the tumour suppressor protein, retinoblastoma (Rb). It is thus evident that miRNAs respond to and are regulated, directly or indirectly, by epigenetic mechanisms. The expression patterns of miRNAs are not uniform however, showing differential expression patterns between different tissues or cell types. There have also been contradictory studies that have identified no change in miRNA expression in the lung cancer cell lines, A549 and NCI-H157, following treatment with epigenetic drugs (Yanaihara *et al.*, 2006; Diederichs *et al.*, 2006).

Similar to the mechanism of repression of tumour suppressor protein coding genes by aberrant DNA hypermethylation at promoter regions, this mechanism has been validated to repress the expression of several miRNAs, miR-1-1, miR-193a, miR-137, miR-342, miR-203 and miR-34b/c, by means of hypermethylated promoter regions (Lujambio *et al.* 2009; Lujambio *et al.* 2008). Although it is not certain if this mechanism contributes to the downregulation of all tumour suppressor miRNAs in cancer, evidence however points to it being the likely cause.

In the context of this chapter, the putative CRC tumour suppressor miRNAs in question in this study, miR-145 and -143, have not yet been validated as being epigenetically silenced by aberrant DNA hypermethylation or histone modifications in CRC. Nevertheless, two independent studies have identified that miR-145 is hypermethylated at the promoter locus causing repression in prostate cancer (Zaman *et al.*, 2010; Suh *et al.*, 2011). MiR-143 has been shown to be repressed by DNA hypermethylation in primary blast cells containing the fusion protein MLL-AF4 in acute lymphoblastic leukaemia (Dou *et al.*, 2012). This repression by DNA hypermethylation was not shown in MLL-AF4 negative ALL derived cells and was also not apparent in normal cells. At the time of the development of this project, there was a lack of evidence on any epigenetic regulation of miR-133b; however a recent finding has provided evidence of epigenetic regulation of miR-133b *via* promoter hypermethylation in CRC (Lv *et al.*, 2015). Literature in regard to epigenetic alterations of miRNA expression however has revealed differential expression

patterns between the various cell and tissue types and stages described by finite regulation in a spatio-temporal manner; therefore it can be assumed that the epigenetic profile of cancer may evolve as the disease progresses through various stages.

The aim of this chapter is to assess epigenetic alterations by means of DNA methylation and histone acetylation on the expression of the three putative tumour suppressor miRNAs in CRC cell lines. In the present study, cell lines from two different progressive stages of CRC were utilised to assess the stage specific alterations in miRNA expression post treatment with the epigenetic agents, 5-Aza-2'-C and Trichostatin A (TSA), respectively. These drugs are described below.

2.1.3 Epigenetic drugs

2.1.3.1 *5-Aza-2'–C and its use as a DNA demethylating agent*

5-Aza-2'-C is used as a DNA demethylating agent in this study. It is essentially an analogue of the naturally occurring nucleoside 2'-deoxycytidine however the carbon at the fifth position has been replaced by nitrogen (Refer to Figure 2.1). It functions as a DNA demethylating agent by incorporating into DNA and therefore binding DNA methyltransferase enzymes irreversibly, as it attempts to methylate the C5 position of the nucleoside. By sequestering the DNA methytransferase enzymes in this manner, it gradually results in global genome DNA hypomethylation and therefore reactivates genes that have previously been silenced (Christman, 2002). This has attracted the use of this compound as an anti-neoplastic agent. The compound was initially synthesised in 1964 by Pliml and Sorm and in 1968 the first sign of anti-leukaemic activity was reported (Sorm & Vesely, 1968). It is more commonly known as Decitabine (trade name Dacogen) after it had been indicated for the treatment of Myelodysplastic syndrome and Chronic Myelomonocytic leukaemia (Kantarjian *et al.*, 2006). Strong anti-leukaemic activity against Acute Myeloid Leukaemia has also been reported for Decitabine in these preceding studies.

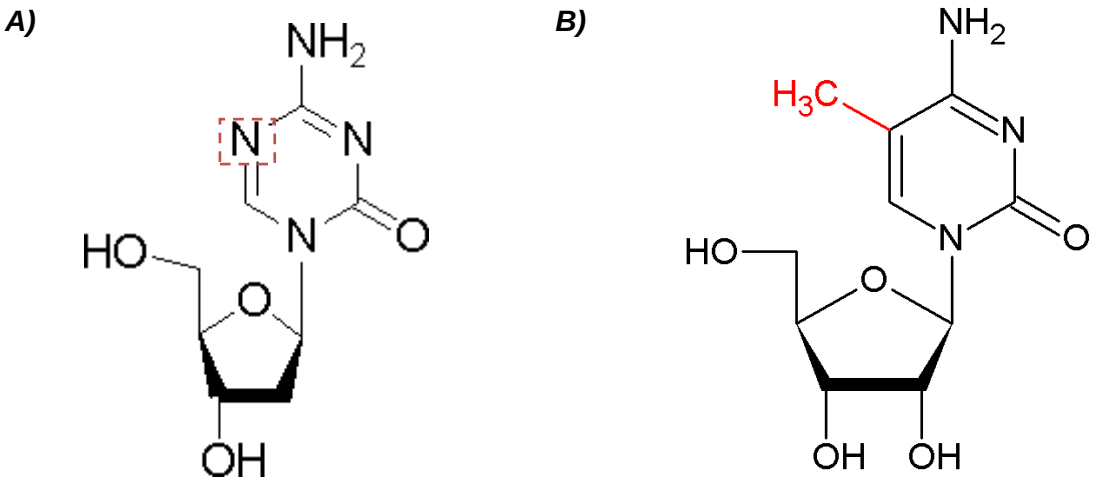

Figure 2.1: Comparison of 5-Aza-2'-C to a methylated cytosine. ***A.*** Chemical structure of 5-Aza-2'-C*:* $C_8H_{12}N_4O_4$. The red dashed box highlights the nitrogen replacement of the carbon molecule at the C5 position. **B.** Chemical structure of methyl cytosine. The methyl group which is added to the cytosine in a CpG island is highlighted in red at the C5 position (Fenaux, 2005).

2.1.3.2 *Trichostatin A and its use as a histone deacetylase inhibitor*

TSA (as depicted by the organic structure in Figure 2.2) was initially isolated and described in 1975 by a group of scientists in Japan (Tsuji, 1975), as an antifungal antibiotic which originated from metabolites of strains of *Streptomyces hygroscopicus*. The compound is organically derived from a primary hydroxamic acid and has a free glycosylated hydromaxate group shown in Figure 2.2. HDACs fall into 3 main families, with 18 HDACs identified to date. TSA inhibits histone deactylation by targeting Zn^{2+} dependent Class I and Class II HDACs, induces histone hyperacetylation and inhibits cell proliferation (Witt *et al.*, 2009). Hydroxamic acids have a high affinity for biometals and TSA specifically interacts with the Zn^{2+} ion in the catalytic unit of Class I and II HDACs with a resulting inhibitory effect. TSA imposes its strongest inhibitory effect on HDACs 1, 2 and 3 of the Class I HDACs, HDAC 4, 7 and 9 of the Class IIA HDACs and HDAC 6 of the Class II B HDACs (Witt *et al.*, 2009).

A)

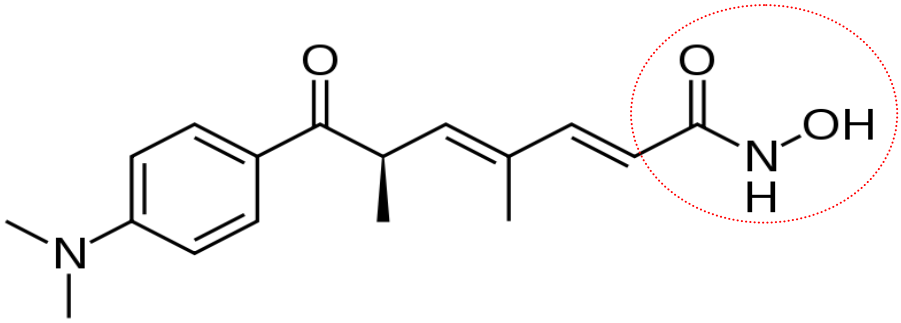

B)

HDACi	Histone Deacetylase										
	Class I				Class II A				Class II B		Class IV
TSA	HDAC1	HDAC2	HDAC3	HDAC8	HDAC4	HDAC5	HDAC7	HDAC 9	HDAC6	HDAC10	HDAC11

Key	
	Strong inhibition
	Weak inhibition
	No effect

Figure 2.2: Trichostatin A structure and targets. *A.* Chemical structure of Trichostatin *A: $C_{17}H_{22}N_2O_3$.* The hydroxamate group is circled in red. **B.** Trichostatin HDAC targets. TSA inhibits the activity of Class I and II HDACs with the strongest inhibitory effect on HDAC 1, 2, 3, 4, 6, 7 and 9. Adapted from Witt *et al.*, (2009).

2.1.4 Methods to isolate and study miRNAs

The small size of miRNAs presents a challenge for amplification and subsequently quantitation of these RNA species. Previously, the most predominant method for miRNA quantitation involved the use of Northern Blots, a convenient and readily accessible electrophoretic and hybridization probe based technique. This method however eventually presented several limitations, most significantly in specificity and reproducibility. Large volumes of sample material are required per lane (approximately 5-10 mg) to detect miRNAs and therefore relatively low abundant

miRNAs are predominantly undetected using this method, as only one miRNA probe is hybridised to the blot at one time. Also, a significant disadvantage lies in not being able to discriminate between miRNAs differing by one nucleotide, using the hybridization probes for Northern analysis. Furthermore, the nature of the experiment requires several assay repeats for statistical significance, yet the reproducibility of the method is not the most reliable due to its laborious nature and lack of automation (Chen *et al.*, 2005).

For these reasons a better method was deemed necessary for the analysis of miRNAs, with the specificity and reliability of PCR (polymerase chain reaction) being the most attractive option. Implementing this method for miRNA analysis however came with its own set of challenges. Initial PCR assays for miRNA detection had relied on the miRNA precursor template and thus could not quantify the active mature miRNA. Furthermore, conventional primers for PCR are approximately the size of a mature miRNA strand which is 21-25 nucleotides in length. In addition, the stem loop structure formed by miRNA precursors do not allow for a convenient template for miRNA amplification. These challenges were overcome with the development of a miRNA PCR Assay utilizing miRNA-specific stem loop reverse transcription primers as depicted in Figure 2.3. In this study, reverse transcription of the miRNA to cDNA was achieved using miRNA-specific stem loop primers for miR-143, -145 and -133b (Applied Biosystems). The stem-loop primers are designed to overcome this problem of the short mature miRNA template by specifically binding to the mature miRNA target and forming a miRNA-primer complex that extends at the 5’ end of the miRNA. There are several advantages conferred by the stem looped structured primer;

1) The short RT priming sequence which is annealed to the 3’ end of the miRNA has better specificity for discriminating between similar miRNAs and has the ability to discriminate single nucleotide differences in sequence.

2) The double stranded stem loop structure prevents hybridization to the miRNA precursor and other longer RNA amplicons.

3) Base stacking in the stem region increases the stability of the miRNA and hetero-duplexes which ultimately enhance reverse transcription efficiency for short reverse transcription primers (the short sequence bound the 3' end).

4) When the stem loop structure unfolds, the presence of a sequence downstream of the miRNA extends the length of the amplicon requiring quantification. The resulting longer amplicon post reverse transcription is conducive to Real Time PCR using TaqMan® technology (Schmittgen *et al.*, 2008).

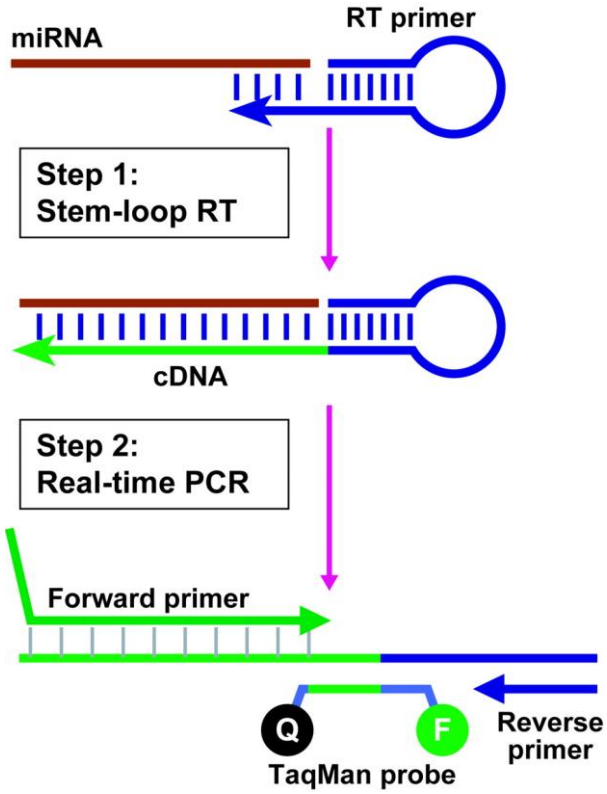

Figure 2.3: TaqMan® miRNA PCR Assay. In Step 1, the miRNA specific RT stem loop primer is shown which confers several benefits in the specificity and sensitivity of the subsequent reactions. After reverse transcription in Step 1, the resulting longer amplicon is then subjected to TaqMan® PCR in Step 2, using miRNA specific forward and reverse primers. The forward primer at the 5' end of the amplicon has an added tail to increase the melting temperature (Chen *et al.*, 2005).

2.1.5 Objectives

The overall aim of this chapter is to seek clarity regarding potential epigenetic regulation of the three putative CRC tumour suppressor miRNAs -143, -145 and -133b in relation to CRC. In this regard, the following objectives were defined:

- To determine the effect of epigenetic treatments (HDAC inhibitor TSA and DNA demethylating agent 5-Aza-2'-C) on the viability of CRC cell cultures
- To detect changes in expression levels of the miRNAs -145, -143 and -133b upon DNA demethylation
- To detect changes in expression of the miRNAs -145, -143 and -133b upon inhibition of histone deacetylation
- To detect stage-specific differences in miRNA expression after treatment with epigenetic treatments
- To compare the effects of DNA demethylation *versus* histone acetylation on the expression of the miRNAs

2.2 Materials & Methods

2.2.1 Cell culture

Aseptic techniques were utilised throughout the cell culture process to ensure prevention of contamination by means of microbacteria, fungi and mycoplasma. This was achieved by performing cell culture procedures under a laminar flow hood that was sterilised with a germicidal UV lamp when not in use. During the use of the hood, a fan was switched on which drew in air through a HEPA filter which ensured that the air was microbe free. All surfaces and gloves were periodically sterilised with 70% $^{v}/_{v}$ ethanol.

The two colorectal adenocarcinoma cell lines, SW1116 (ATCC CCL 233) and DLD1(ATCC CCL 221) were obtained from the Health Science Research Resources Bank (HSRRB) of the Health Science Foundation of Japan. These cell lines are representative of stage I and stage III (metastatic) CRC, respectively. These cell lines were routinely cultured in DMEM-F12 (Lonza-Biowhittaker®) culture media supplemented with 2% $^{v}/_{v}$ and 10% $^{v}/_{v}$ heat inactivated foetal bovine serum (FBS), respectively; and with 0.2% Penicillin/Streptomycin (Lonza BioWhittaker®).

The cell lines were initially rapidly thawed from the -70°C storage facility, rinsed by centrifugation in sterile Phosphate-Buffered Saline (PBS) solution and then placed into culture. Cells were plated into cell culture flasks and placed into the 37% incubator supplied with 5% CO_2 in air. Cells were subcultured at 80% confluency, that is, when approximately 80% of the surface of the cell culture flask had been occupied by the dividing cells. After removing the remaining cell culture media, confluent SW1116 and DLD1 cell cultures were rinsed with PBS and then incubated with 0.25 % deactivated Trypsin/ EDTA for 5 and 3 minutes, respectively. Once in suspension, the cells were pelleted by centrifugation at low speed (300rpm) for 1 minute. After removing the supernatant, the cell lines were re-suspended in fresh culture media and transferred to new cell culture flasks and placed in the incubator for subsequent cell expansion. Surpluses of the cell lines were harvested and stored cryogenically.

With regards to the ethical considerations pertaining to the use of *in vitro* cell cultures for research purposes, the use of cell lines purchased from an accredited cell bank do not require approval from the Wits Human Research Ethics Committee (Wits HREC). However an ethics waiver was obtained for the study (Ref: W-CJ-090317-4). (Refer to Appendix A).

2.2.2 Epigenetic drug treatments

To evaluate the contribution of epigenetic modulation on the regulation of miR-143, -145 and -133b expression in CRC, the CRC cell lines SW1116 and DLD1 were

subjected to epigenetic treatments involving two entities of epigenetic regulation; DNA methylation and histone acetylation, respectively.

Cell cultures were starved of serum overnight to synchronise the cells in the G0 (quiescent) phase of the cell cycle prior to drug treatment, therefore creating a homogenous baseline.

To assess the effects of DNA methylation on the expression of miRNAs, cell cultures were treated with 5-Aza-2'-C. The DNA de-methylating agent, 5-Aza-2'-C (Sigma Aldrich), was dissolved at a concentration of 50mg/ml in 99% acetic acid:PBS at a 1:1 ratio and stored at -70°C. Post thawing, 5-Aza-2'-C was added to cell culture media at concentrations of 1µM and 3µM, respectively.

The stock solution of 5-aza-2'deoxytydine (50mg/mL) involved dissolving 10mg 5-aza-2'-C in 200µL of an acetic acid (99%):PBS solvent in a 1:1 ratio. The 50mg/mL stock solution therefore contained 49.5% acetic acid. A 10µM stock solution was then created using 2.5µL of the 50mg/mL stock solution added to 50mL cell culture medium. The resultant acetic acid percentage reduced to 0.0025%. Further dilutions to 1µM and 3µM decreased the acetic acid percentage to 0.000125% and 0.000375% respectively. At these concentrations, there is no reported effect of acetic acid on cell viability, gene expression or DNA methylation. Marina *et al* in 2010 had reported on the effects of acetic acid on mammalian cell culture in which it was determined that 0.03% of acetic acid had minimal effect on pH when cells were maintained at 37˚C. It was argued that this minimal effect was due to metabolising cells maintained at 37˚C having superior internal cellular pH control. Furthermore, DNA methylation has previously been documented to remain stable during pH changes (Ernst *et al.*, 2008). An acetic acid control was therefore not deemed necessary in this experiment. No treatment controls were treated as per standard cell culture protocol as described above under paragraph 2.2.1. Cell cultures of the two cell lines were treated with 5-Aza-2'-C for 48 hours, with a daily replacement of the drug treatment due to the instability of the 5-Aza-2'-C compound.

To assess the effects of histone acetylation on the expression of miRNAs, cell cultures were treated with TSA, a HDACi. TSA (Sigma-Aldrich), reconstituted at a

concentration of 5mM in dimethyl sulfoxide (DMSO) (stored at -20°C) was diluted down to a 1000nM stock solution. The stock solution was then added to cell culture media at a 300nM concentration. Following serum starvation, SW1116 and DLD1 cell cultures were subjected to a 24 hour treatment of 300nM TSA. A DMSO (Sigma-Aldrich) carrier control was included in the treatments, to evaluate non-specific effects that may be induced by DMSO itself. Dimethyl sulfoxide (DMSO) is an amphipathic solvent characterised by its ability to penetrate the cell membrane. This property has allowed for the solvent to be used as an effective drug delivery molecule, owing to its ability to dissolve both polar and non-polar compounds (Santos *et al.*, 2003). It is also known to have various effects on gene expression and therefore warrants a control sample.

2.2.3 Cell viability

Post treatment with the epigenetic treatments, both cell lines were harvested and re-suspended in 1mL PBS. One part filtered Trypan Blue (Biorad) was added to one part cell suspension (in cell culture media). The mixture was allowed to react at room temperature for approximately 3 minutes. A drop (100µL) of the Trypan Blue/cell suspension was added to a haemocytometer and placed on the stage of the inverted bifocal microscope. Once focused on the cells, the number of viable (clear) and non-viable (blue) cells were counted within the specified area. Cell viability was calculated according to the equation below:

$$\% \text{ viable cells} = \frac{\text{Total number of viable cells per 1 mL of aliquot}}{\text{Total number of cells per 1mL of aliquot}} \times 100$$

2.2.4 MicroRNA isolation

To assess the effect of the epigenetic drug treatments on the miRNAs in question the first step post- treatment was to isolate good quality RNA. Due to the small size of miRNAs and the notorious instability of RNA, it was deemed necessary to source an RNA extraction method that preserved the integrity of these small RNA's. Initially,

homogenised cell culture lysates were subjected to the MicroRNA “Cells to Ct” kit from Applied Biosystems, which eliminates the RNA isolation procedure and reverse transcribes RNA into cDNA directly from the cell lysate (Ho *et al.*, 2013). Although the elimination of the RNA extraction step is intended to prevent contamination and hence the degradation of RNA, low RNA yields together with high salt concentrations were obtained, as determined by the A260/A230 OD ratio. This negatively impacted RNA quality and purity and thus PCR performance, emphasizing the requirement for a more suitable method. For this reason the mirVana miRNA isolation kit available from Ambion was evaluated.

There are two popular methods for the extraction of RNA, chemical extraction and solid-phase extraction, either of which is incorporated in the various commercial kits available for RNA extraction. Chemical extraction involves the use of a concentrated chaotropic salt, such as guanidinium thiocyanate, sodium acetate and phenol:chloroform. The chaotrope allows for the denaturing of macromolecules, such as DNA, RNA and proteins. After centrifugation, the acidic solution then separates these macromolecules into different phases. RNA remains in the aqueous upper phase, while proteins remain in the interphase and DNA is contained in the lower organic phase. RNA is precipitated out of the aqueous phase with the use of isopropanol or ethanol (Chomczynski & Sacchi, 2006)

Solid-phase extraction involves the use of high salt concentrations or salt and alcohol mixtures to decrease the affinity of RNA for water, resulting in increased affinity to the solid material (glass fibre) used to precipitate the RNA (Tan and Yiap, 2009).

The mirVana miRNA isolation kit uses the most convenient combination of both methods to extract high quality RNA enriched with small RNAs. This is done by eliminating the steps that would compromise the extraction of small RNAs, such as routine alcohol precipitation and high concentrations of denaturing salts. For these reasons the mirVana kit was chosen as the optimal and most appropriate method to extract RNA suitable for this protocol.

Treated and control cell cultures were subjected to the miRvana miRNA isolation kit (Ambion). The kit provides separate procedures for the isolation of total RNA containing conserved small RNAs or the extraction of RNA enriched with small RNAs below 200 bases in size. For the purpose of this experiment, the purification of total RNA was followed, as miRNA with preserved integrity of the flanking regions were required for the procedures to follow.

Approximately 1 x 10^6 cells were harvested and then lysed by adding 300-600µL of Lysis/Binding Solution contained within the kit. To ensure complete homogenisation, the lysates were vortexed briefly. The homogenates were then subjected to organic extraction. First, a 1/10 volume of miRNA homogenate additive was added to preserve the integrity of miRNAs. This was left on ice for 10 min. Then 300-600µL of Acid-Phenol: Chloroform was added to the homogenate, vortexed for 30-60 seconds and centrifuged for 5 minutes at maximum speed (10 900 x g) to separate the aqueous and organic phases of the mixture. After centrifugation the aqueous phase containing RNA was carefully removed, without disturbing the interphase (proteins) and lower phase (DNA), and transferred to a fresh tube. The volumes removed were noted and subsequently 1.25 volumes of room temperature ACS grade 100% ethanol were added. Exactly 700µL of the mixture was then transferred to a filter cartridge placed in a collection tube, and centrifuged at 10 000rpm to pass the mixture through the filter. The flow-through was discarded and the step repeated until all the ethanol/lysate mixture had passed through the filter. Subsequently, 700µL of Wash 1 (provided in the kit) was then added to the filter and centrifuged at 10 000rpm for 5-10 seconds. The flow-through was discarded; following which 500µL of Wash 2/3 was added to the filter and centrifuged. Flow-through was discarded and the wash step with Wash 2/3 was repeated, followed by a 1 min centrifugation at 10 000rpm to remove any residual fluid that may have been left in the filter. The filter cartridges were then transferred to fresh, clean collection tubes and the RNA contained in the filter was eluted with 100µL of 95°C pre-warmed Elution Solution (contained in the kit). This was done by transferring the Elution Solution to the centre of the filter followed by centrifugation at 10 000rpm for 20-30 seconds. The eluate

collected in the collection tube, containing the RNA samples, were then stored at -80°C until use.

2.2.5 RNA quantitation and quality assessment

A crucial step post RNA extraction was to assess the concentrations and purity of the RNA isolated. The purity and integrity of RNA influences the credibility of the results of downstream applications, such as reverse transcription and ultimately PCR performance. Nucleic acids (DNA and RNA) achieve optimal absorbance of light absorbance (optical density) at a 260nm wavelength. By measuring the optical density (OD) at 260nm and hence determining the concentration of RNA by using the Beer Lambert Law, there is an assumption that the sample being assessed contains purely RNA and does not contain DNA. Therefore, it is a crucial step to eliminate DNA in the RNA extraction procedure. By separating the RNA, protein and DNA layers in organic extraction, and by ensuring that only the aqueous phase was carried over to the following procedures, the probability of DNA contamination was significantly reduced.

Approximately 1.5µL of each isolated RNA sample was added to the pedestal of a NanoDrop Spectrophotometer ND-1000. Nanodrop Spectrophotometers provide scanning data at various wavelengths that can be analysed to assess the concentration and purity of RNA. The ratio of the OD readings recorded at 260nm and 280nm (260/280) indicates the purity of the RNA and likely contamination by proteins, phenols and aromatic compounds, which absorb optimally at 280nm. Highly pure RNA generally has an OD A260/A280 ratio of between 1.8 and 2.1. The ratio of the absorbance readings at 260nm over 230nm (260/230) gives an indication of the salt contamination in the RNA sample (this being carried over from the high concentrations of salts used during the RNA extraction procedure). Contamination with salts is generally indicated by an OD A260/A230nm ratio outside the range of 1.5-2.1. Please refer to Table 2.1 below for concentrations and absorbance ratios calculated for the RNA samples extracted.

Table 2.1: RNA concentrations and A260/A280 and A260/A230 ratios for each sample of RNA extracted.

Drug	Treatment	Cell line	[1][ ] ng/µL	A_{260}/A_{280}	A_{260}/A_{230}
5-Aza-C	NTC	SW1116	191.35	2.07	2.09
		DLD1	443.05	2.08	2.17
	1µM	SW1116	161.2	2.01	1.78
		DLD1	157.5	2.08	1.84
	3µM	SW1116	165.5	2.05	2.01
		DLD1	223.45	2.07	1.97
TSA	NTC	SW1116	233.55	2.07	2.01
		DLD1	280.65	2.09	2.14
	300nM	SW1116	161.45	2.06	1.88
		DLD1	173.2	2.09	1.86
	DMSO	SW1116	276.3	2.09	2.02
		DLD1	341.95	2.08	2.12

[1] Concentration

2.2.6 miRNA reverse transcription

The RNA samples that had achieved high levels of purity, as determined by the OD A260/A280 and A260/A230 ratio's in Table 2.1 were then subjected to miRNA RT-PCR. The first step was to convert the extracted total RNA to cDNA. This was achieved using the miRNA Reverse Transcription kit from Applied Biosystems. Reverse transcription of the total RNA to cDNA was achieved using miRNA-specific stem loop primers for miR-143, -145 and -133b, respectively (Applied Biosystems). These primers, as discussed in the introduction of this chapter, assist in preparing longer cDNA templates that are more amenable to the PCR procedure to follow. Table 2.2 contains the reaction mixes that were used for a 15µL volume of RT reaction. RNA concentrations were standardised for all samples prior to the Reverse Transcription assay.

Table 2.2: Reaction mix volumes for a 15µL Reverse Transcription mix.

RT reaction component	Volume per 15µL reaction volume (µL)
100mM dNTPs (with dTTP)	0.15
MultiScribe™ Reverse Transcriptase (50U/µL)	1.00
10x Reverse Transcription Buffer	1.50
RNase Inhibitor (20U/µL)	0.19
Nuclease-free water	4.16
Total RNA	5
miRNA specific stem loop primer (miR-143, -145 or -133b)	3
Total	**15**

RT Master mixes were prepared prior to addition of the RNA samples and RT primers. The RT Master mix was centrifuged and separated into 7µL aliquots. Volumes of 5 µL of total RNA at a standardized concentration was then added and subsequently the addition of 3µL of the miRNA RT primers to each aliquot, adding up to the 15µL reaction volumes. These volumes were scaled up according to the cDNA end product volumes required for PCR. Reaction mixes were kept on ice for 5 min and then transferred to the thermal cycler and run with the parameters shown in Table 2.3.

Table 2.3: Thermal cycler parameters for the Reverse Transcription procedure.

Step type	Time (min)	Temperature (°C)
HOLD	30	16
HOLD	30	42
HOLD	5	85
HOLD	∞	4

The above mentioned Reverse Transcription procedure was followed for all cDNA samples required for the amplification of miRNAs. The RT reaction for the amplification of 18SrRNA did not contain specific reverse transcription primers and hence was not done using the miRNA reverse transcription kit. The RT procedure was carried out with a conventional TaqMan® Reverse Transcription kit, using Random hexamers as the primers to convert total RNA to cDNA. The RT reaction mix is detailed in Table 2.4 below.

Table 2.4: RT reaction mix for a conventional Reverse Transcription reaction.

Component	Volume per 10µL reaction volume (µL)
10x Reverse Transcription Buffer	1
$MgCl_2$	2.2
dNTP mix	2
Random Hexamer[2]	0.5
RNase Inhibitor	0.2
MultiScribe™ Reverse Transcriptase	0.25
Nuclease-free water and RNA	3.85
Total	**10**

2.2.7 miRNA PCR amplification

Real time PCR proceeded using a TaqMan® Universal PCR Master Mix and TaqMan® MicroRNA Assays (Applied Biosystems). Refer to Figure 2.5 for the reaction volumes per mix. TaqMan® technology utilises the basic concepts of polymerase chain reaction (PCR) and fluorescence resonance electron transfer (FRET) in combination to yield a superior version of the conventional PCR, more accurately amplifying the target being investigated (Kessler *et al*., 2009). MiRNA expression was normalised to the housekeeping non-coding RNA 18s rRNA and detected relative to "no treatment controls" in a 7500 Real Time PCR Machine (Applied Biosystems). Input cDNA concentrations were standardised prior to experimental runs on each cell line. MiRNA-specific TaqMan® MGB probes and primers were used to detect expression of the respective miRNAs. Samples were run in triplicate to establish a mean Ct value for the amplification of each sample. The parameters programmed into the 7500 Real Time PCR machine for each run are shown in Figure 2.6.

[2] Random Hexamers were used for the subsequent amplification of the housekeeping gene and endogenous control, 18SrRNA.

The housekeeping non-coding RNA 18SrRNA was amplified using an assay containing the specific primers and probes targeting this gene. This assay was commercially available through Applied Biosystems.

Table 2.5: Reaction volumes for a 20µL PCR mix.

Component	**Volume/ 20µL reaction (in µL)**
TaqMan® miRNA assay 20x or housekeeping gene assay	1
Product from RT reaction (cDNA)	1.33
TaqMan® 2X Universal PCR Master Mix, No AmpErase UNG	10
Nuclease-Free Water	7.67
Total	**20**

Table 2.6: Parameters programmed in the Applied Biosystems 7500 Real Time PCR Machine for each run.

Step	**AmpliTaq Gold Enzyme Activation**	**Polymerase Chain Reaction**	
	HOLD	CYCLE (40 cycles)	
		Denature	Anneal/ Extend
Time	10 min	15 sec	60 sec
Temperature (°C)	95	95	60

2.2.8 Data analysis

Sample reactions were run in triplicate. The mean Ct values were determined during the experimental runs and subsequently the miRNA expression levels from the treated samples were first normalised to 18SrRNA and then calculated relative to “no treatment controls|, according to the $2^{-\Delta\Delta Ct}$ method described by Livak and Schmittgen in 2001 (Appendix C).

To compare the relationship between the sample means before and after treatment with the epigenetic treatments (for the cell viability assays and the RT-PCR reactions), a paired two-tailed Student’s t-test was performed with the confidence interval set at 95%.

2.3 Results

2.3.1 The effect of DNA demethylation on cell viability in early and late stage colorectal cell lines

To evaluate the susceptibility of SW1116 and DLD1 cell lines to 5-Aza-2’-C treatment, the cell lines were subjected to cell viability assays post-treatment with the epigenetic drug and compared to the untreated controls.

Visual changes observed (images not shown) after epigenetic treatment with 5-Aza-2’-C were evidenced by an altered growth characteristic of DLD1 cells, demonstrating a slight decrease in adherent cell growth, recognised by the detachment of several cells from the cell culture flask surfaces. The detached cells had lost their epithelial morphology and were more granular in appearance.

In contrast, treating SW1116 cells with 5-Aza-2’-C resulted in a very marginal increase in the rate of cell growth. This effect was observed as the cell cultures had reached confluency at a slightly faster rate with the treatment of 5-Aza-2’-C. Passage cycles were shorter when treated with 5-Aza-2’-C compared to the untreated

SW1116 cell cultures. This ultimately meant that the time for the flask surface to be 100% confluent was shortened upon treatment with 5-Aza-2'-C.

These visual changes were supported by the quantitative results obtained from cell viability assays completed after treatment with 5-Aza-2'-C. The "no treatment control" (NTC) samples for the DLD1 cell line yielded a 97% cell viability while treatment with 1µM 5-Aza-2'-C decreased cell viability by 6% yielding a value of approximately 91% live cells (where t(1) = 4.0288 and *p*=0.0157; m=97, SD=12.16, n=3) . The number of live cells were further decreased to 89% at the increased dose of 3µM 5-Aza-2'-C (where t(1) = 5.3718 and *p*=0.0058; m=89, SD=2.16, n=3) (Figure 2.4).

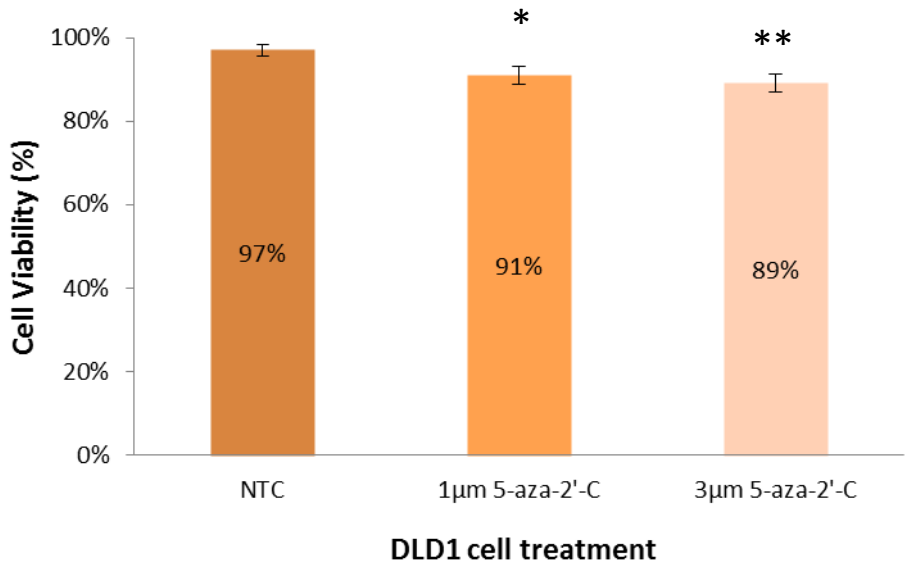

Figure 2.4: DLD1 cell viability post treatment with 5-Aza-2'-C. DLD1 cells were treated with differential doses of 5-Aza-2'-C for 48 hours, with a daily replacement of the drug. A slight decrease in cell viability was observed with 5-Aza-2'-C treatment at 1µM and a further decrease noted with 3µM where *p*=0.0157 and *p*=0.0058, respectively. * Significant (p<0.05); ** Very significant (p<0.01)

Cell viability assays conducted on SW1116 cells pre- and post- treatment with 5-Aza-2'-C correlated with the visual changes that were recognised during cell culture with the number of live cells increasing by 1% to a level of approximately 97%

viability when treated with 1µm 5-Aza-2'-C (where t(1) = 0.06718 and *p*=0.5387; m=97, SD=1.41, n=3), compared to 96% viability for the untreated equivalent of the cells. However, with an increased concentration (3µm) of the DNA demethylating agent, cell viability decreased with a 3% drop in viability to 93%, compared to the untreated equivalent (where t(1) = 1.7010 and *p*=0.1642; m=93, SD=2.16, n=3) These results are illustrated in Figure 2.5.

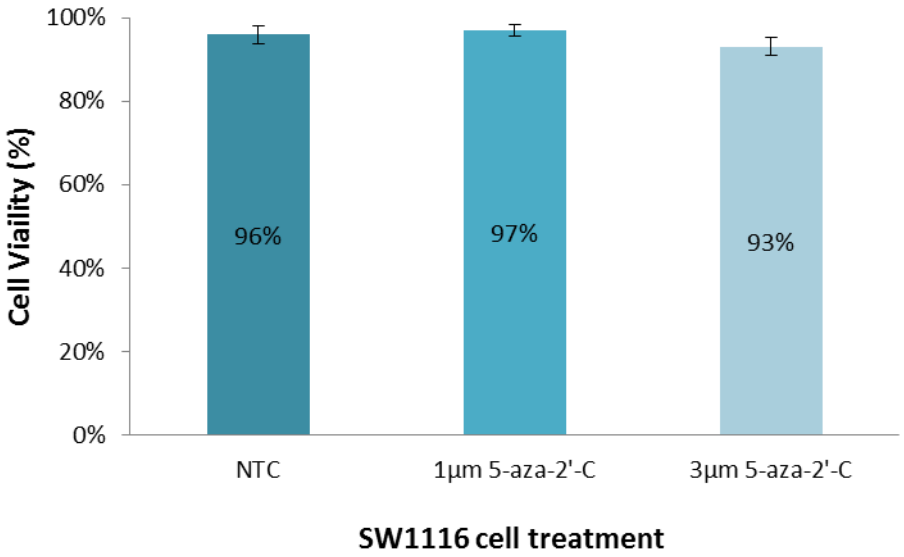

Figure 2.5: SW1116 cell viability post treatment with 5-Aza-2'-C. SW1116 cells were treated with differential doses of 5-Aza-2'-C for 48 hours with a daily replacement of the drug. There was a slight increase in viability at 1µm (*p*=0.5387, not significant) and a slight decrease in viability at 3µm 5-Aza-2'-C (*p*=0.1642, not significant).

2.3.2 The effect of histone acetylation on cell viability in early and late stage colorectal cancer cell lines (SW1116 and DLD1 cells)

The evaluation of the susceptibility of SW1116 and DLD1 cells to the HDACi TSA was assessed by performing cell viability assays on the cell lines pre- and post-treatment as described in Chapter 2.2.3.

A microscopy assessment of the DLD1 cells after treatment with 300nM of TSA indicated a noticeable increase in non-adherent cells, in suspension in the culture

medium. In contrast, DMSO treated cultures were similar to untreated controls, where cells remained predominantly attached to the surface of the culture vessel, indicating an effect on the cells due to the TSA treatment.

In corroboration with the above observations, the cell viability assay showed untreated cells to be 99% viable, whilst DMSO carrier control cells had a minimally decreased viability of some 6% where t(1) = 5.095 and *p*=0.0047; m=93, SD=1.63, n=3. TSA treatment in comparison, resulted in a 15% decrease in DLD1 cell viability where t(1)=15.9773 and *p*=0.0001; m=84, SD=1.41, n=3, denoting a probable effect of the drug on proliferation (See Fig 2.6 below).

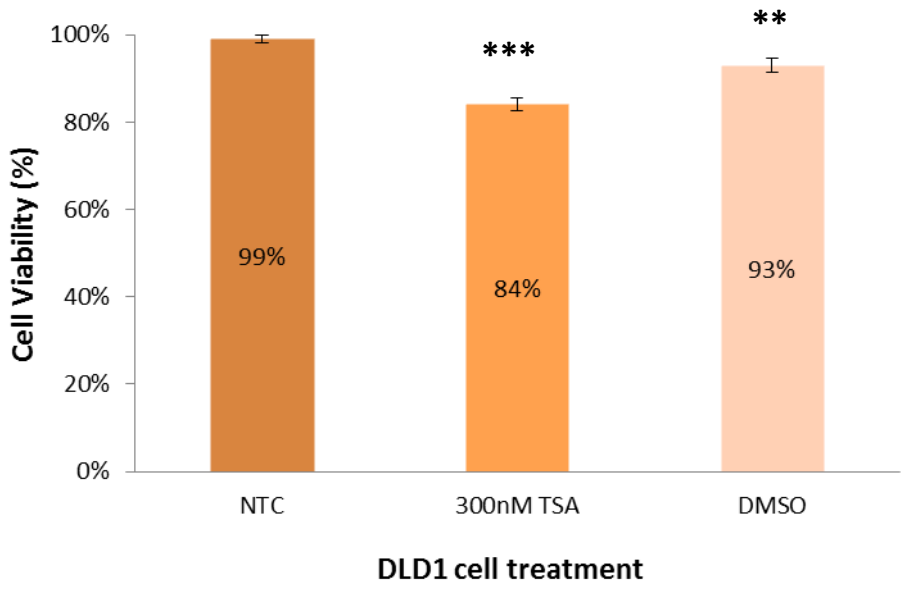

Figure 2.6: DLD1 cell viability post treatment with TSA. DLD1 cell cultures were treated either with 300nM TSA or an equivalent concentration of DMSO (carrier control); or were untreated (NTC) for 24 hours. TSA decreased viability of DLD1 cells to 84% relative to the "no treatment control" (*p*=0.0001) whereas DMSO treatment only decreased the viability by 6% (*p*=0.047). ** Very significant (*p*<0.01), *** Extremely significant (*p*<0.001)

Similar to the DLD1 cells, the effect of TSA on SW1116 cells resulted in an increase in non-adherent cells and an altered cell viability. More specifically, cells in suspension were granular in appearance and similar to those seen after the treatment of DLD1 cells with 5-aza-2'-C.

Also, a uniform pattern of decreased viability was demonstrated in SW1116 cell cultures after treatment with 300nM TSA. The dramatic percentage decrease in viable cells compared to the untreated control cells was 18% where t(1)=17.1286 and *p*=0.0001; m=80, SD=1.63, n=3. This drop was independent of DMSO as the DMSO treated control cells had diminished the percentage of live cells by 6% where t(1)=5.7095 and *p*=0.0047; m=92, SD=1.63, n=3, as shown in Figure 2.7.

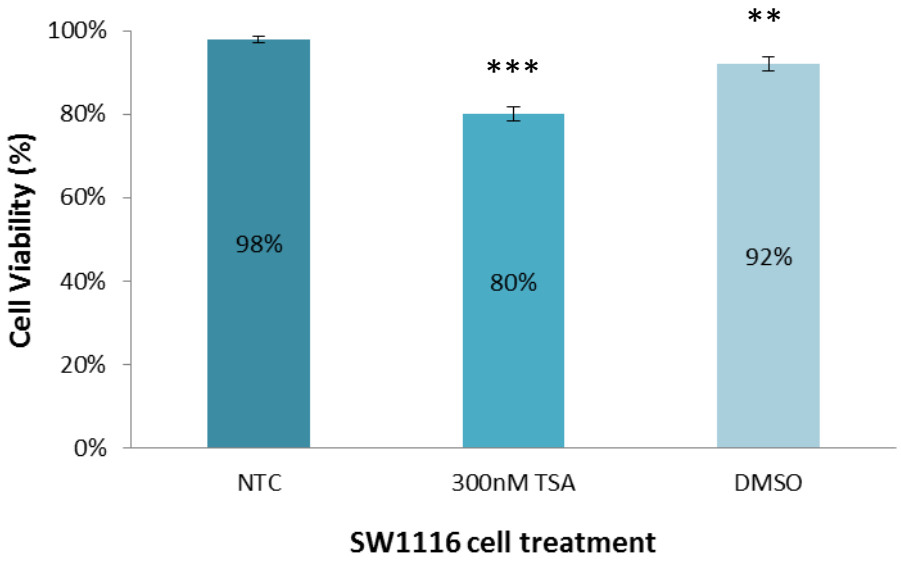

Figure 2.7: SW1116 cell viability post treatment with TSA. SW1116 cell lines were treated with either 300nM TSA or an equivalent concentration of DMSO (carrier control) for 24 hours. Decreased viability of SW1116 cells was demonstrated upon treatment with TSA (*p*=0.0001), compared with DMSO treatment (*p*=0.0047) and the NTC. ** Very significant (*p*<0.01), ***Extremely significant (*p*<0.001).

2.3.3 The effect of DNA de-methylation on miRNA expression in early stage colorectal adenocarcinoma

To assess the contribution of DNA de-methylation on the expression of the three miRNAs in question in early stage CRC, SW1116 cells were treated with both a low and a high dose of 5-Aza-2'-C. After isolating RNA and subsequent conversion to

cDNA by reverse transcription, the samples were subjected to real time PCR to detect relative expression of the miRNAs to the untreated controls. The Ct values were first normalised to the endogenous control, 18s rRNA, after which fold changes in expression were calculated according to the $2^{-\Delta\Delta Ct}$ method (Livak & Schmittgen, 2001). The sample ΔCt mean values for treatment and untreated samples were compared for statistical significance using a paired two-tailed Student's t-test, with the confidence interval set at 95%.

2.3.3.1 *The effect of 5-Aza-2'-C treatment on the expression of miR-133b*

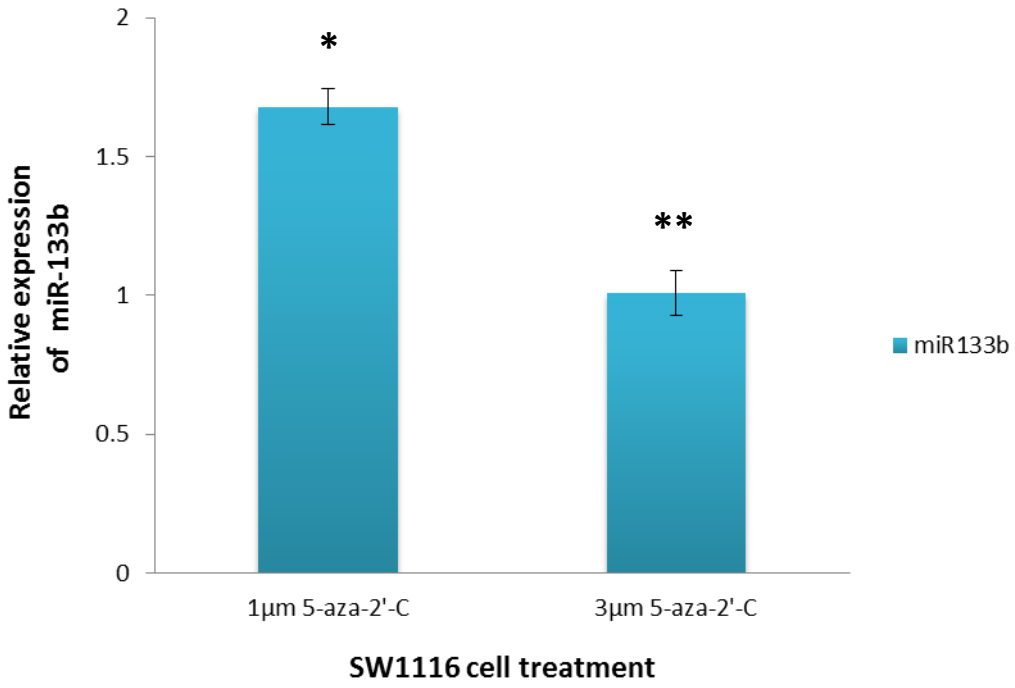

Figure 2.8: Relative expression of miR-133b in SW1116 cells after treatment with 5-Aza-2'-C. Low and high dose 5-Aza-2'-C treatment yield increased miR-133b expression by 1.6 (p=0.0282) and 1 fold (p=0.0047) respectively. *Significant (p<0.05), ** Very Significant (p<0.01).

The effect of the two dosages of 5-Aza-2'-C on the expression of miR-133b is illustrated in Figure 2.8. MiR-133b expression increased by over 1.6 fold after treatment with 1µM 5-Aza-2'-C, compared to the no treatment control (NTC), where

t(1) = 22.5577 and *p*=0.0282 (m=5.865, SD=0.26, n=3). A similar trend is shown for the treatment of SW1116 cells at the higher dose of 3µm 5-Aza-2'-C; miR-133b was also significantly up-regulated, where t(1) = 5.69382) and *p*=0.0047 (m=3.21, SD = 0.481, n=3), albeit some 0.5 fold less than the increase exhibited with the low dose treatment. From this, it would seem that there may be a dose dependent relationship of the 5-Aza-2'-C treatment on miR133b expression.

2.3.3.2 *The effect of 5-Aza-2'-C treatment on the expression of miR-143*

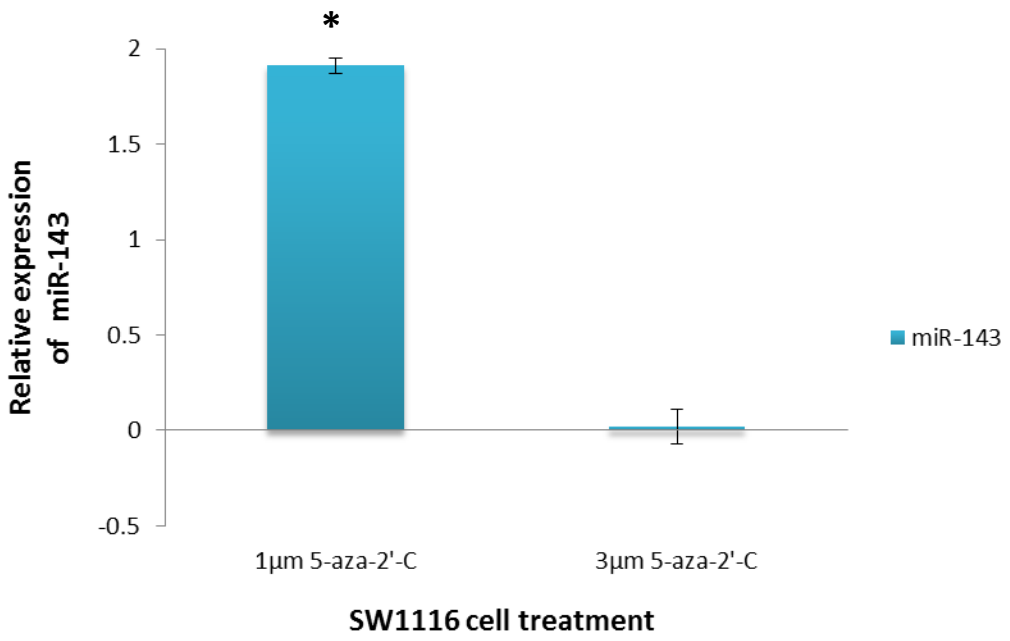

Figure 2.9: Relative expression of miR-143 in SW1116 cells after treatment with 5-Aza-2'-C. Low dose (1µm) 5-Aza-2'-C yielded increased miR-143 expression by almost 2 fold (*p*=0.0157), while there was a marginal increase of 0.01 fold (*p*=0.503, not significant) after high dose (3µm) 5-Aza-2'-C treatment. * Significant (*p*<0.05).

To evaluate the effect of DNA de-methylation on miR-143 expression in early stage CRC cells, expression levels of miR-143 relative to the untreated controls were compared, after treating SW1116 cells with a low and a high dose of 5-Aza-2'-C, respectively (Figure 2.9).

The expression of miR-143 was effectively induced by the treatment of 1µm 5-Aza-2'-C by almost 2 fold (where t(1)=40.5576 and *p*=0.0157 (m=6.50950, SD=0.16,n=3)). However at a higher concentration (3µm) this induced expression was lost, demonstrating a marginal but insignificant up-regulation of 0.018 fold, compared to the untreated control (where t(1)=0.735 and *p*=0.503 (m=-0.264, SD=1.003, n=3)). The expression of miR-143 was more responsive to the lower dose of 5-Aza-2'-C than the higher 3µm dose, demonstrating a dose-specific response.

2.3.3.3 *The effect of 5-Aza-2'-C treatment on the expression of miR-145*

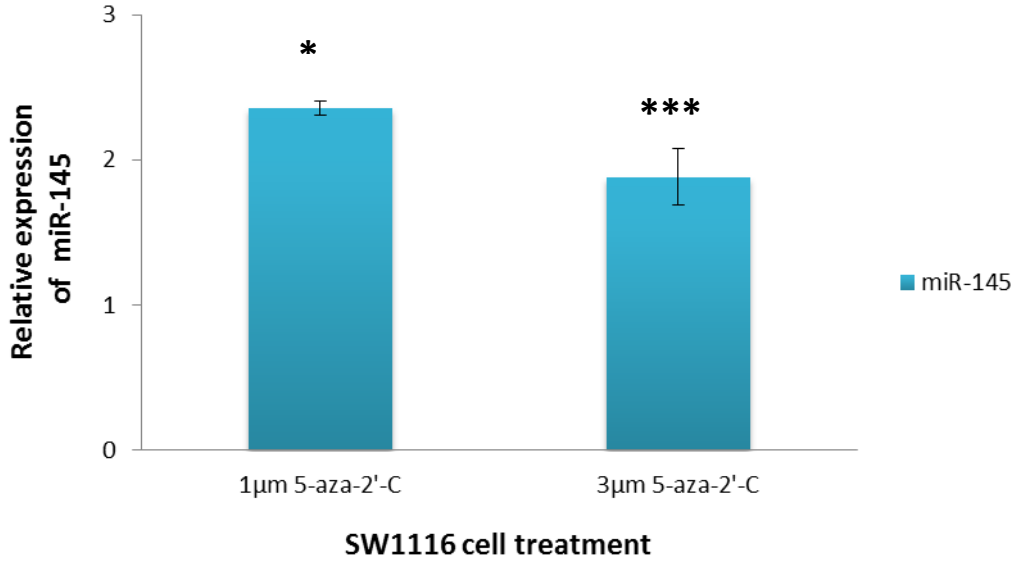

Figure 2.10: Relative expression of miR-145 in SW1116 cells after treatment with 5-Aza-2'-C. Low dose (1µm) and high dose (3µm) 5-Aza-2'-C yield increased miR-145 expression by 2.3 fold (*p*=0.0177) and 1.8 fold (*p*=<0.00001) respectively. * Significant (*p*<0.05), *** Extremely significant (*p*<0.001).

SW1116 cells were treated with a lower (1µm) and higher dose (3µm) of 5-Aza-2'-C and its effect on miR-145 expression was evaluated (Figure 2.10). At the lower dose, miR-145 was significantly up-regulated by 2.4 fold, relative to the control cells; the mean decrease in the Ct value was significant, where t(1)= 36.0390 and *p*=0.0177 (m=7.388, SD = 0.205, n=3). Similarly with a dose of 3µm 5-Aza-2'-C, miR-145 was effectively up-regulated by 1.8 fold compared to the untreated control samples; where the mean decrease in Ct was highly significant, with t(1) = 33.2513 and

p<0.00001 (m=6.24, SD=0.771, n=3). Additionally, miR-145 expression seemed to be more susceptible to the lower dose of 5-Aza-2'-C, with an almost 0.5 fold increase in expression when compared to the lower dose.

2.3.4 The effect of DNA methylation on miRNA expression in late stage colorectal adenocarcinoma

To determine the contribution of DNA de-methylation on the expression of the three miRNAs in question in late stage CRC, DLD1 cells were treated with low and high dose 5-Aza-2'-C. Isolated RNA was reverse transcribed and miRNA expression levels were assessed as described previously, relative to the endogenous control 18s rRNA.

2.3.4.1 *The effect of 5-Aza-2'-C treatment on the expression of miR-133b*

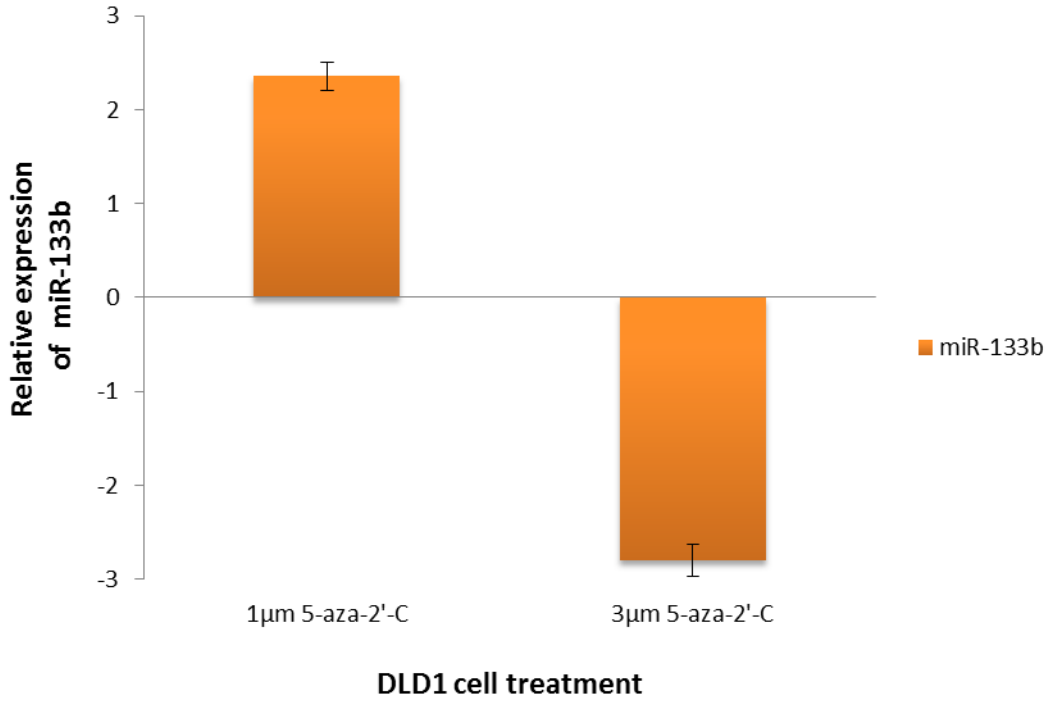

Figure 2.11: Relative expression of miR-133b in DLD1 cells after treatment with 5-Aza-2'-C. Low dose (1µm) yielding an increased expression of miR-133b by 2.3 fold (*p*=0.1179, not significant) while high dose (3µm) 5-Aza-2'-C exhibits down-regulation of miR-133b by 2,8 fold (*p*=0.0870, not significant). Relative expression is shown as log($2^{-\Delta\Delta Ct}$,base 2).

To quantify the effect of DNA de-methylation on miR-133b expression in late stage colorectal adenocarcinoma, DLD1 cells were treated with low (1µm) and high (3µm) dose 5-Aza-2'-C for 48 hours each and qRT-PCR was subsequently conducted to detect the expression of miR-133b pre- and post- treatment. According to Figure 2.11, relative expression of miR-133b compared to untreated controls yielded a trend of upregulation by 2.3 fold when treated with 1µm 5-Aza-2'-C where t(1)=5.3399 and *p*=0.1179 (m=6.747, SD=1.264, n=3). Alternatively, a trend of down-regulation of miR-133b by 2.8 fold, where t(1)=7.2755 and *p*=0.0870 (m=-9.811, SD=1.349, n=3), is evident when DLD1 cells are treated with the higher dose of 5 aza-2'-C. This implies a dose sensitive response of miR-133b to the DNA de-methylating agent. In comparison to Figure 2.5, where early stage colorectal carcinoma cells (SW1116) were treated with 5-Aza-2'-C and the expression of miR-133b evaluated, it would seem that miR-133b expression in SW1116 cells was more susceptible to DNA 5-Aza-2'-C at the higher dose of 3µm than in DLD1 cells. In contrast however, the susceptibility to the 1µm dose was retained in both cell lines, with highest susceptibility being shown in the DLD1 cell line.

2.3.4.2 *The effect of 5-Aza-2'-C treatment on the expression of miR-143*

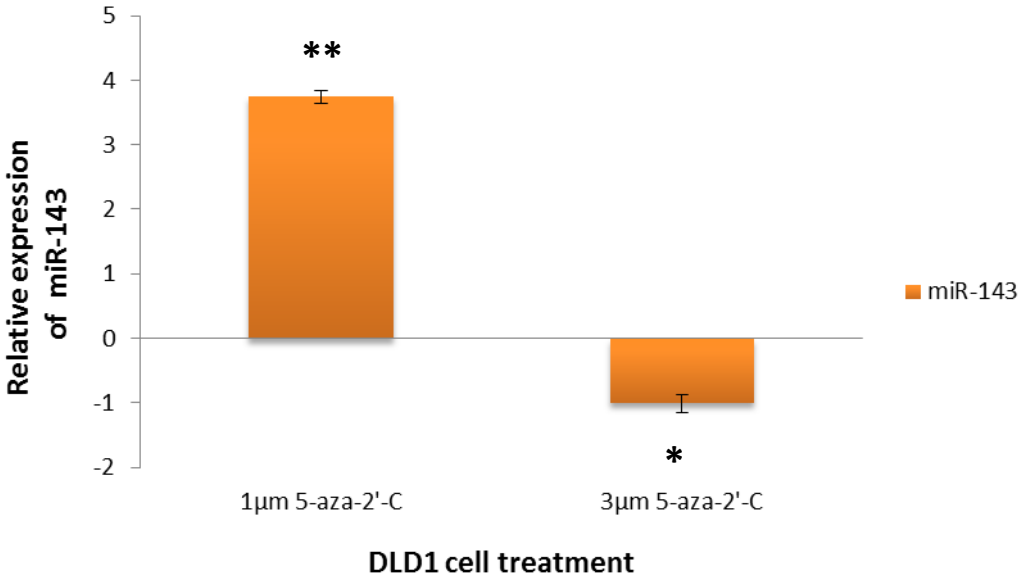

Figure 2.12: Relative expression of miR-143 in DLD1 cells after treatment with 5-Aza-2'-C. Low dose (1µm) yielding an increased expression of miR-143 by 3.7 fold (p=0.005), while high dose (3µm) 5-Aza-2'-C exhibits down-regulation of miR-143 by 1 fold (p=0.0238). Relative expression is shown as log($2^{-\Delta\Delta Ct}$, base 2). * Significant, (p<0.05), ** Very Significant (p<0.01).

MiR-143 expression was assessed in DLD1 cells after treatment with 1µm and 3µm doses of 5-Aza-2'-C for 48 hours (Figure 2.12). Quantification of miR-143 by qRT-PCR revealed that when the DLD1 cells were treated with 1µm 5-Aza-2'-C, the mean decrease in Ct was found to be significant, where t(1)=126.246 and p=0.005 (m=11.804, SD=0.093, n=3), implying that miR-143 was significantly up-regulated by 3.7 fold. In contrast, a mean increase in Ct was found to be significant where t(1)=26.7616 and p=0.0238 (m=3.76, SD=0.14, n=3), indicating that treatment with the higher dose of 3µm resulted in down-regulation of miR-143. When comparing these results to the quantitative results of the effect of 5-Aza-2'-C on miR-143 in the early stage CRC cell line SW1116 (Figure 2.9), it is immediately recognised that in both cell lines miR-143 is more susceptible to 1µm 5-Aza-2'-C than the higher dose of 3µm.

2.3.4.3 *The effect of 5-Aza-2'-C treatment on the expression of miR-145*

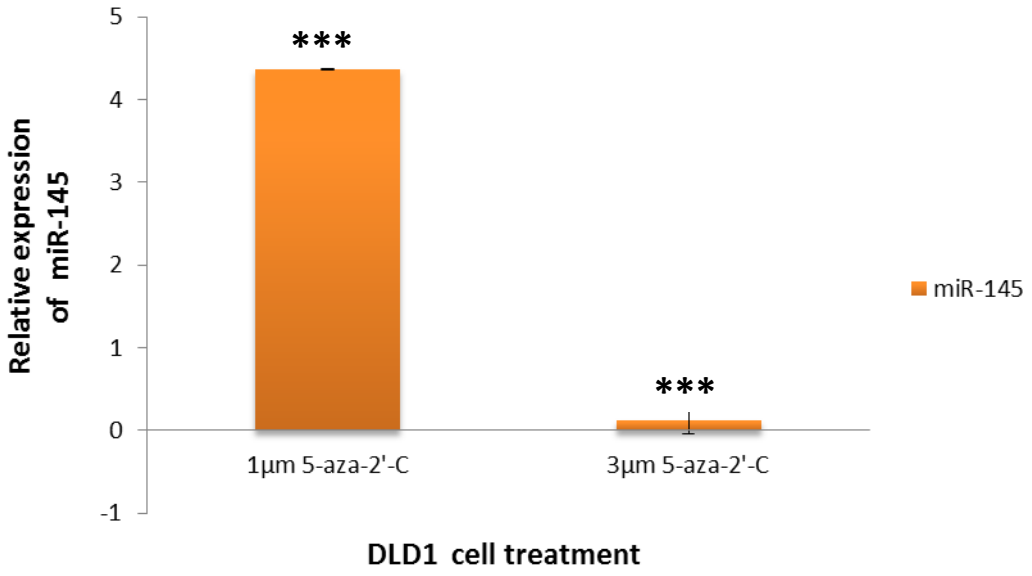

Figure 2.13: Relative expression of miR-145 in DLD1 cells after treatment with 5-Aza-2'-C. Low dose (1µm) yielded an increased expression of miR-145 by 4.3 fold (p=0.001) while high dose (3µm) 5-Aza-2'-C exhibited marginal increase of miR-143 by 0.1 fold (p=0.00001). Relative expression is shown as log ($2^{-\Delta\Delta Ct}$, base 2). *** Extremely significant (p<0.001)

Assessing the relative expression of miR-145 to the untreated controls in DLD1 cells after treatment with 1µm 5-Aza-2'-C revealed a mean decrease in Ct that was found to be significant where t(1)=610.3696 and p=0.001 (m=14.0385, SD-0.023, n=3), substantiating that miR-145 was effectively up-regulated by 4.3 fold relative to the untreated controls. On the other hand, when DLD1 cells were treated with 3µm 5-Aza-2'-C, only a slight increase in the expression of the miRNA was apparent. This result was found to be significant, where t(1)=28.070365 and p=0.00001 (m=0.3275, SD-0.314, n=3). Refer to Figure 2.13 for the illustration of these quantitative results.

2.3.5 The effect of histone de-acetylation on miRNA expression in early stage colorectal cancer

To assess the contribution of histone de-acetylation on the expression of the three miRNAs in question in early stage CRC, SW1116 cells were treated with TSA (300nM) and additionally with the carrier control DMSO. After isolating RNA and subsequent conversion to cDNA by reverse transcription, the samples were subjected to real time PCR to detect relative expression of the miRNAs to the untreated controls. After normalizing, the Ct values to the endogenous control, 18s rRNA, fold changes in expression were calculated according to the method of Livak & Schmittgen, 2001. The sample ΔCt mean values for treatment and untreated samples were compared for statistical significance using a paired two-tailed Student's t-test, with the confidence interval set at 95%.

2.3.5.1 *The effect of TSA on the expression of miR-133b*

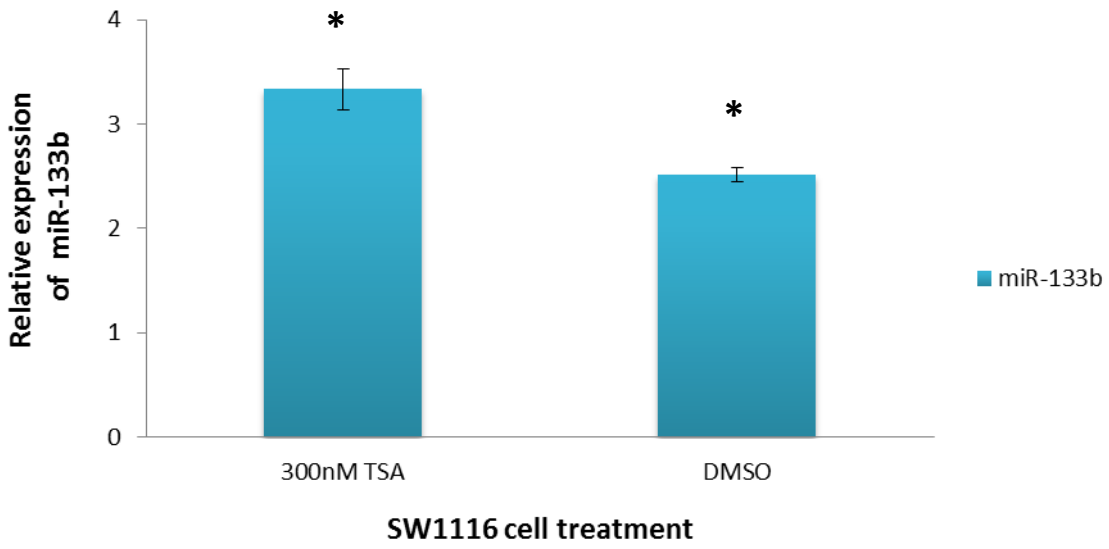

Figure 2.14: Relative expression of miR-133b in SW1116 cells after treatment with TSA. Treatment with the HDACi TSA increased the expression of miR-133b by 3.3 fold (p=0.0353) in comparison to 2.5 fold by DMSO (p=0.0101). Relative expression is shown as log($2^{-\Delta\Delta Ct}$, base 2). * Significant ($p<0.05$)

The impact of histone acetylation on the expression dynamics of miR-133b in early stage colorectal adenocarcinoma was assessed by treating SW1116 cells with 300nM TSA and thereafter quantitatively determining the expression of miR-133b by qRT-PCR (Figure 2.14). The histone de-acetylase inhibitor had significantly increased the expression of miR-133b by 3.3 fold, where t(1)=18.0408 and p=0.0353 (m=10.175, SD=0.564, n=3). To eliminate the effects of the carrier control, DMSO, on the result received by the treatment of TSA, a DMSO control was assessed for expression of miR-133b. As shown in Figure 2.11, DMSO had induced a significant increase in miR-133b expression by 2.5 fold, where t(1)=62.7744 and p=0.0101 (m=8.349, SD=0.133, n=3). Although DMSO had also induced expression of the miR-133b, this was 0.8 fold less than the expression for miR-133b after treatment with 300nM TSA. The net result of TSA treatment remains an up-regulation of miR133-b expression.

2.3.5.2 *The effect of TSA on the expression of miR-143*

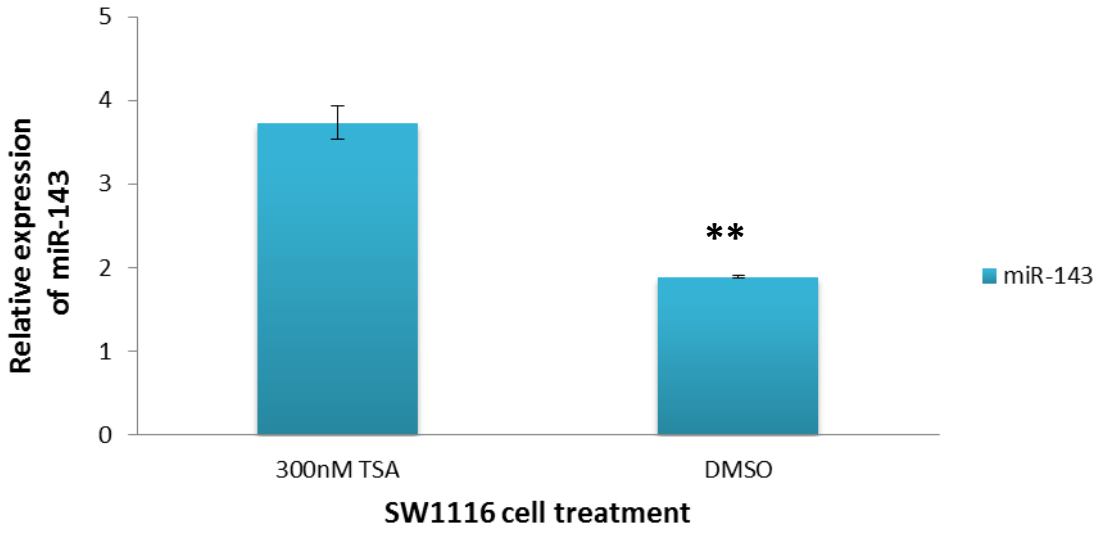

Figure 2.15: Relative expression of miR-143 in SW1116 cells after treatment with TSA. Treatment with the HDACi TSA increased the expression of miR-143 by 3.7 fold (p=0.0759, not significant) in comparison to 1.8 fold by DMSO treatment (p=0.0028). Relative expression is shown as $\log(2^{-\Delta\Delta Ct}$, base 2). **Very significant (p<0.01)

To assess the impact of histone de-acetylation on miR-143 expression in early stage colorectal adenocarcinoma, SW1116 cells were treated with 300nM TSA for 24 hours, after which miR-143 was quantified by qRT-PCR (Figure 2.15). It was determined that relative to the no treatment controls, when the cells were treated with 300nM TSA, miR-143 had increased in expression by 3,7 fold (where t(1)=8.3488 and p = 0.0759 (m=12.0765, SD=1.446, n=3). Despite not being a significant correlation, DMSO alone only increased the expression of miR-143 by 1.8 fold, almost 1.9 fold less than that of 300nM TSA. The quantification of miR-143 post treatment with DMSO was found to be significant where t(1)=227.9091 and p=0.0028 (m=6.2675, SD=0.027, n=3). The results indicate that TSA treatment of SW1116 cells yielded a net upregulation of miR-143 by 1.9 fold.

2.3.5.3 *The effect of TSA on the expression of miR-145*

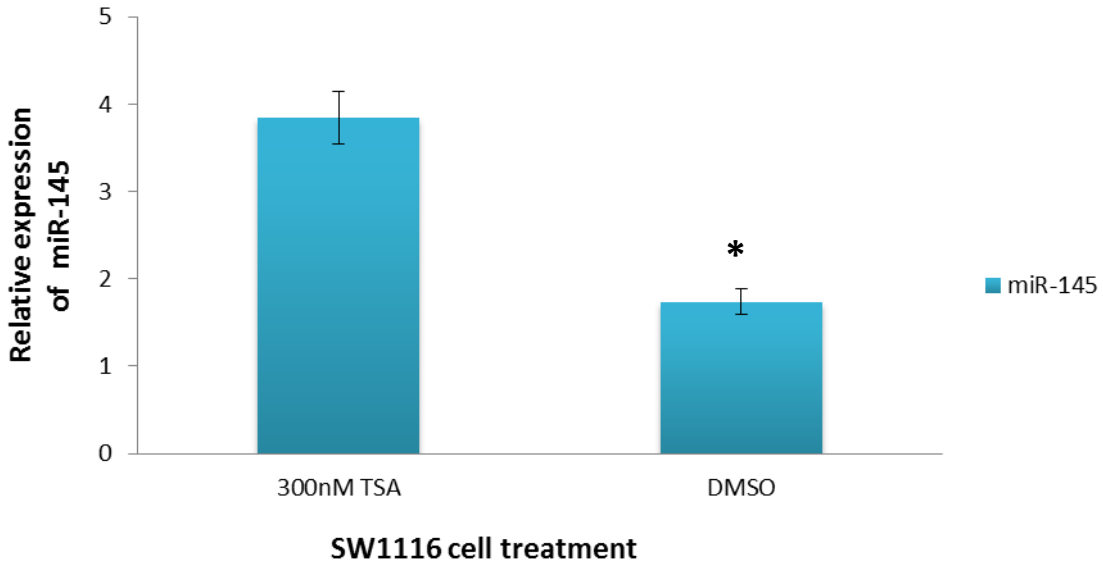

Figure 2.16: Relative expression of miR-145 in SW1116 cells after treatment with TSA. Treatment with the HDACi TSA increased the expression of miR-145 by 3.8 fold (p=0.0508, not significant) in comparison to 1.7 fold with DMSO (p=0.0332). Relative expression is shown as log($2^{-\Delta\Delta Ct}$,base 2). *Significant (p<0.05).

When SW1116 cells were treated with TSA and its effect on the expression of miR-145 was quantified, a similar expression pattern to miR-143 (Figure 2.15) was realised. Treatment with 300nM TSA resulted in a mean decrease in Ct, where t(1)=12.5174 and p=0.0508 (m=11.178, SD=0.893, n=3), providing evidence that treatment with TSA demonstrates a trend of up-regulation of miR-145 by 3.8 fold, relative to the no treatment control. DMSO treatment alone had induced the expression of miR-145 by 1.7 fold, where t(1)=19.1536 and p=0.0332 (m=5.7365, SD=0.3, n=3), yielding a significant result that is approximately 2 fold lower than the TSA treatment inclusive of DMSO. This result indicates a net up-regulation of miR-145 after treatment of 300nM TSA by about 2 fold from the no treatment controls. (Figure 2.16)

2.3.6 The effect of histone acetylation on miRNA expression in late stage colorectal cancer

The effect of histone acetylation in late stage CRC was assessed by treating DLD1 cells with 300nM TSA and the DMSO carrier control after which the three miRNAs in question, miR-143, 145 and 133b, were quantified by miRNA qPCR, relative to the no treatment controls. Mean Ct values for triplicate samples were analysed for fold change and subjected to a paired two-tailed Students t-test to evaluate the statistical significance with the confidence interval set at 95%.

2.3.6.1 *The effect of TSA on the expression of miR-133b*

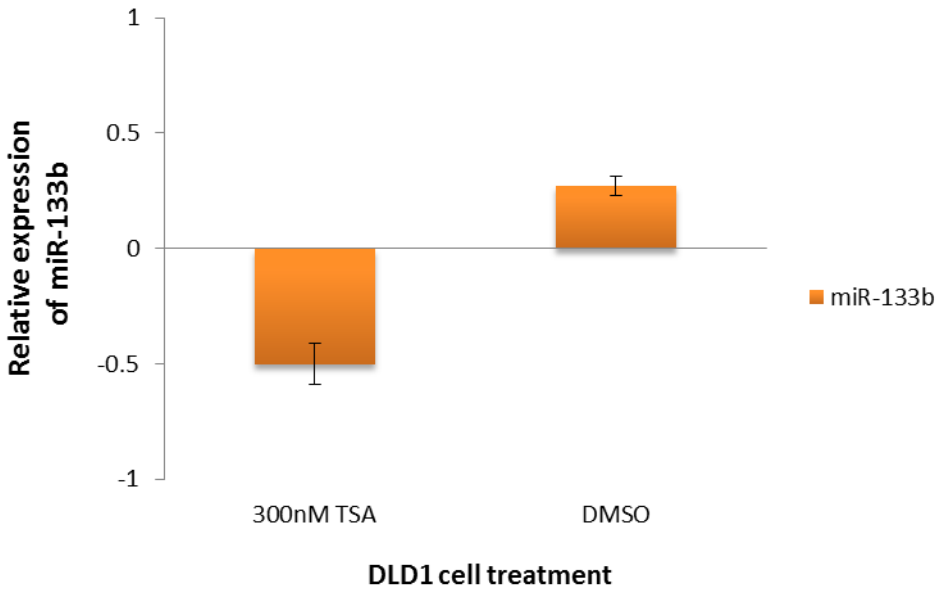

Figure 2.17: Relative expression of miR-133b in DLD1 cells after treatment with TSA. Treatment with the HDACi TSA decreased the expression of miR-133b by 0.5 fold (p=0.32, not significant). DMSO treatment increased miR-133b expression by 0.2 fold (p=0.1171, not significant). Relative expression is shown as $\log(2^{-\Delta\Delta Ct}$, base 2).

During late stage colorectal adenocarcinoma by virtue of DLD1 cells, miR-133b expression was assessed after treatment with 300nM TSA and the carrier control

DMSO (Figure 2.17). An antagonistic relationship between the treatment with TSA and miR-133b is demonstrated whereby treatment with TSA resulted in a mean increase in Ct, exhibiting a decrease in miR-133b expression by 0.5 fold from the no treatment control [t(1) = 1.8189, p=0.32 (m=-1.6725, SD=0.919, n=3)]. This effect seems to be independent of the DMSO vehicle, as DMSO alone had demonstrated a mean decrease in Ct, where t= 5.3758, *p*=0.1171 (m=0.887, SD=0.165, n=3), showing increased expression of miR-133b by 0.26 fold.

2.3.6.2 *The effect of TSA on the expression of miR-143*

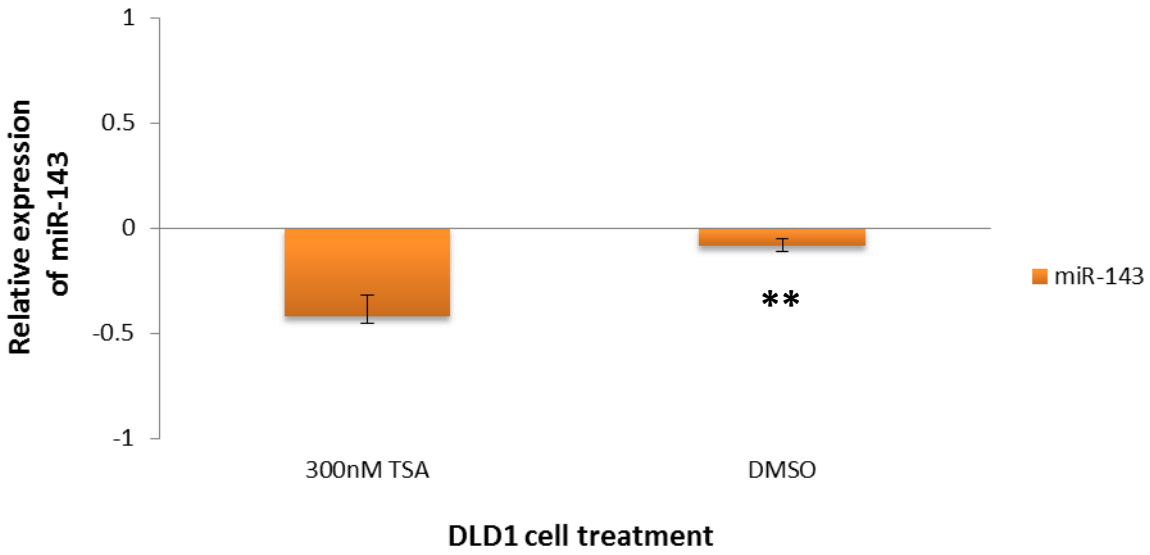

Figure 2.18: Relative expression of miR-143 in DLD1 cells after treatment with TSA. Treatment with the HDACi TSA decreased the expression of miR-143 by 0.4 (*p*=0.3277, not significant) fold while DMSO treatment decreased miR-143 expression by 0.08 fold (*p*=0.007515). Relative expression is shown as log($2^{-\Delta\Delta Ct}$,base 2). ** Very Significant (*p*<0.01).

MiR-143 expression in late stage colorectal adenocarcinoma after treatment with 300nM TSA revealed a result reminiscent of the effect of the epigenetic drug treatment on miR-133b (see Figure 2.17). As depicted in Figure 2.18, miR-143 had decreased by 0.4 fold relative to the no treatment. This mean increase in Ct was found to be non-significant where t(1)=1.7683 and *p*=0.3277 (m=-1.038, SD=0.587, n=3). This result was also found to be independent of the DMSO carrier molecule.

Treatment with DMSO alone had significantly decreased miR-143 expression by 0.08 fold, where t(1)=6.463078 and *p*=0.007515 (m=-0.9665, SD=0.252, n=3). Thus here, the observed decrease in miR-143 was specifically in response to the treatment with TSA.

2.3.6.3 *The effect of TSA on the expression of miR-145*

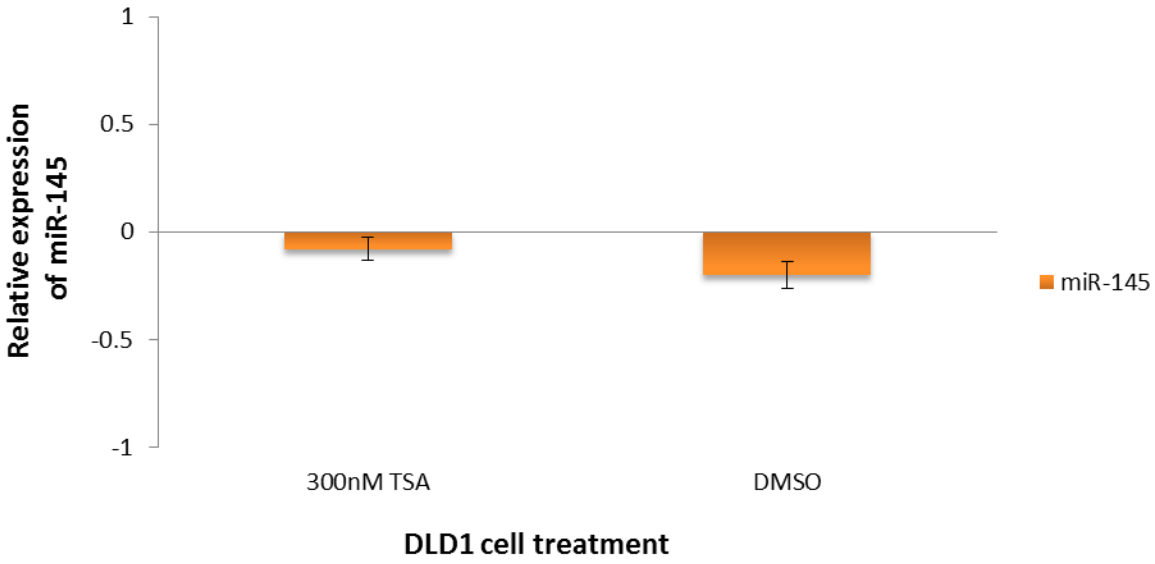

Figure 2.19: Relative expression of miR-145 in DLD1 cells after treatment with TSA. Treatment with the HDACi TSA decreased the expression of miR-145 by 0.07 (*p*=0.6591, not significant) fold whereas DMSO treatment alone decreased miR-1245 expression by almost 0.2 fold (*p*=0.3383, not significant). Relative expression is shown as log($2^{-\Delta\Delta Ct}$,base 2).

MiR-145 expression in late stage colorectal adenocarcinoma was also found to be marginally affected by the treatment with 300nM TSA. The mean Ct was slightly increased compared to the no treatment control, where t(1)=0.5934 and p=0.6591 (m=-0.1255, SD=0.211, n=3). Therefore miR-145 expression decreased slightly by 0.07 fold, relative to the no treatment control. It is however questionable whether this result was caused by TSA, as the DMSO carrier control exhibited a mean increase in

Ct, where t(1)=1.7012 and *p*=0.3383 (m= -0.427, SD=0.251, n=3). An almost 0.2 fold decrease in expression was noted with the treatment of DMSO alone (Figure 2.19).

2.4 Discussion

The consistent pattern of downregulation of miRNAs -143, -145 and -133b in CRC and several other cancers proposes these miRNAs as potential targets of epigenetic regulation. To evaluate the effect of epigenetic regulation by virtue of DNA methylation and histone acetylation on the expression of these CRC associated miRNAs, the colorectal adenocarcinoma cell lines SW1116 and DLD1, representing an early and late stage of CRC, respectively, were treated individually with one of two categories of epigenetic drugs, either a DNA demethylating agent, 5-Aza-2'-C or a HDACi, TSA.

2.4.1 Appropriate use of cell lines

The use of established cancer cell cultures remains the most accessible and reproducible *in vitro* method for cancer research purposes (Kao *et al.*, 2009). For this study the CRC cell lines SW1116 and DLD1 were selected as they represent distinct yet progressive stages of CRC tumours. SW1116 cells are a Dukes' stage A, Grade III colorectal adenocarcinoma obtained from a 73 year old Caucasian male. The DLD1 cells are a Dukes' stage C colorectal carcinoma from a Caucasian adult male. The use of these two disparate stages allows for the evaluation of the response of early and late stage tumours to the aforementioned pharmacological treatments.

The classification of CRC was first devised by the pathologist Cuthbert Dukes, a British pathologist (Dukes, 1932). The classification system, evidently termed Dukes' staging, classifies colorectal tumours into four stages, from A-D. Stage A (SW1116) refers to tumours that are confined to the mucosa. Stage B is represented by tumours invading the bowel wall and penetrating the muscle layer, however without any involvement of lymph nodes. Stage C (DLD1) CRC tumours present with lymph node involvement and Stage D is depicted by tumours with widespread metastasis. The Dukes' staging classification is however outdated in clinical practice and has

been replaced by the more detailed TNM staging. Refer to Figure 2.20 below which describes the associated TNM classification for the SW1116 and DLD1 cell lines.

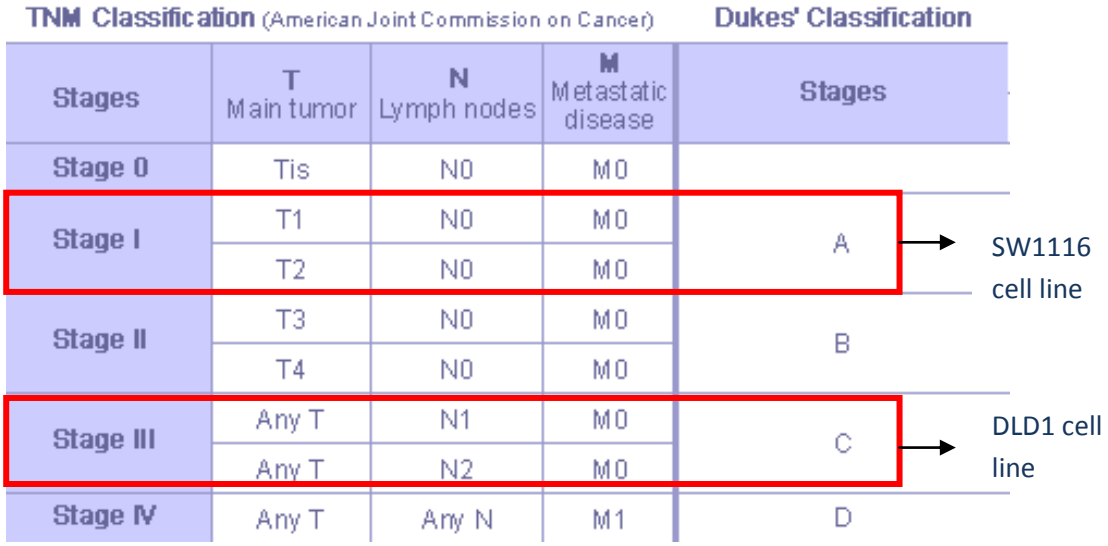

Figure 2.20: TNM staging *vs* Dukes Staging. TNM staging has been formulated by the American Joint Commission on Cancer. The more detailed TNM staging has replaced the outdated Dukes staging. Key: Tis = carcinoma *in situ,* T0= no primary tumour evidence, T1 = tumour has invaded the submucosa, T2 = tumour has penetrated the muscularis propria, T3 = Tumour has invaded subserosa and into peritonalised pericolic or perirectal tissues, T4 = the tumour invades other organs or structures and/or piercing the visceral peritoneum. N0 = no evidence of metastasis to any lymph nodes, N1 – one to three lymph node involvement, N2 – metastasis to four or more lymph nodes. M0 = no evidence of distant metastases, M1=distant metastases present (Hopkins Colon Cancer Center, 2015).

Cancer cell lines have also been reported to be suitable *in vitro* models to study epigenetic features of cancer (Ferreira *et al.*, 2013). To allow for an accurate analysis of the assays conducted with these cell lines, it is important to understand the molecular characteristics of each cell line. The established characteristics for the SW1116 and DLD1 cell lines are outlined in Table 2.7.

Table 2.7: Genetic and Epigenetic features of SW1116 and DLD1 cell lines.[3]

SW1116 cell line	DLD1 cell line
Dukes' Stage A/Stage I	Dukes' Stage C/Stage III
MSS (Microsatellite Stable)/CIN +	MSI (Microsatellite Instable)/CIN -
*CIMP Panel 1 +	CIMP Panel 1 +
**CIMP Panel 2 -	CIMP Panel 2 +
KRAS mutant [G12A]	KRAS mutant [G13D]
wt BRAF	wt BRAF
wt PIK3CA	PIK3CA mutant [E45K; D549N]
wt PTEN	wt PTEN
TP53 mutant [A159D]	TP53 mutant [S241F]

(Adapted from Ahmed *et al*., 2013)

2.4.2 The effect of DNA demethylation on cell viability in early and late stage colorectal cancer

As a first approach here, cell viability of each cell line was assessed following treatment with 5-Aza-2'-C, since it has previously been shown to suppress tumour cell line growth (Bender *et al*., 1998). This served to indicate the effects of DNA demethylation on the *in vitro* growth of the early and late stage CRC cells. Foreseeably, DLD1 cells displayed decreased cell viability in a dose dependent manner upon treatment with 5 aza-2'-C. However, in the SW1116 cells although there was a marginal increase in the percentage cell viability at the lower dose of 1µm 5-Aza-2'-C, there was nevertheless a slight decrease in cell viability at the higher dose (3µm) of 5-Aza-2'-C.

The non-susceptibility of SW1116 cells to 5-Aza-2'-C is inconsistent with published literature reporting on the antitumour effects of 5-Aza-2'-C. Although the mechanisms whereby 5-Aza-2'-C accomplishes its anti-tumour effects are not fully

[3] *CIMP Panel 1+ indicates mutations in CDKN (p16), MINT 1, MINT 2, MINT 31 and MLH1

**CIMP Panel 2+ indicates mutations in CACNA1G, IGF2, NEUROG1, RUNX3 and SOCS1

elucidated. The first postulated mechanism of cytotoxicity relates to the reactivation of aberrantly silenced genes that ultimately function to control and regulate cell proliferation and apoptosis. The second idea relates to the treatment with 5-Aza-2'-C being recognised as DNA damage due to the covalent DNMT-DNA adducts that form, following which the DNA damage response pathways would then be responsible for the cytotoxic effects (Palii *et al.*, 2008).

A key difference in the characteristics of the two cell lines is that DLD1 cells are microsatellite instable (MSI), whereas SW1116 cells are microsatellite stable (MSS) (see Table 2.7; Ahmed *et al.*, 2013). SW1116 cells being microsatellite stable (MSS) indicates the presence of unstable chromosome translocations with gains or losses of whole chromosomes as described in Chapter 1.2 (Lengauer *et al*., 1998). Generally this transient instability of the chromosomes occurs early in the development of cancer which is likely the case as SW1116 represents Dukes' Stage A or Stage I of CRC.

As already mentioned in Chapter 1.2, the MSI phenotype is characterised by deficiencies in the DNA mismatch repair (MMR) pathway specifically as a result of mutation or hyper-methylation of the MLH1, MSH2 or MSH6 genes (Peltomaki *et al.*, 2001). The susceptibility of DLD1 cells to 5-Aza-2'-C as shown here is potentially a result of reactivated MLH1, which is aberrantly silenced by hyper-methylation in MSI CRC. It has previously been reported that 5-Aza-2'-C treatment was able to re-express MLH1 in the colon cancer xenograft SW48 (MSI) in which MLH1 was silenced through promoter hyper-methylation (Plumb *et al*., 2000). Moreover, this re-expression of MLH1 sensitised the xenografts to several chemotherapeutic agents.

MLH1 is known to induce apoptosis and cell cycle arrest in response to DNA damage, by signalling for p53 mediated apoptosis. MLH1 p53-independent apoptosis mediated by c-Abl/p73α/GADD45α has also been reported (Fukuhara *et al.*, 2014). This p53-independent apoptotic pathway may be relevant to DLD1 cells should MLH1 be reactivated after treatment with 5-Aza-2'-C as DLD1 cells are carriers of a p53 mutation, a common feature of MSI CRC (Ahmed *et al.*, 2013). Confirmation of

apoptosis in response to 5-Aza-2'-C treatment however has not been determined in this study and would require further analysis.

In addition to MLH1, promoter hyper-methylation of p16 has also been demonstrated in MSI CRC which also associates with advanced Dukes' staging, such as DLD1 cells (Shannon *et al.*, 2001). P16 is a cyclin-dependent kinase inhibitor and functions as a tumour suppressor by binding and inactivating cyclin D-cyclin-dependent kinase 4 thereby inactivating the Retinoblastoma protein which blocks transcription of cell cycle genes and which ultimately triggers cell senescence (Ligget *et al.*, 1998).

In summary, the MSI CRC cell lines such as DLD1 are more susceptible to treatment with 5-Aza-2'-C potentially through the reactivation of silenced tumour suppressor genes. The differential susceptibility demonstrated by SW1116 cells concurs with the evidence that MSI tumours are likely to show higher levels of methylation than MSS tumours; and also that increased methylation is associated with a more advanced tumour stage (Hawkins *et al.*, 2002).

2.4.3 The effect of histone acetylation on cell viability in early and late stage colorectal cancer

In keeping with the ability of epigenetic modulators to inhibit proliferation of cancer cells, cell viability assays post treatment with TSA was performed for both cell lines. TSA treatment at concentrations of 300nM for 24 hours potently decreased the viability of both early (SW1116) and late (DLD1) stage CRC cell lines. DMSO was used as a TSA drug vehicle to enable cellular access of the HDACi. DMSO however has also been found to alter gene expression, cell morphology and cell viability in a dose dependent manner (Pal *et al.*, 2012). To determine whether the cytotoxic effects were an independent result of TSA treatment, cell viability after treatment solely with an equivalent DMSO concentration was also assessed. The resulting decrease in cell viability in response to DMSO treatment was much lower in both cell lines in comparison to TSA, indicating here that TSA is responsible for cell death in early and late stage CRC cell lines.

These results are not unexpected as HDACi's have long been known and appreciated to induce cell cycle arrest and cell death in cancer cells (Dokmanovic *et al*., 2007). TSA in particular causes cell cycle arrest in the G1 and G2 cell cycle phases (Yoshida *et al.*, 1988). In addition, TSA treatment has been shown to upregulate proteins that are pro-apoptotic and downregulate proteins that repress apoptosis (Meng *et al.*, 2012; Liu *et al.*, 2013; Duan *et al.*, 2005; Kim *et al.*, 2006; Moore *et al.*, 2004). Cell death induced by HDACi has been characterised by several mechanisms as depicted in Figure 2.21 below. Apoptosis was induced *via* the intrinsic (Duan *et al.*, 2005) and extrinsic (Kim *et al.*, 2006) pathways upon inhibition of HDAC. In addition, HDACi treatment can also induce autophagic cell death; autophagy is a catabolic pathway in which proteins and organelles in the cytoplasm are sequestered into vacuoles and transported to the lysosome for degradation and recycling (Rikiishi, 2011). Another mechanism of HDACi induced cell death is through mitotic catastrophe caused by alterations in G2M checkpoint gatekeeper proteins, DNA repair mechanisms and alterations in proteins involved in mitotic spindle formation and chromosome segregation during mitosis (Cornago *et al.*, 2014). Treatment with HDACi is also associated with senescence, an irreversible halt on cell division (Vargas *et al.*, 2014), and cell death facilitated by an increase in reactive oxygen species (ROS) (Ungerstedt *et al.*, 2004).

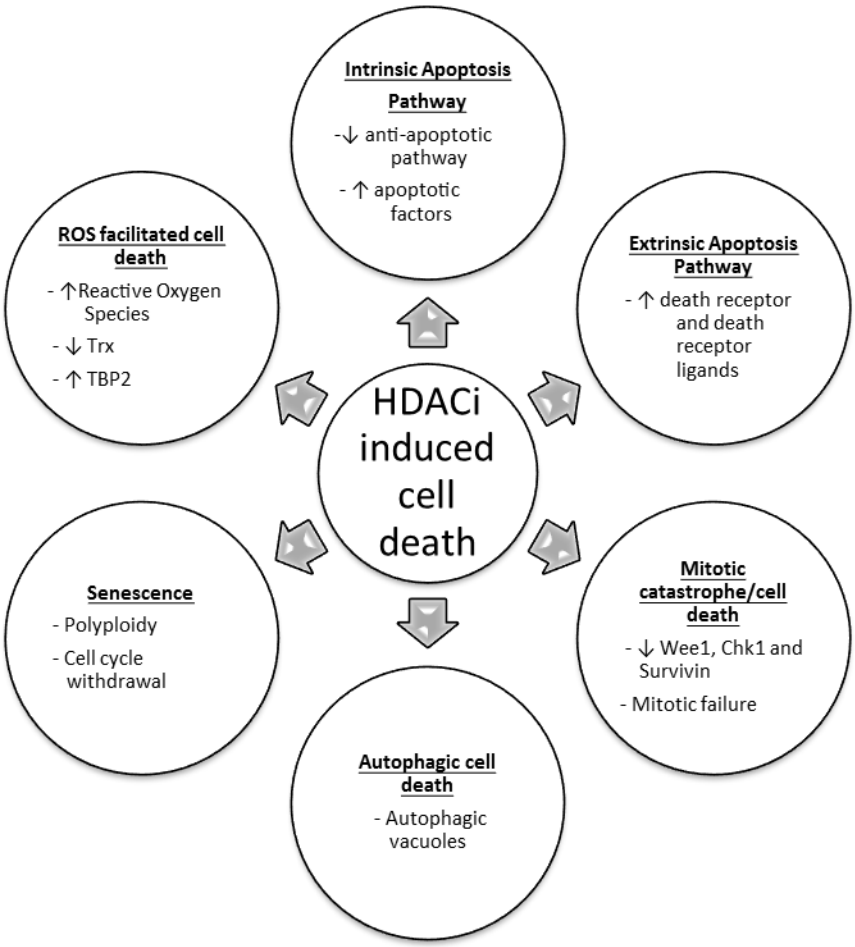

Figure 2.21: HDACi induced cell death. HDACi mediates cell death through various pathways, including the intrinsic and extrinsic pathway, mitotic catastrophe, autophagy, senescence and ROS facilitated cell death (Adapted from Xu, *et al*., 2007).

In CRC TSA has demonstrated cytotoxicity in various ways. Chen *et al.* in 2004 elucidated the growth inhibitory role that TSA plays in SW1116 cells. TSA had induced G1 phase arrest in SW1116 cells and had demonstrated a significant increase in p21(WAF1) expression. In addition, it was shown that Histones 3 and 4 in the chromatin associated with the p21 (WAF1) gene was acetylated, indicating a direct effect of TSA and histone acetylation on the expression of p21(WAF1). P21 (WAF1) functions as a CDK inhibitor and therefore limits the progression of the cell cycle. An intimate relationship between p21 (WAF1) and p53 has been documented thoroughly in which p53 mediates growth arrest, following DNA damage, by inducing

p21 (WAF1) which in turn alters DNA replication by forming complexes with PCNA (proliferating cell nuclear antigen), an auxiliary factor to DNA Polymerase δ and ε, a preceding event to altering DNA replication (Xiong *et al.*, 1992). SW1116 and DLD1 cells are however p53 deficient and therefore the induction of p21 (WAF1) in SW1116 cells would indicate alternative mechanisms that are independent of the relationship with p53. P53 independent induction of p21 has been reported despite the mechanisms not being fully elucidated (Macleod *et al.*, 1995). One potential path of p21 (WAF1) activation in a p53 deficient environment is through STAT1 (Chin *et al.*, 1996). Another described mechanism of p21 (WAF1) induction is through histone deacetylases. HDAC3 is overexpressed in colon cancer and has been found to regulate the expression of p21 (WAF1) in an inverse proportional manner (Wilson *et al.*, 2006). Furthermore, HDAC inhibitors have been reported to directly induce p21 (WAF1) by hyperacetylation of histones in the chromatin region around the p21 (WAF1) promoter (Richon *et al.*, 2000). These two mechanisms are potentially the cause of the potent reduction in cell viability.

In the present study, when comparing the effect of DNA demethylation *versus* that of histone deacetylase inhibition on the cell viability in both cell lines, it is evident that TSA decreases the cell viability in both cell types more so than DNA demethylation, this possibly being due to various cell death pathways being initiated (see Fig. 2.21 above).

2.4.4 The stage specific effect of DNA demethylation on the expression of miRNAs

All three miRNAs in question had demonstrated clear upregulation in both cell lines upon treatment with 5-Aza-2'-C at the lower dosage of 1µm. The susceptibility of miRNAs in both cell lines to 5-Aza-2'-C was however much less at a higher dosage of 3µm with the DLD1 cell line showing the least susceptibility of the miRNAs to the higher dose, where downregulation patterns of miR-133b and miR-143 were obtained. A negligible change was also achieved for miR-143 in SW1116 cells in

response to the higher dose. These results demonstrate a dose sensitive response to the DNA demethylating agent 5-Aza-2'-C, wherein miRNAs are upregulated at low doses of 5-Aza-2'-C.

The initial use of 5-Aza-2'-C as a therapeutic anti-tumour agent was assessed at the maximum tolerated dose in several cancers and the result was of high toxicity and low efficacy, with exceptions in Myelodysplastic Syndrome (MDS) and Acute Myeloid Leukaemia eventually leading to its approval by the FDA for treatment of MDS (Kantarjian *et al.*, 2006). Increased efficiency of the "pro-drug" was however recognised only when low transient doses were used (Wijermans *et al.*, 1997; Wijermans *et al.*, 2000; Tsai *et al.*, 2012). In the present study, the susceptibility of the miRNAs to the lower dose concurs with this finding. It is thought that the low dosage levels induce more hypomethylation, while the higher doses induce more cytotoxicity which confounds the effects of DNA demethylation. This was also supported by the evidence that 5-Aza-2'-C treatment produces a U-shaped hypomethylation response curve, which indicates that DNA hypomethylation levels increase with increasing doses of 5-Aza-2'-C until a point at which it reaches a trough of maximum hypomethylation, after which with increasing doses the hypomethylation effect decreases (Qin *et al.*, 2009). If it is verifiable that the lower doses of the DNA demethylating agent are more able to re-express silenced tumour suppressor genes in CRC, then the present result achieved here is indicative that at 1µM the miRNAs are transcriptionally activated by DNA demethylation. This could be directly through removal of methyl groups from the promoter regions of each miRNA, or indirectly through the activation of transcription factors that are themselves reactivated through DNA demethylation and are involved in miRNA-transcription factor feedback regulation loops. To confirm if the miRNA activation is through the direct effect of DNA demethylation of CpG islands in the promoter regions, sequencing of bisulfite modified DNA coupled with methylation specific PCR will need to be completed pre- and post- treatment with 5-Aza-2'-C.

A previous study has determined that miR-145 is repressed by DNA methylation in which the promoter region was found to be hypermethylated in prostate cancer cells and various other cell lines (Suh *et al.*, 2011). In the study, it was also determined

that downregulation of miR-145 in tumour cell lines was highly correlated with cell lines containing p53 mutations. Furthermore, miR-145 has also recently been found to be epigenetically silenced by promoter hypermethylation in oesophageal carcinoma (Harada *et al.*, 2015). Although Suh *et al.* (2011) had also reported miR-145 promoter methylation in several colon cancer cell lines, interestingly the SW1116 cell line was found to be negative for miR-145 methylation. In the same study the HT29 and SW620 colorectal cell lines were also tested and found to be positive for miR-145 methylation. HT29 and SW620 cell lines are both Dukes' Stage C and have p53 mutations, resembling the molecular characteristics of DLD1 cells. It is possible that DLD1 cells are positive for miR-145 methylation, which could explain the increased susceptibility of miR-145 in DLD1 cells, when compared to SW1116 cells in response to 5-Aza-2'-C.

MiR-145 and miR-143 are polycistronic miRNAs, indicating that they are transcribed from the same promoter (Iio *et al.*, 2010). This would signify that the promoter methylation status should impact both miRNAs. Silencing of miR-143 *via* promoter methylation has only been reported thus far in MLL-AF4 acute lymphocytic leukaemia (Dou *et al.*, 2012). In the present study, although both miRNAs were induced by 1µM 5-Aza-2'-C, these were at varying levels. These differential levels of induction of both miRNAs by 5-Aza-2'-C could be explained by post-transcriptional regulation of the miRNA maturation process. P53 has been demonstrated to be involved in inducing the expression of the miR-143/145 cluster in a transcription-independent manner; however as SW1116 and DLD1 cells are p53 deficient, it could be assumed that a different transcription factor may be involved in the post transcriptional maturation of the miRNAs (Suzuki *et al.*, 2009).

MiR-133b expression, also induced by 5-Aza-2'-C in this study in both cell lines at the lower dose and only in SW1116 cells at the higher dose, correlates with the recent finding by LV *et al.* (2015) who reported that miR-133b promoter hypermethylation is causal for its low levels in CRC. No further evidence has been determined regarding epigenetic regulation of miR-133b.

When comparing early *versus* late stage CRC expression of miRNAs after 5-Aza-2'-C treatment, all miRNAs are more responsive to the lower dose of 5-Aza-2'-C in DLD1 cells compared to SW1116 cells. For miR-145 this could be explained by the discrepancy in the promoter hypermethylation at different stages as indicated by the lack of promoter hypermethylation in SW1116 cells and the presence of miR-145 methylation in several Dukes' stage C/p53 mutant CRC cell lines (Suh *et al.*, 2011).

Another potential reason for a discrepancy in susceptibility is that 5-Aza-2'-C is an S-phase acting drug which means that it induces its effect in cells that are actively replicating. SW1116 is a slow growing cell line with a higher doubling time than DLD1 cells. Thus it may be assumed that the SW1116 cells have a proportionately lower ratio of cells in the S-phase than DLD1 cells at a given time point. Considering that the treatment times were the same for both cell lines, a discrepancy in DNA demethylation levels could explain the lower levels of upregulation of miRNAs in the SW1116 cell line. This would need to be confirmed by measuring the methylation levels of the cell line pre- and post- treatment with 5-Aza-2'-C.

In addition to the above, miRNA signatures have been insinuated to discriminate between MSI *versus* MSS colorectal tumours (Lanza *et al.*, 2007). Although this initial study did not report on differential patterns between miR-145, -143 and -133b in MSI as opposed to MSS CRC, a later study in 2011 by Balaguer *et al.*, demonstrated that all three miRNAs were differentially expressed in MSI *versus* MSS CRC by 1.5 fold or more. Whether the differential patterns of miRNA expression between the two cell lines is due to DNA methylation is a matter of question. However if this may be the case, it would explain at least in part the differences that have been recognised in the SW1116 cells *versus* the DLD1 cells.

When comparing the responsiveness of each miRNA to the DNA demethylating agent, it is evident that miR-145 is most susceptible to DNA demethylation, followed by miR-143 and then miR-133b. This pattern is consistent regardless of the stage of the cancer cell line and therefore it may be assumed that the miRNA regulation occurs in the same manner in both the early and late stage CRC cells, with the likely cause being DNA methylation.

2.4.5 The stage specific effect of histone acetylation on the expression of miRNAs

In the early stage CRC cells, all three miRNAs were induced by over 3 fold, following a 24 hour treatment with TSA. The miRNAs were also upregulated by DMSO by approximately 2 fold. Overall a net upregulation by 0.82, 1.85 and 2.11 for miR-133b, miR-143 and miR-145, respectively can be seen. In comparison TSA does not seem to induce miRNA expression in the late stage CRC cell line, showing slight levels of downregulation. This trend was also evident in the DMSO carrier control in DLD1 cells, for miR-143 and miR-133b and with only slight upregulation of miR-145. From this it would seem that the susceptibility of these miRNAs to the HDACi appears to be dependent upon the stage of the cell line.

In the study by Zaman *et al.* in 2010, in which miRNA expression was detected after treatment of late stage metastatic prostate cancer cell lines with 5-Aza-2'-C, TSA and 5-Aza-2'-C plus TSA, miR-145 had only increased significantly with treatments containing 5-Aza-2'-C, while a minimal effect was shown for miR-145 expression upon treatment with TSA alone. This is similar to the results reported in this study, whereby late stage cells showed no effect on miR-145 when treated with TSA. However, significant upregulation of the miRNA is attained after treatment with 5-Aza-2'-C. Similarly, miR-143 was upregulated in TSA treated early stage SW1116 cells. This finding agrees with raised levels of miR-143 reported in the non-invasive early stage MCF7 breast cancer cell line, upon treatment with TSA alone (Rhodes *et al.*, 2012). In comparison, mir-133b expression increased in the Dukes' stage C (late stage) cell lines, HT29 and SW620, following TSA treatment (Lv *et al.*, 2015); thereby diminishing the correlation between the susceptibility of the miRNAs to TSA and cell staging.

In studies where tumours were treated with HDACi's, researchers became aware of a phenomenon in which cells would acquire resistance to the HDACi (Fedier *et al.*, 2007; Dedes *et al.*, 2009). Imesch *et al.* in 2009 had further determined that resistance to TSA in colon cancer cells is caused specifically by a deficiency in the MLH1 gene, as the acquired resistance was only present in MSI cells. As mentioned

previously the MLH1 gene is involved in DNA repair and its silencing by promoter hypermethylation characterises MSI cells. Resistance to TSA in MSI colon cancer cells was also accompanied with a loss in the accumulation of histone acetylation, lack of p21 induction and reduced apoptotic ability (Imesch *et al*., 2009). In the present study, this could potentially explain why TSA had no effect on miRNA expression, as the loss in histone acetylation would ultimately not allow for the re-expression of silenced tumour suppressor genes due to enduring condensed chromatin formation. Moreover, the DMSO treated DLD1 cells lacked a response to TSA, unlike the DMSO induced miRNA expression in the SW1116 cells. It may be that DLD1 cells could be resistant to TSA at the concentrations used in this study. A relationship between DMSO and miRNA expression in MSI cells has not as yet been elucidated and may merit further investigation.

2.4.6 Comparison of DNA demethylation *versus* histone acetylation on expression of miRNAs

In the early stage CRC cell line SW1116, DNA demethylation seems to have a moderate influence on the expression of miRNA, this taking into account the expression of all three miRNAs post-treatment with the low dose 5-Aza-2'-C. MiRNA expression levels increased significantly in the late stage DLD1 cells for all miRNAs. A higher frequency of promoter DNA hypermethylation of all three miRNAs is a plausible justification of the increased induction of the miRNAs in DLD1 cells. This may well relate directly to the adenoma to carcinoma sequence postulated by Fearon and Vogelstein in 1990, which alluded to the accumulation of genetic and epigenetic alterations in a stepwise manner in the transformation from normal colon epithelium to adenocarcinoma. More specifically, an accumulation of DNA methylation through the transformation process is highlighted in this model. Thus it follows that DLD1 late stage CRC cells have a higher degree of DNA methylation than SW1116 cells. This could explain the tendency of the miRNAs to be more highly induced in DLD1 cells compared to SW1116 cells when treated with the DNA demethylation agent. This concept is further supported by Frigola *et al.* (2005) who demonstrated that carcinoma cells contained increased hypermethylation levels

compared to adenomas. Further to this, several tumour suppressor genes were shown to be more frequently methylated in advanced stages of colon cancer; p16 methylation occurs more in Dukes' stage C and D than in Dukes' stage A and B (Yi *et al.*, 2001); CDKN2A hypermethylation is more prevalent in Dukes' stage C (Maeda *et al.*, 2003); DKK1 is selectively hypermethylated in advance CRC neoplasms (Aguilera *et al.*, 2006); and miR-143 was also proven to be expressed at its lowest level in advanced stage cancer associated with lymph node metastasis (Qian *et al.*, 2013) . In addition miR-133b had lower expression levels in late as compared to early stages of cancer (Duan *et al.*, 2013).

In the present study, when compared to 5-Aza-2'-C treated SW1116 cells, TSA shows comparable induction of miRNAs in the early stage CRC cell line. However when evaluating the effect of 1µM 5-Aza-2'-C *versus* 300nM TSA in late stage CRC, there is a marked difference in the transcriptional induction of all three miRNAs. From these results it can be inferred that DNA methylation seems to play a more influential role in the regulation of miRNAs in the later stages of CRC, as discussed above. However in contrast histone acetylation plays a moderate role in early CRC, while on its own does not seem to have an influence during the later stage of CRC. In this study, although the differences between the two stages were sought, it must however also be considered that the genotypes differ between the two cell lines.

Chapter 3: COMPUTATIONAL TARGET PREDICTION FOR MIR-143, MIR-145 AND MIR-133B AND FUNCTIONAL ANALYSIS

3.1 Introduction

With over a thousand miRNAs identified so far and with each miRNA potentially targeting up to a hundred target genes each, it is not surprising that miRNAs regulate over 50% of mammalian protein coding genes (Friedman *et al.*, 2009) exhibiting widespread functions in critical cellular processes. It is thus a vital task to identify and validate their targets to further understand the roles that each miRNA plays in regulating critical cellular processes and henceforth the development of diseased states upon their de-regulation. Identification of miRNA targets is contingent on sequence complementarity between mature miRNA sequences and the 3' UTR of mRNA transcripts. Basic alignment tools, such as BLAST, lack in their ability to align short sequences such as miRNAs, thus motivating the development of specific target prediction algorithms. Almost perfect complementarity between mature miRNA sequences and their respective targets in plant cells allows for a simple and easy prediction (Voinnet *et al.*, 2009). In stark comparison however, the imperfect complementarity displayed by animal/metazoan mature miRNAs to their targets posed a challenging task in the miRNA target prediction field. Consequently, this has led to the development of sophisticated computational algorithms to assist in the prediction of putative miRNA targets. *In silico* miRNA target prediction is a rapidly evolving field in miRNA research with increasing amounts of bioinformatic tools becoming available. There are several parameters that are considered in the algorithms based on a number of principles of miRNA target recognition which are elaborated below.

3.1.1 Principals of miRNA target recognition

3.1.1.1 *Sequence complementarity*

miRNA recognition of a target was first discovered when it was found that the miRNA *lin*-4 regulates the expression of lin-14 in *C.elegans* (Wightman *et al.*, 1993). This study also determined that the 3'UTR of lin-14 was sufficient to confer this regulation pattern. In 2004, Doench and Sharp had determined that the 5' end of the miRNA was crucial for the repression of its target while the 3' end had minimal value. It has also been shown that targets with the same sequence from nucleotides 2 to -7 of the 5' end of the miRNA share the same targets. This region from nucleotides 2 -7 of the 5' end of the miRNA has further been described as the "seed" region and requires strict Watson-Crick pairing in the miRNA-target duplex. The majority of miRNA target sites have perfect complementarity with the seed region. These sites deemed "canonical binding sites" are further categorised by three types (depicted in Fig 3.1 A). The 7mer-A1 site contains complementarity to the seed region and has an adenine at the position corresponding to position 1 of the 5' miRNA end. It is thought that the adenine in this position increases the target recognition efficiency (Lewis *et al.*, 2005). The 7mer-m8 site consists of complete seed region complementarity to its target, in addition to complementary base pairs at position 8 flanking the seed region. The third canonical binding type termed 8mer, consists of the flanking adenosine in the target site corresponding to position 1 of the miRNA and has complementarity to position 8 flanking the miRNA seed region. There are some sites with perfect pairing to the seed region only. These 6mer sites are however associated with reduced efficiency and are only marginally available (Figure 3.2 B). The efficiency of site binding is ranked where 8mer > 7mer-m8 > 7mer-A1 > 6mer (Nielsen *et al.*, 2007; Grimson *et al.*, 2007). Target binding to the 3' end of the miRNA also occurs and in these instances is thought to enhance the binding efficiency of the seed region pairing. These sites have 3' supplementary binding with perfect seed matches (Figure 3.3 C). Mismatches and imperfect seed region pairing are also tolerated in some efficient binding sites. In these cases the mismatch in the

seed region is compensated for by extensive 3' binding. 3' compensatory binding seems to be preferentially located around nucleotides 13-16 (Figure 3.4 D). G:U wobbles have also been recognised in seed regions, wherein a guanine is allowed to bind to a uracil instead of a cytosine (Doench & Sharp, 2004).

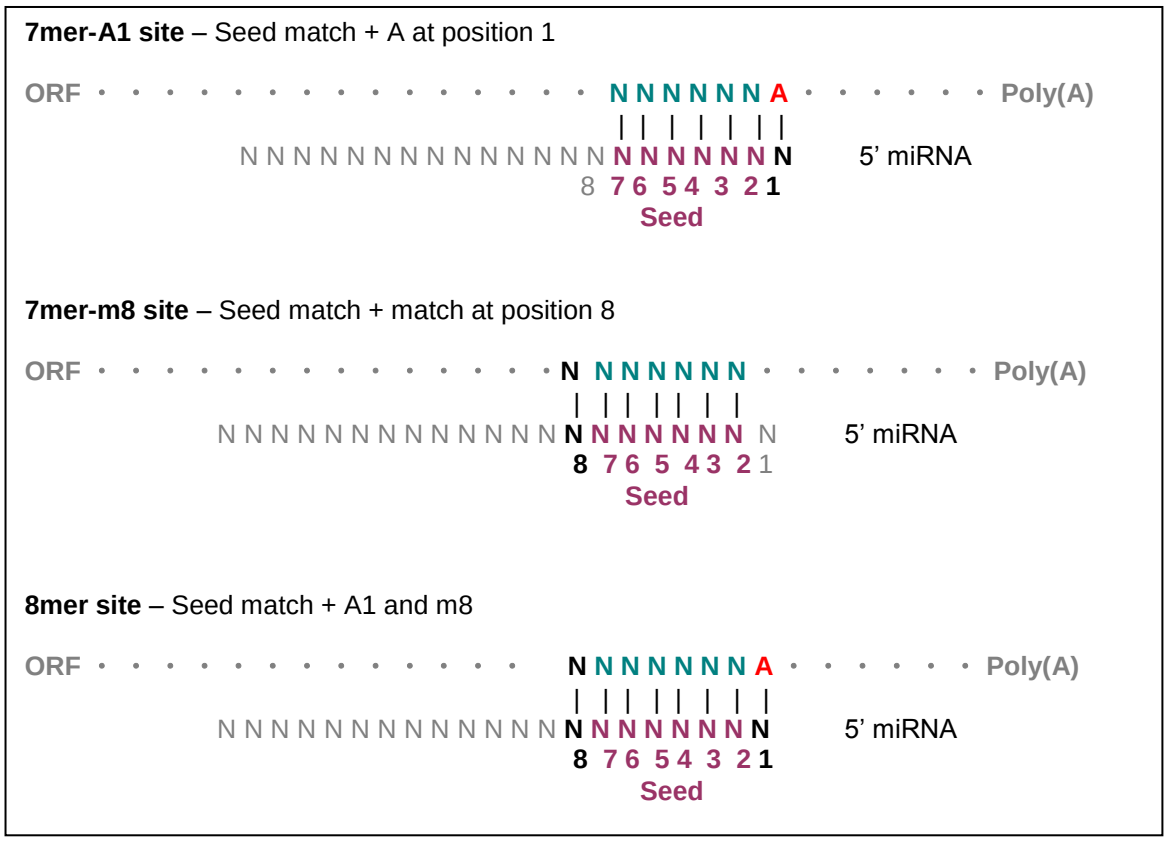

Figure 3.1 : Canonical miRNA-target binding types. Experimental evidence has determined three defined types of miRNA-target binding based on partial hybridisation of miRNA to target. A) perfect complementarity to the seed region is a minimal requirement for 5' dominant binding types. An Adenine in position 1 allows for preferential binding (Adapted from Bartel, 2009).

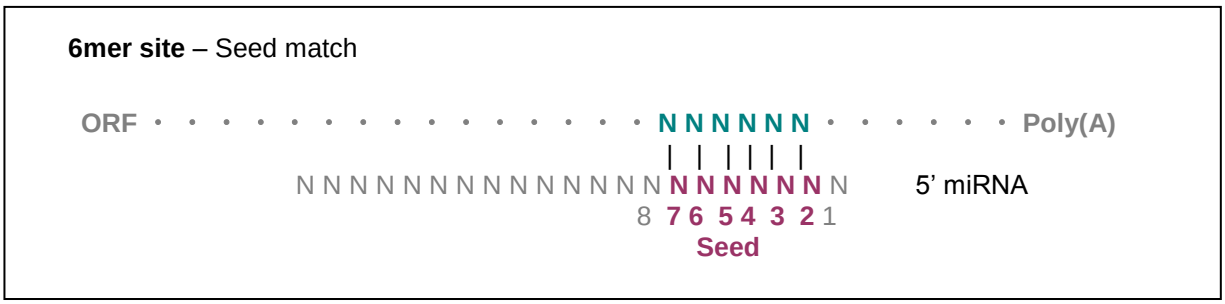

Figure 3.2 : Marginal binding sites. 6mer sites contain perfect binding to the seed region only. These sites are the least common binding site (Adapted from Bartel, 2009).

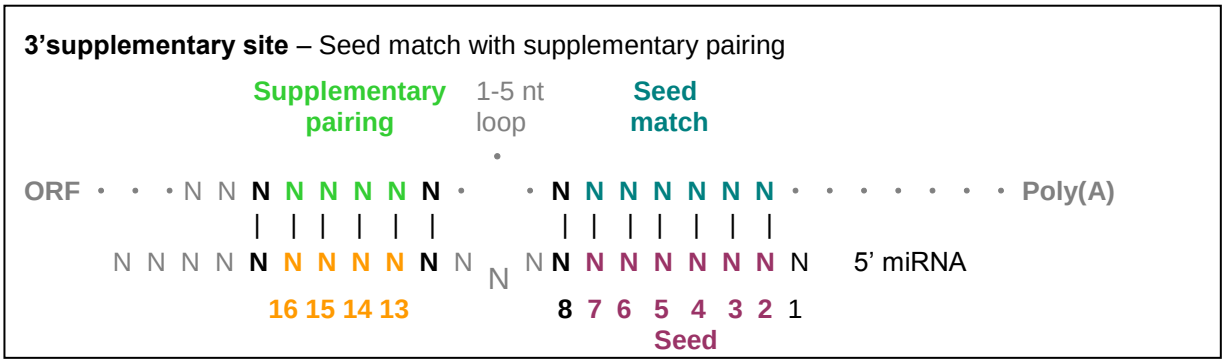

Figure 3.3 : 3' Supplementary binding site. Binding of the mRNA to the 3' end of the miRNA with a characteristic bulge in the middle constitutes a 5'-dominant canonical site (Adapted from Bartel, 2009).

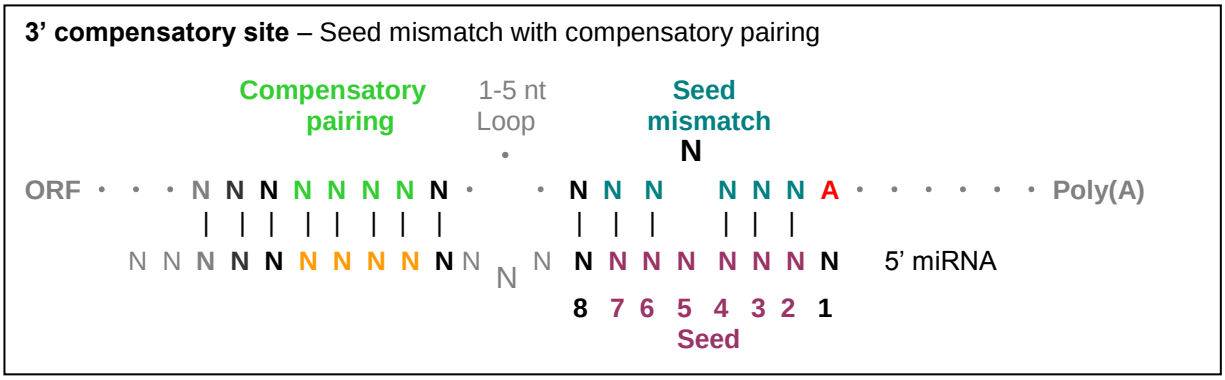

Figure 3.4 : 3' compensatory site. A mismatch in the seed region can be compensated for by extra binding at the 3' end of the miRNA (Adapted from Bartel, 2009).

3.1.1.2 *Conservation of miRNA-target interactions*

Considering conservation of miRNA-target interactions between orthologous 3'UTR sequences from several species significantly reduces the number of false positive predictions in bioinformatic target prediction programs. It has been of the notion that mammalian target sequences are retained through evolution due to selective pressure and that by comparing the 3'UTR of orthologous sequences allows for a more efficient miRNA target prediction. Early studies recognised that seed regions matched between orthologous sequences of flies and worms (Stark *et al.*, 2003). Lewis *et al.* (2003) highlighted that about a third of human genes contain conserved targets of miRNAs. Subsequently, this volume increased to more than 60% of protein coding human genes under selective pressure to retain sites in the 3' UTR as targets for miRNAs (Friedman *et al.*, 2009). Despite the overwhelming level of conservation observed, there are still a considerable number of non-conserved sites that will not be identified with algorithms being highly dependent on alignment with orthologous sequences. A target prediction strategy relying on stringent conservation would fail to identify any non-conserved sites that may have developed through selection events. It is therefore important to combine conservation analysis with other principles of binding for a more precise prediction.

3.1.1.3 *Thermodynamics of miRNA:target binding*

The likelihood of a miRNA binding to its target appears to rely on the thermodynamic stability of duplex formation. This essentially denotes that the net energy required for the formation of the miRNA:mRNA duplex impacts the probability of the duplex interaction. The change in free energy (ΔG) is calculated as the difference between the energy spent on opening the mRNA target site and the energy gained by the formation of the miRNA-miRNA duplex formation (Kertesz *et al.*, 2007). A lower energetic cost is generally indicative of the physiologic interaction. The RNA secondary structure influences the free energy required for the structure to unfold, as illustrated in Figure 3.5. Therefore programs that predict the secondary structure and

energy required to unfold the 3'UTR sequence are both incorporated in target prediction algorithms (Ding *et al.*, 2004; Lorenz *et al.*, 2011; Zuker *et al.*, 2003).

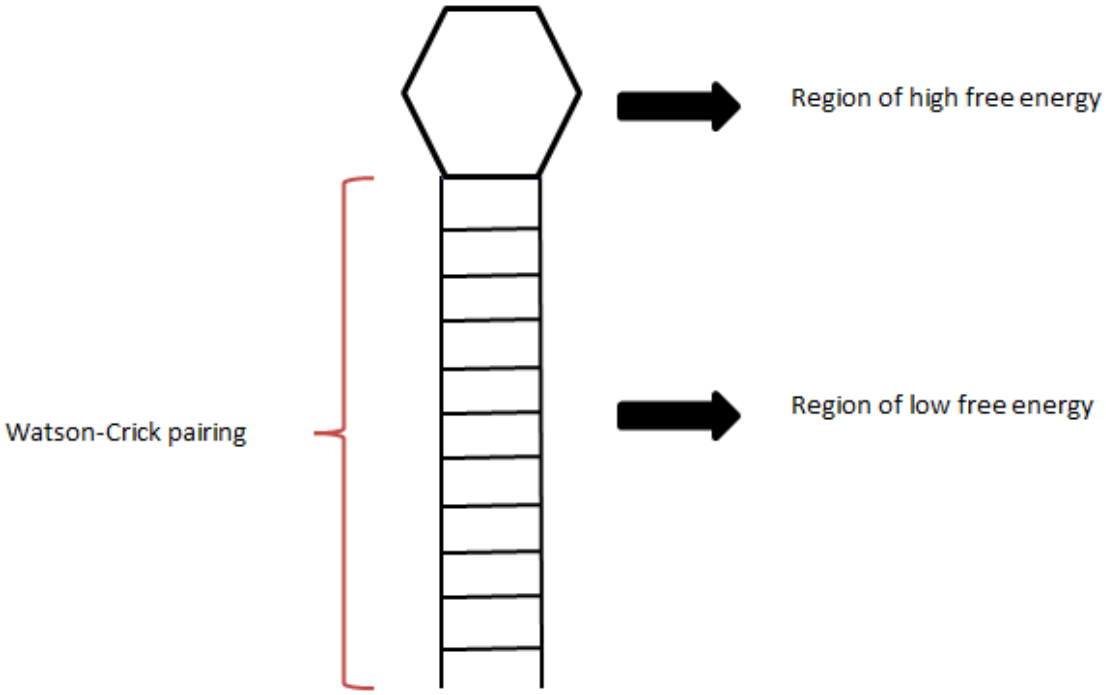

Figure 3.5: Free Energy of binding. Areas of complementary base pairing have a lower net energy than areas that are not bound. This principle is considered when measuring the free energy of binding of a miRNA to its target.

3.1.1.4 *Target site accessibility*

The accessibility of the mRNA target site to the miRNA seed region has an effect on the association and dissociation to and from the RNA Induced Silencing Complex (RISC). When assessing this component in computational prediction programs only the mRNA target site accessibility is considered as the mature miRNA is already lodged into the RISC, in a formation that exposes the seed region to its targets. The accessibility of the mRNA target is dependent upon the secondary structure of the sequence and also to the free energy of unbinding, as described above. Another factor to consider is the local AU content in the mRNA target. A higher AU content

allows for a weaker mRNA secondary structure making the target amenable to unfolding and therefore increasing the access of the target to the miRNA-RISC complex (Grimson *et al.*, 2007).

3.1.1.5 *3'UTR context*

The position of the target site within the 3'UTR influences the efficacy of miRNA mediated silencing of the target (Grimson *et al.*, 2007). It is required that the position of the target site is within 15nt of the stop codon, a feature which may have evolved due to the placement of the ribosomal complex. The length of the 3'UTR also affects the position of the target site whereby in short 3'UTRs the target sites are most likely in the 5' end of the 3'UTR and in long 3'UTRs the target site is generally not located in the centre, due to inaccessibility to the silencing complex. It has also been shown that some mRNA target site have multiple sites for the miRNA which seems to enhance the level of repression (Doench *et al.*, 2003; Brennecke *et al.* 2005; Grimson *et al.*, 2007). Target sites that are located close together have also demonstrated synergistic behaviour by revealing optimal downregulation when two target sites are between 13 – 35 nt apart (Saetrom *et al.*, 2007). Furthermore, an AU rich nucleotide composition of the sequence flanking the target site is also a feature of efficient miRNA target sites, especially owing to its contribution to site accessibility, as discussed above.

3.1.2 Choosing the right target prediction tools

Although the exact mechanisms of miRNA targeting is not yet fully elucidated, the aforementioned principals, which have been experimentally validated, have provided researchers with parameters to exploit and incorporate in the development of computational miRNA target prediction tools. The first programs developed took advantage of sequence complementarity of the target to the miRNA seed region, which the majority of miRNA target prediction tools still utilise to date. Conservation became a key consideration when programs that used a conservation parameter had

a lower rate of false positives (Lewis *et al.*, 2005). Since each computational program applies the different miRNA binding features with different weighting scales and combinations, the results from each program do not exactly match the next, therefore making it difficult to assess which program performs best. To assist in estimating the performance of the algorithms, programs are assessed according to two key factors, specificity or the "true negative rate" and sensitivity, referred to as the "true positive rate" (Lalkhen & McCluskey, 2008). The "true negative rate" (specificity) essentially refers to the number of non-targets correctly predicted not to be targets of the miRNA; whilst the "true positive rate" (sensitivity), reflects the number of validated targets that are correctly predicted as targets by the miRNA prediction program. Certain components which are included in the algorithm will have an influence on specificity and/or sensitivity; for example, by implementing stricter thresholds for conservation or thermodynamic stability the specificity may be increased, while the sensitivity may be compromised significantly. Essentially a trade-off between specificity and sensitivity is required to achieve optimal performance of the program. A reliable method of assessing the performance of the algorithm is by plotting sensitivity/specificity pairs for each prediction at different cut offs on a ROC curve (Figure 3.6), which is the plot of sensitivity *versus* 100-specificity (Lalkhen & McCluskey, 2008). The closer the curve is to the upper left corner, the more reliable the test is. The Area under the Curve (AUC) is the measure used to quantify the reliability of the program.

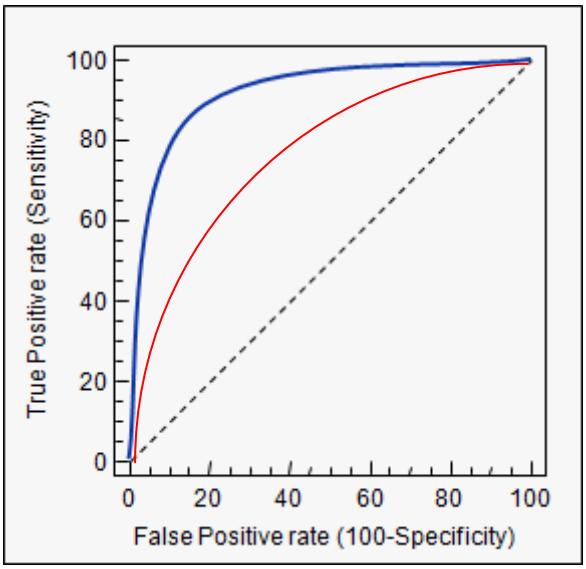

Figure 3.6: ROC (Receiver Operating Characteristic) Curve. The blue line depicts the plot of an excellent program. The red line depicts a good performance while the black dashed line depicts a random (non-specific) performance. A larger "area under the curve" or AUC would indicate a more reliable test/program/algorithm (Lalkhen & McCluskey, 2008).

3.1.3 Functional analysis of putative targets

Prediction of miRNA targets, with the use of computational tools, provides a lengthy list of potential targets to be validated further. There are several methods used to determine if the potential targets are valid targets. These methods typically rely on three premises of miRNA/mRNA target relationships:

1. The first and most overt premise is that the miRNA reduces the expression of the target by binding to the 3'UTR (Bartel, 2009). Validation using this method involves the use of a reporter plasmid in which the 3'UTR of the target gene is cloned downstream of a luciferase or green fluorescent protein (GFP) open reading frame. Once the recombinant plasmid is transiently transfected into a neutral host cell along with the miRNA of interest, the levels of fluorescence is assessed in cells with miRNA *versus* those without the miRNA. Undoubtedly

in the case of a true target, the fluorescence level would be decreased in the cells hosting increased levels of miRNA.

2. The second avenue of validation is based on the premise that if an mRNA is a target of a miRNA, then the two should be co-expressed in a cell in order for the miRNA to regulate the mRNA target (Kuhn *et al.*, 2008). Using this premise the levels of miRNA and mRNA are assessed for co-expression using Northern blots or quantitative PCR. *In situ* hybridization is also used to confirm co-expressed miRNA and mRNA sets.

3. The third premise on which miRNAs are being validated relies on the fact that ultimately the miRNA would affect the levels of the biological product of mRNA, that is, the protein (Thomson *et al.*, 2011). Validation of miRNA targets using this premise involves the transfection of anti-miRNA or precursor miRNAs into a homeostatic cell and then assessing the levels of protein within the cell approximately 24-48 hours after transfection.

3.1.4 Objectives

To further understand the role that the putative CRC-related tumour suppressor miRNAs play in cancer, an imperative task is to identify its targets. This chapter describes and discusses the identification of putative targets for miRNA-143, -145 and -133b through the following objectives:

- By selecting appropriate bioinformatics tools to predict targets for each miRNA
- Next, developing a curating strategy to filter predicted targets for further functional analysis
- Ultimately assessing the effect of the miRNA on protein levels of the predicted targets

3.2 Methodology and Materials

3.2.1 Computational tool selection

As discussed above, it is clear that each bioinformatic tool will yield results that may differ to the next. In this study three tools were selected to predict targets for the miRNAs of interest. The tools were selected to encompass the various principles of miRNA-target binding. Also, a key consideration is the sensitivity and specificity of each program which justifies the reliability of the results retrieved through the program. The motivation behind using three different target prediction programs lies upon the hypothesis that if all three programs predict the same target by using different algorithms, then it is more likely to be a true target. Only targets that were predicted by all chosen programs were considered for further filtering. The features of each program are described below:

3.2.1.1 *Program 1: TargetScan v5.1 (http://targetscan.org)*

TargetScan utilises a rule based algorithm that first searches for full seed region complementarity and thereafter extends the search to regions outside the seed region (approximately 21-23 nucleotide fragments) until a mismatch is detected. Classifications are then made on the length of perfect complementarity and an adenine at position 1. Imperfect seed matches with 3' compensatory pairing are also considered in this algorithm to accommodate G:U wobbles. The complementary regions are then analysed by the RNAfold program to determine the minimum free energy secondary structure. Conservation is considered in this algorithm by aligning orthologous 3'UTRs from up to 5 different species and then determining if the seed region is located in an island of conservation. The resulting score is calculated per 3'UTR. The scoring relies on several parameters; the type of seed matching, any pairing that occurs outside of the seed region, AU content upstream and downstream of the seed region and the overall distance of the site to the nearest untranslated region (Lewis *et al.*, 2005).

3.2.1.2 *Program 2: PicTar – Probabilistic Identification of Combination of Target sites (http://pictar.bio.nyu.edu)*

Unlike TargetScan, PicTar is a data-driven algorithm, rather than a rule-based one. This essentially means that prediction of miRNA targets, using this algorithm, is not only reliant on a given set of requirements but rather on available data. The program searches for near to full complementarity of conserved 3'UTRs. The alignment across up to 8 vertebrate species is an important consideration in the program to reduce the number of false positives. Once the complementarity and conservation checks are complete, it then uses RNAHybrid to calculate the energy spend of miRNA-3'UTR duplex formation. The program uses energy-cutoffs for different types of binding. Therefore a seed region with a mismatch may be selected as long as it is within a specified energetic range. Predicted targets are then scored using a Hidden Markov Model (HMM) which is based on a Bayesian classifier model. This statistical model is used to analyse chains or sequences in which the rules governing the production of the chain is not known. By "studying" experimentally validated datasets the model uses a maximum likelihood approach to determine the probability of an observation occurring (Krek *et al.*, 2005; Lall *et al.*, 2006).

3.2.1.3 *Program 3: DIANA-MicroT v3.0 (http://diana.pcbi.upenn.edu)*

DIANA MicroT v3.0 requires strict seed region base pairing and shows preference for 7mer Watson-Crick paired sites. 6mer sites and seed matches with G:U wobbles are considered if supplementary 3' binding of miRNA is present, or if binding energy is favourable. Thermodynamic parameters are considered by a 38nt window progressively scanning across a 3'UTR sequence subsequently using a modified dynamic programming approach to calculate free energies of potential binding sites at each step. Conservation is also included in the final scoring, however a non-conserved site may also be considered. Once the target sites are identified they are compared to targets identified from mock sequences and a signal-to-noise ratio and precision score is obtained for each site. Mock sequences are essentially random sequences designed per miRNA that have the same number of seed sites per

3’UTR. These sites are not biologically functional and therefore the ability of the program to recognise the difference allows for the SNR to be determined (Kiriakidou *et al.*, 2004).

3.2.2 Strategic curation of predicted targets

Relying only on the aforementioned computational programs to identify miRNA targets would be premature. Validation of miRNA targets is a lengthy and relatively expensive procedure and therefore additional analysis and curation of the predicted targets should be completed to filter the potential targets and essentially reduce the number of false positives. In this study, only targets that were predicted across all three programs were considered for the strategic curation developed for this study.

As miR-145, miR-143 and miR-133b seem to commonly be downregulated in CRC, the hypothesis was made that ultimately the combination of the three miRNAs would affect pathways related to the tumourigenesis process and potentially in CRC development. Under this inference the targets identified per miRNA, and that were predicted by all three programs, were loaded into DIANA mirPATH v1, a program that identifies the KEGG pathway enrichment of the combined miRNA predicted targets. KEGG, the **K**yoto **E**ncyclopedia of **G**enomes and **G**enes, is a collection of manually transcribed pathways representing the current knowledge of molecular systems. Once the list of overrepresented pathways were identified, all miRNA targets within these pathways were outlined. Targets linked to more than one CRC identified pathway were weighted more and therefore ranked higher than those only associated with one pathway. Subsequent systemic literature analyses was conducted for all filtered targets to determine a strong reference to CRC, most specifically an increased expression which demonstrates an antagonistic relationship to the downregulated miRNA recognised in CRC.

Figure 3.7 illustrates the manual curation methodology used to streamline the selection of potential miRNA targets for further functional analysis.

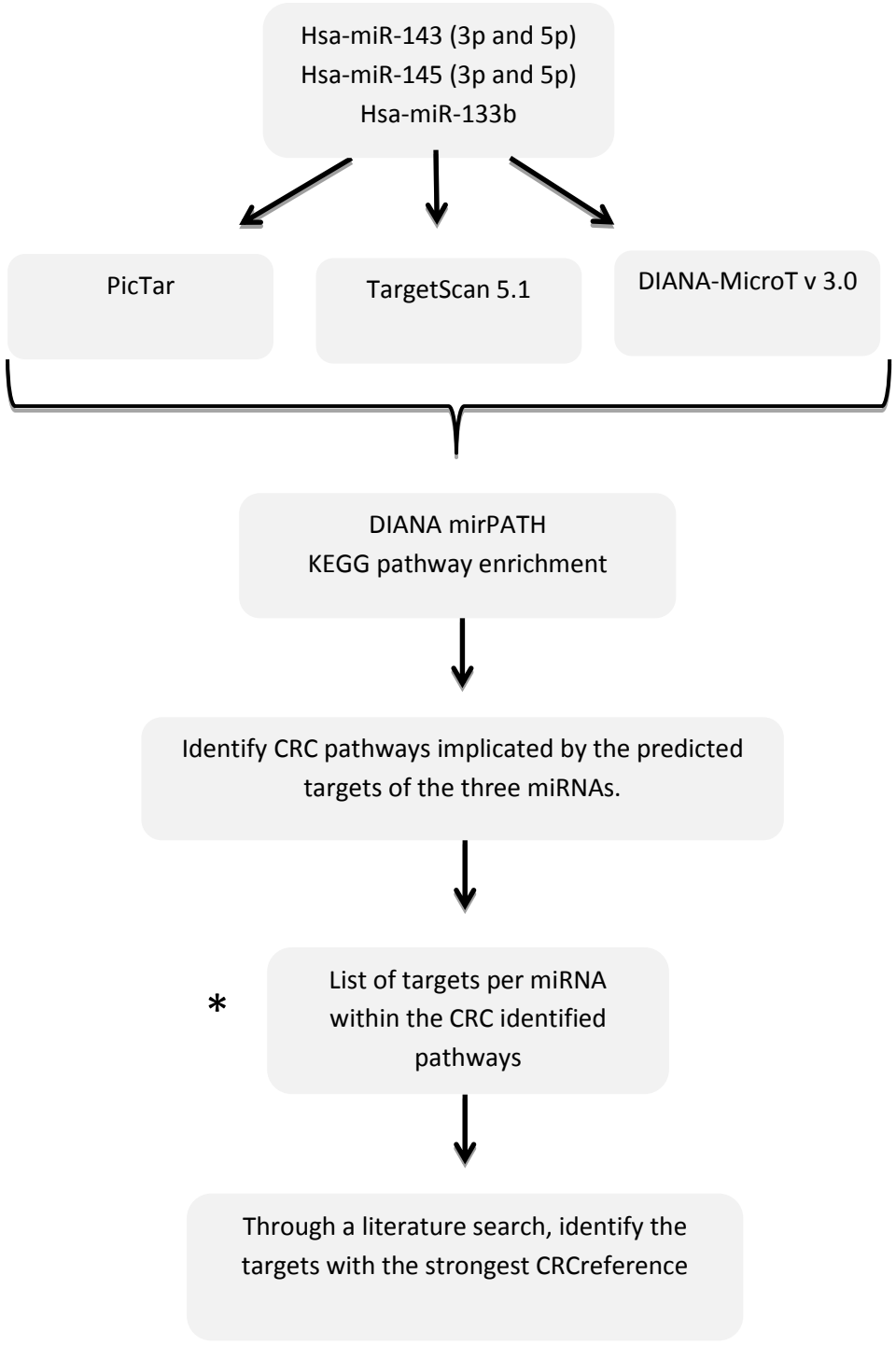

Figure 3.7: Target prediction methodology and selection of targets for functional analysis. *List of targets within CRC identified pathways were further ranked according to number of associated pathways in addition to the ranking of the pathways by significance.

3.2.3 Functional Analysis of selected putative targets

3.2.3.1 *Cell culture*

For a reliable assessment of miRNA target genes, a cell line without potentially downregulated miR-143, -145 and -133b was used. In this case the HET1A cell line was utilised. This cell line is derived from a normal human oesophagus and has been shown to demonstrate normal levels of the miRNAs in question. Aseptic techniques were used in the cell culturing procedure as described previously in Chapter 2.2. The cells were however grown in a special growth medium, BEBM (bronchial epithelial basal medium) obtained from Lonza.

3.2.3.2 *Anti-miR transfection*

Once the HET1A cells had reached 80% confluency, the cells were washed with PBS (Sigma Aldrich) and transfected with Anti-miR™ 143, 145 and 133b oligomers (Ambion) using the siPORT NeoFX Transfection agent (Ambion), as per manufacturer's instructions. Prior to the experiment, the concentrations of the Anti-miR™ oligomers and the transfection reagent were optimised to ensure optimal transfection. Anti-miR™ oligomers were used at a concentration of 30nM and the siPORT NeoFX transfection reagent was used at a concentration of 3µL in the treated cells. The transfection mix was incubated with the HET-1A cells for 24 hours. Three controls were included to identify confounding effects from other reagents and to assess the effects of the Anti-miR™ with confidence. The first control was an untransfected cell line, cultured as per normal cell culture procedures, in the absence of transfection. In the second control, cells were treated with the transfection mixture lacking the transfection reagent (siPORT NeoFX transfection agent) and only the Anti-miR™. The third control involved transfection with Anti-miR™ miRNA Inhibitor Negative Control #1 (Ambion) which is a random oligomer that is not biologically relevant, with no effect on miRNA expression.

3.2.3.3 *Fluorescence microscopy*

Following transfection for 24 hours with the transfection mixture or the controls, cells were harvested by centrifugation and thereafter the pellet was resuspended in 6mL of BEBM (Lonza), of which 1 mL was re-suspended in 7mL fresh room temperature BEBM. Prior to harvesting the cells, glass coverslips were immersed in a 70%$^{v}/_{v}$ ethanol solution, then heat sterilised by flaming and placed in petri dishes. The resuspended cell mixture was carefully transferred on-to the glass coverslip to ensure full coverage, without spilling over into the petri dish. The coverslips were then incubated at 37˚C with 5% CO_2 for 5 hours to ensure cell adherence to the surface of the coverslip. Once the cells were adhered to the glass surface, fresh BEBM was added to the petri dish and maintained overnight for the cells to grow on the coverslip surface.

After overnight incubation, the next step involved fixing of the cells to the coverslip. A 3%$^{v}/_{v}$ formaldehyde solution was prepared by mixing 3mL formaldehyde (Univar) in 33mL PBS which was used as a fixative solution. Medium was removed from the petri dish containing the seeded coverslip. The cells were washed in PBS three times to remove excess growth medium. After this, the fixative solution was added to the petri dish containing seeded coverslips and kept at room temperature for 10-15 min. Fixative was aspirated off and safely discarded in a fume hood drain. The coverslips were washed three times with PBS to remove excess fixative solution. Finally, the fixed coverslips were then immersed in PBS solution in petri dishes, sealed with Parafilm® and stored at 4˚C overnight.

Prior to adding the primary antibody to the fixed cells seeded on coverslips, a 0.5%$^{w}/_{v}$ solution of BSA (bovine serum albumin)/PBS was prepared. 125µL Triton X-100 detergent was added to 25mL BSA/PBS. PBS was removed from the petri dishes containing fixed seeded coverslips that were stored overnight. The 0.5%$^{v}/_{v}$ Triton X-100 detergent solution was added to the petri dish and kept at room temperature for 10 minutes. Triton X-100 is a non-ionic surfactant which permeabilises the cell membrane, subsequently allowing the primary antibody entry

into the cell. Once the cell membrane was permeabilised the cell-free side of the coverslips were dried without disturbing the cell monolayer and placed cell surface up on a dry microscope slide. A 1:100 dilution of primary antibody in 0.5%$^{v}/_{v}$ BSA/PBS was then prepared and 100µL of the primary antibody solution was added to the coverslip. The coverslips and slides were then transferred to an airtight container that was kept humid with wet filter paper and stored at 4˚C overnight. Table 3.1 indicates the primary antibody employed for each miRNA gene target.

Prior to staining with the secondary antibody, three beakers were filled with autoclaved PBS. The cover slips containing primary antibody were removed from the microscope slide with forceps and drained of liquid on paper towel to remove the primary antibody solution. The coverslips were then sequentially dipped 10 times in each of the three beakers of PBS before being dried again and transferred to the clean microscope slide, cell side uppermost. A 1:200 dilution of secondary antibody in 0.5%$^{v}/_{v}$ BSA/PBS was then prepared and 100µL of the secondary antibody solution was added to the coverslip. The slides were then transferred to the airtight humid container and stored in a dark cupboard for 1 hour at room temperature (25˚C). The relevant secondary antibodies used to detect each primary antibody are indicated in Table 3.1 below.

Table 3.1: Primary and secondary antibodies used per transfected cell line.

Anti-miR Transfection	Primary Antibody/Predicted miRNA Target	Secondary Antibody
Anti-miR™ 143	KRAS mouse monoclonal IgG_{2a} (Santa Cruz Biotechnologies)	AlexaFluor® 568 conjugated anti-mouse (Life Technologies)
Anti-miR™ 145	FZD7 goat polyclonal IgG (Santa Cruz Biotechnologies)	AlexaFluor® 568 conjugated anti-goat (Life Technologies)
Anti-miR™ 133b	ß-TRCP goat polyclonal IgG (Santa Cruz Biotechnologies)	AlexaFluor® 568 conjugated anti-goat (Life Technologies)

Once the secondary antibody staining was complete, the nucleus of the cell was then stained with DAPI, 4', 6-diamidino-2-phenylindole (Boehringer Ingelheim). DAPI is a stain containing blue fluorescence which specifically binds to AT-rich areas of double stranded DNA (Kapuscinski, 1995). Coverslips were drained of the secondary antibody mixture and dipped serially in three beakers of autoclaved PBS, ten times each, in order to remove excess secondary antibody mixture. DAPI was diluted 1:10000 in PBS and added to the coverslips and transferred back to the clean microscope slides. The slides were returned to the airtight humid container and stored for 30-45 min in a dark cupboard at 25˚C.

Once DAPI staining was completed, the coverslips were drained and rinsed serially in PBS before being transferred cell surface down onto a new microscope slide using Gel Mount ™ aqueous mounting medium (Sigma-Aldrich). The mounted coverslips were left to dry and then stored at 4˚C, until viewed under the Olympus IX71 inverted fluorescence microscope and Zeiss LSM 780 laser scanning microscope, using a 63x objective.

3.3 Results

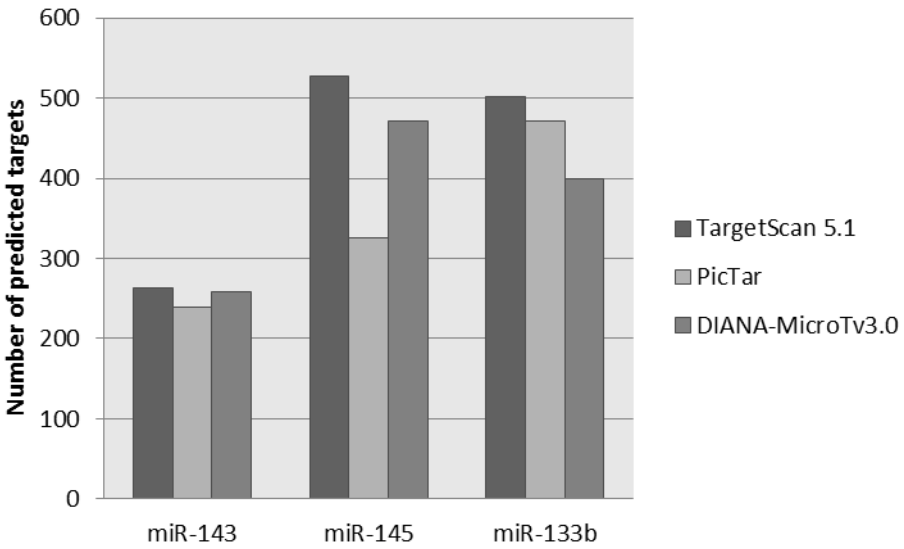

Figure 3.8: Predicted number of target genes per miRNA.

The mature miRNA sequences for hsa-miR-143-3p, hsa-miR-143-5p, hsa-miR-145-3p, hsa-miR-145p and hsa-miR-133b were submitted into the target prediction algorithms TargetScan 5.1, PicTar and DIANA-Micro T v3.0, as described in section 3.2.1. Overall miR-143 was predicted to have the least number of targets by all three programs, where TargetScan 5.1 predicted 263 conserved targets, PicTar predicted 239 targets and DIANA-Micro T v3.0 predicted 259 target genes. For TargetScan 5.1, there were 272 conserved target sites and 134 poorly conserved target sites within the 263 target genes. Of the 259 genes predicted by DIANA-MicroT v3.0, there were 307 target sites predicted within these genes. MiR-145 yielded large numbers of miRNA targets, most specifically when using TargetScan 5.1 and DIANA-microTv3.0 predicting 528 and 471 target genes. Although PicTar had predicted a lower number of targets for miR-145 compared to the other two computational programs, this number (326) is still higher than the number of target genes predicted for miR-143. TargetScan 5.1 predictions for miR-145 resulted in 585 conserved sites and 174 poorly conserved sites within the 528 target genes. For DIANA-MicroT v3.0 a total of 502 target sites were identified. MiR-133b had also produced large numbers of predicted targets from each program. Some 502 target genes, of which were 530 conserved sites and 80 were poorly conserved sites, were identified from TargetScan 5.1, a total of 471 targets were identified from PicTar and 399 targets (421 target sites) were identified with DIANA-MicroTv3.0.

These results demonstrate that each program yields differential sets of target genes and sites per miRNA. All three programs derive the miRNA mature sequences from mirBase and use RefSeq sequences to map 3'UTRs. The differences in predictions are purely as a result of the different algorithms and weighted scoring and thresholds for the principles of miRNA-target binding considered by each program. The resulting dataset of almost 3500 miRNA targets required further curation and filtering to make the data more meaningful.

The 3458 targets predicted for all miRNAs were then submitted into the DIANA mirPATH v1 algorithm. The resulting KEGG pathways enriched by the combined predicted targets for the three miRNAs were determined. Figure 3.9 below represents in histogram format the output of the pathway enrichment. It shows the

probabilities of the pathway association when assessing the union of all targets, those targets predicted for each miRNA per target prediction program and also the intersection of the combined targets.

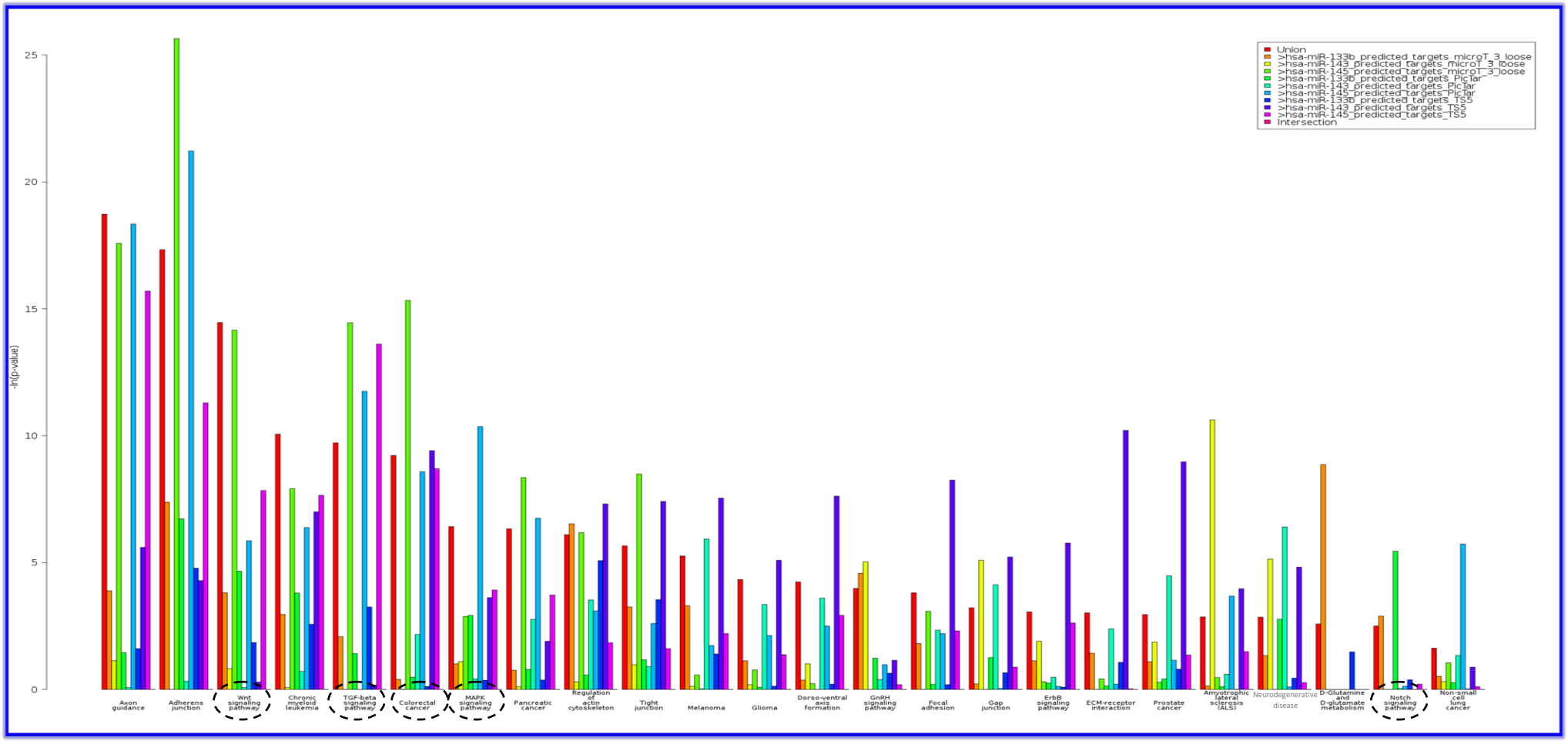

Figure 3.9: KEGG pathway enrichment of the combined miRNA targets. miR-143, miR-145 and miR-133b predicted targets from TargetScan, PicTar and DIANA MicroTv3.0 were transferred to DIANA mirPATH to obtain enrichment of KEGG pathways. CRC related pathways were identified to be associated with the combined miRNA targets (circled)

The top 25 significantly enriched pathways from the predicted miRNA targets illustrated in Figure 3.9 reveals that pathways potentially influenced by the combined expression of the three miRNAs fall within clearly recognizable categories listed below:

- Cancer (Chronic Myeloid Leukaemia (CML), Colorectal Cancer (CRC), Pancreatic Cancer, Melanoma, Glioma, Prostate Cancer, Non-small cell lung cancer(NSCLC)
- Growth signalling pathways (Wnt signalling pathway, TGF-beta signalling pathway, MAPK signalling pathway and Notch signalling pathway)
- Cell-cell and cell-ECM interactions (Adherens Junctions, Regulation of actin cytoskeleton, Tight junction, Focal adhesion, Gap junction, ECM-receptor interaction)
- Neuron signalling and related disease (Axon guidance, Amyotrophic lateral sclerosis (ALS), Neurodegenerative Disease)

Of particular interest in this study, “Colorectal Cancer” was a KEGG pathway found to be enriched by the combined targets of the three putative tumour suppressor miRNAs. Additionally, several growth signalling pathways previously reported to be deregulated in CRC have also been enriched here with most of them listed within the Top 10 pathways enriched from the combined miRNA predicted targets. This information provides some indication of the involvement of these miRNAs in the development of CRC specifically through these pathways. From these results, one could easily infer that these three miRNAs potentially regulate key CRC-related pathways and could possibly explain the relationship of the miRNAs in the development of CRC. However, as the target prediction programs are essentially just a prediction tool with percentages of false positive rates, these findings require further validation.

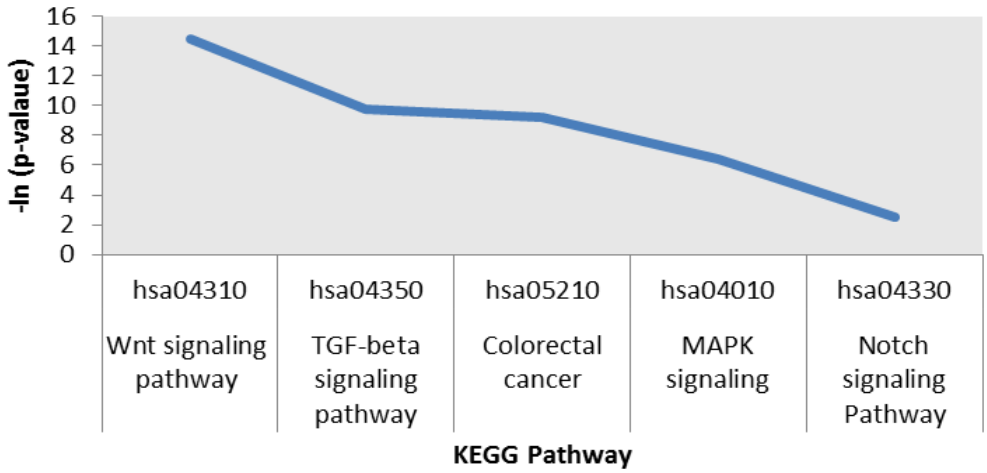

Figure 3.10: KEGG Pathway enrichment of CRC-related pathways. Combined targets of miR-143, miR-145 and miR-133b predicted using PicTar, TargetScan and DIANA MicroT. Obtained from DIANA MicroT V1.0

Based on the DIANA mirPATH v1 output, the CRC-related pathways were ranked for significance according to the probabilities of the pathway being enriched by the miRNA targets (see Figure 3.10 above). The Wnt signalling pathway is the most enriched CRC related pathway followed by the TGF-beta signalling pathway, sequentially followed by “Colorectal cancer”, the MAPK signalling pathway and lastly a slight enrichment of the Notch signalling pathway. All predicted targets that fell within these pathways were determined per miRNA and only those targets predicted across all three computational programs were listed for further analysis. Targets falling within more than one CRC-related pathway were ranked higher than those only linked to one; and those linked to a more significantly enriched pathway ranked higher than a less significant pathway. The filtered list of potential miRNA targets are shown in Table 3.2

Table 3.2: List of potential targets per miRNA associated with KEGG CRC-related pathways.

miRNA	Target Gene	CRC pathway involvement
miR-143	**KRAS***	**CRC, MAPK**
	PDGFRA	CRC, MAPK
	BCL2*	CRC
	FGF1	MAPK
	GLI3	NOTCH
	CSNK1G3	NOTCH
miR-145	SMAD3*	TGF-beta, Wnt, CRC
	FZD7	**Wnt, CRC**
	PPP3CA*	Wnt, MAPK
	CTNNBIP	Wnt
	CCND2	Wnt
	ZFYVE9	TGF-beta
	INHBB	TGF-beta
	FLNB	MAPK
	RASA2	MAPK
	DUSP6	MAPK
	RASA1	MAPK
miR-133b	*PPP2CB	TGF-beta, Wnt
	*PPP2CA	TGF-beta, Wnt
	FBXW11	**Wnt, NOTCH**
	NFAT5	Wnt
	SP1*	TGF-beta
	EVI1	MAPK
	FGFR1*	MAPK
	MAP3K3	MAPK
	CRK	MAPK
	CSNK1G3	NOTCH

*Experimentally validated targets

A systemic literature search was conducted on each predicted target represented in Table 3.2. The search involved assessing gene or protein expression in CRC and their potential roles in CRC development. Most importantly however, evidence of oncogenic potential of the target was assessed. If the predicted gene is a true target of the miRNAs in question, then upon downregulation of the specific miRNAs, one could expect to see a resultant increased expression of the target in CRC. After the literature search was completed, the targets boxed in red in Table 3.2 were chosen for functional analysis due to their strong inference of an increased expression in CRC. A detailed view of the putative miRNA-target binding sites is described further.

Three sites in the KRAS gene (ENSG00000133703) were predicted by all three programs as miR-143 targets. Two 8mer sites were conserved across several vertebrate species. A 7mer-1A site demonstrated poor conservation amongst aligned vertebrate orthologues. MiR-143-KRAS binding sites are depicted in Figure 3.11:

Conserved sites:

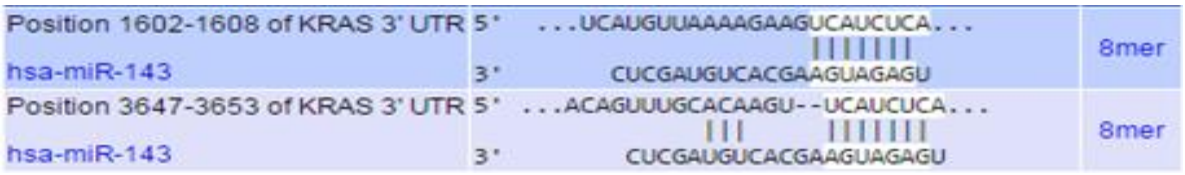

Poorly conserved site:

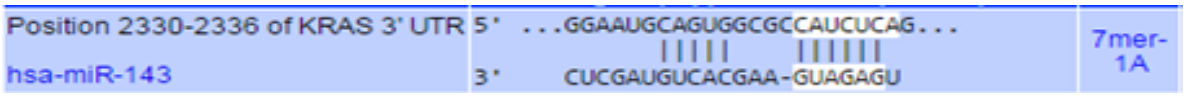

Figure 3.11: miR-143 binding sites in the KRAS gene. Two 8-mer sites were predicted with the seed regions positioned at region 1602-1608 and 3647-3653 of the KRAS 3'UTR.

Within the FZD7 (ENSG00000155760) gene chosen as a potential miR-145 target for further functional analysis, a single 7mer-m8 site was predicted across all three computational programs. The seed region of the site is located at position 518-524 of the FZD7 3'UTR. MiR-145-FZD7 putative binding is depicted in Figure 3.12 below.

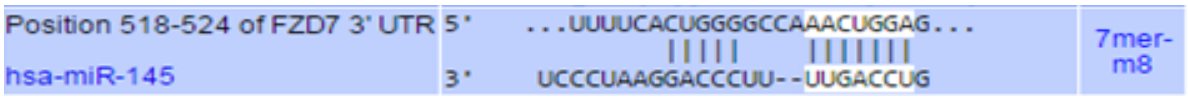

Figure 3.12: miR-145 binding site in the FZD7 gene. A single 7mer-m8 site was predicted with the seed region positioned at region 518-524 in the FZD7 3'UTR.

For miR-133b, the FBXW11 (ENSG00000072803) gene was selected as a putative target for further functional analysis. A single 7mer-m8 site wherein the seed region is located at position 1622-1628 of the FBXW11 3'UTR was predicted across all three computational target prediction programs used in this study. The miR-133b-FBXW11 binding site is depicted below in Figure 3.13.

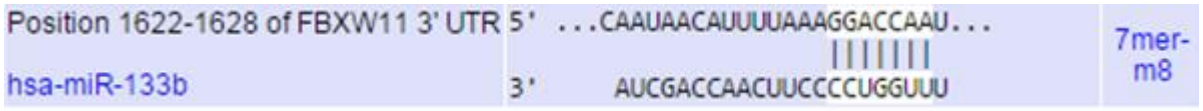

Figure 3.13: miR-133b binding site in the FBXW11 gene. A single 7mer-m8 site was predicted with the seed region positioned at 1622-1628 in the FBXW11 3'UTR.

In silico miRNA target prediction provided a platform to identify potential targets for each miRNA and the chosen targets were supported by scientific literature in relation to CRC development. In order to test the functionality of these potential targets, the protein levels were measured by immunofluorescence, before and after HET1a cells were transfected with Anti-miRs.

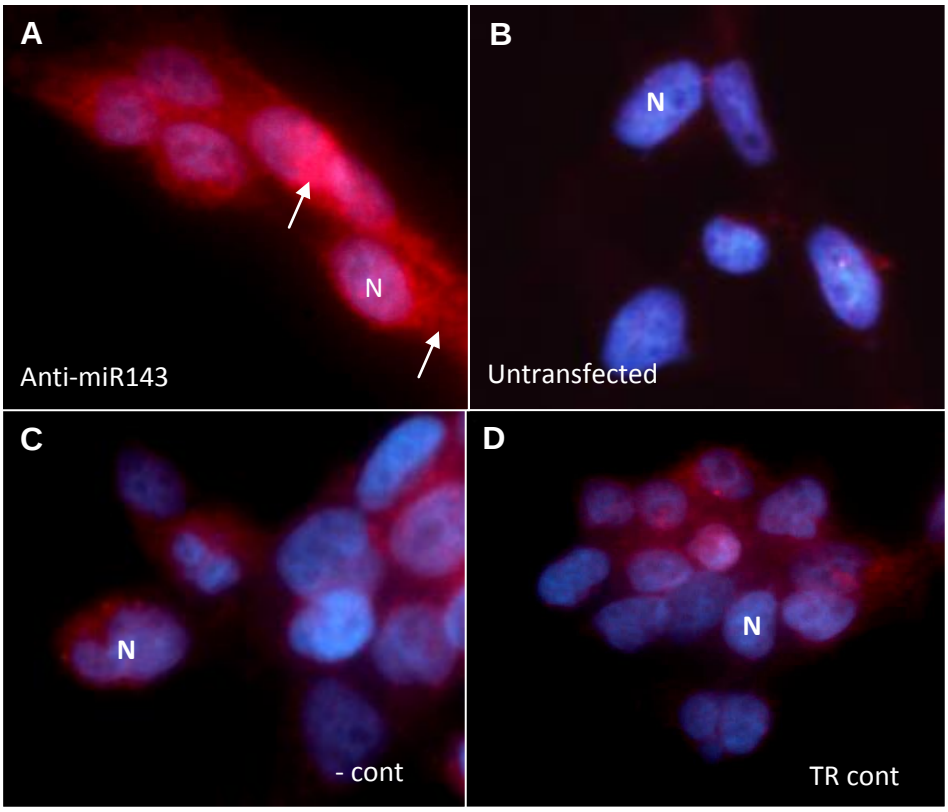

Figure 3.14: Immunofluorescence confocal microscopy image of KRAS protein in Anti-miR™ 143 transfected HET1A cells. (A) KRAS is strongly expressed in the nucleus (N) and nuclear periphery extending into the cytoplasm, after miR-143 inhibition. B) Untransfected control. C) Negative control D) Transfection reagent control. Blue = nucleus (N), Red = KRAS protein (Original magnification of 63x)

After HET1A cells were transfected with anti-miR-143 miRNA inhibitor and thereafter stained with anti-KRAS, it can be clearly seen in Figure 3.14 that KRAS expression appears to be intensely increased (A) when compared to the untransfected control (B), the negative control (C) and the TR control (D). Thus, the increased fluorescence representing KRAS protein expression appears to increase with decreased expression of miR-143. Moreover, this increase in expression is not due to the transfection reagent, but is specifically related to transfection with the anti-miR for miR-143. An antagonistic relationship is represented here between miR-143 and KRAS protein, which is indicative of a miRNA-target relationship. In anti-miR-143 transfected cells KRAS is intensely expressed in the nucleus, the nuclear periphery and the cytoplasmic regions of the cell, however in the absence of anti-miR-143

transfection, KRAS expression is sparsely located along the periphery of the nucleus and does not extend into the cytoplasmic region.

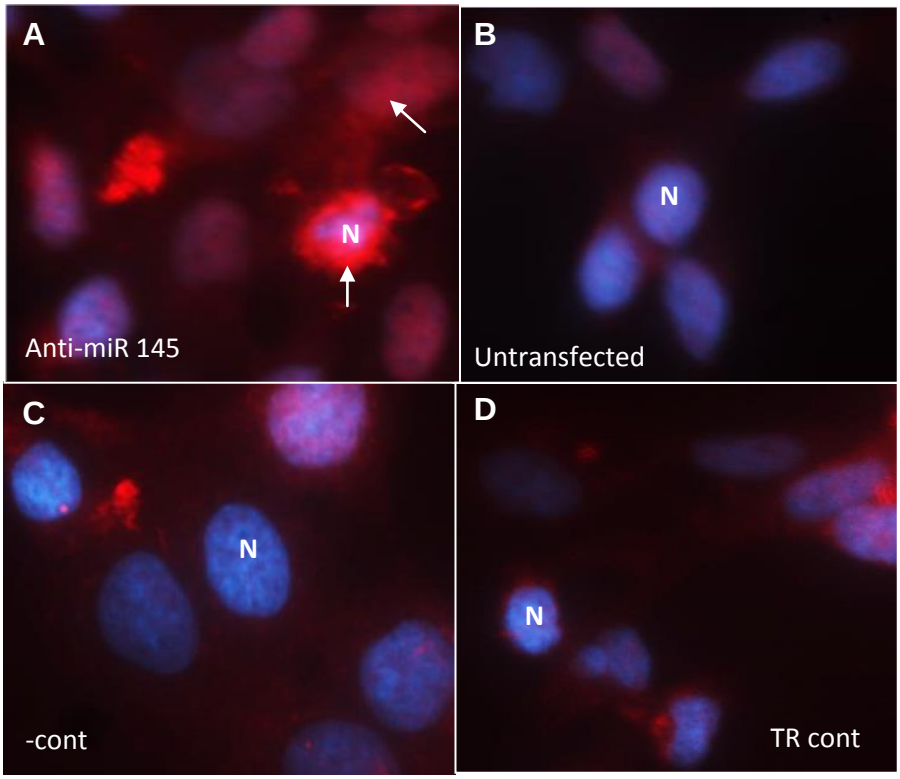

Figure 3.15: Immunofluorescence confocal microscopy image of FZD7 expression in Anti-miR™ 145 transfected HET1A cells. (A) FZD7 localises peri-nuclearly after miR-145 inhibition B) Untransfected control. C) Negative control D) Transfection reagent control. Blue = nucleus (N), Red = FZD7 protein (Original magnification of 63x)

HET1A cells were transfected with anti-miR-145 miRNA inhibitor to decrease the expression of miR-145 and to determine the subsequent effect on the expression of FZD7. Figure 3.15 depicts the immunofluorescence staining of the cells with anti-FZD7 before and after the transfection with anti-miR-145, revealing an overexpression of FZD7 (A), when compared to the untransfected cells (B). Although there seems to be a marginal increase in FZD7 expression upon transfection with the negative control sequence (C) and the transfection reagent control (D), there is a concentrated increase in fluorescence in the anti-miR-145 transfected sample. FZD7

is localised evenly in the cytoplasm of the cells that were not transfected with anti-miR-145, however when transfected with anti-miR-145, there is intense nuclear and peri-nuclear associated fluorescence.

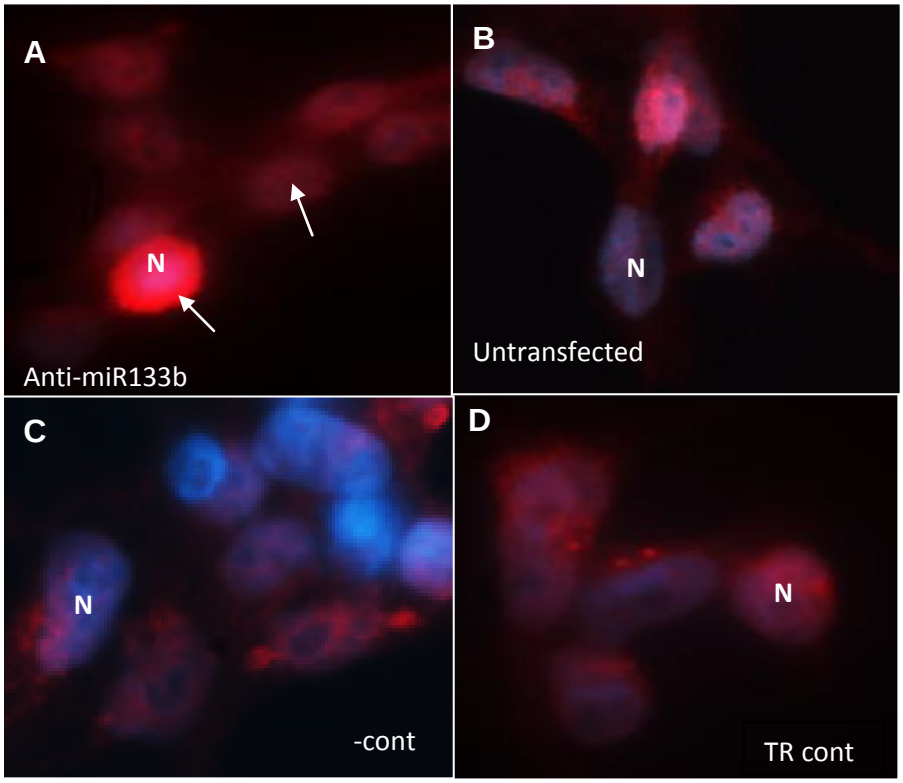

Figure 3.16: Immunofluorescence confocal microscopy image of FBXW11/ßTRCP expression in Anti-miR™ 133b transfected HET1A cells. (A) FBXW11/ßTRCP protein expression is increased in the nucleus and cytoplasm post miR-133b inhibition. B) Untransfected control. C) Negative control D) Transfection reagent control. Blue = nucleus (N), Red = FBXW11/ßTRCP protein (Original magnification of 63x)

To assess the effect of miR-133b on the proteomic expression of FBXW11, HET1A cells were first transfected with anti-miR-133b miRNA inhibitor and then stained by immunofluorescence to detect FBXW11. Figure 3.16 demonstrates the expression of FBXW11 protein pre- and post-transfection with the anti-miR-133b inhibitor. MiR-133b inhibition increases the nuclear expression of FBXW11 (A) when compared to

the untransfected cells (B). FBXW11 localises primarily in the cytoplasm with marginal nuclear staining in the untransfected cells, however FBXW11 does not extend towards the plasma membrane. Upon miR-133b inhibition, FBXW11 is intensely localised to the nucleus and nuclear periphery, with a marginal increase in the cytoplasmic region. The negative control transfected cells (C) and the transfection reagent control cells (D) yield FBXW11 expression patterns similar to the untransfected cells and therefore the intense increase in FBXW11 expression and altered localization is a specific response to anti-miR-133b.

3.4 Discussion

Identifying miRNA targets manually can be a laborious and indirect process. With thousands of identified miRNAs each targeting over 100 target genes, an overwhelming task to identify all targets of identified miRNAs still continues despite the progress made in this field in the past two decades. Furthermore, methods to validate a target can be protracted and expensive, this requiring supplementary evidence before a potential target is selected for validation. Computational programs assist greatly in mining large datasets by using sophisticated algorithms to combine principles of miRNA-target recognition to identify targets in published transcriptomes. In this study computational target prediction programs were utilised to specifically predict gene targets of miR-143, miR-145 and miR-133b to further elucidate the role that these miRNAs play in CRC.

3.4.1 Selection of miRNA target prediction tools

The first objective of this chapter was to select appropriate computational tools to assist in predicting targets for three miRNAs under study. TargetScan, PicTar and DIANA microTv3 were selected for this study based on their favourable scores in precision and sensitivity compared to other available algorithms (Summarised in Table 3.3). Despite the miRanda program exhibiting high levels of sensitivity (Sethupathy *et al.*, 2006; Alexiou *et al.*, 2009) in comparison to most other programs listed, it nevertheless yields exceptionally high numbers of false positives and was therefore not selected for the present analysis.

All three programs used in this study incorporate alignment with orthologous 3'UTRS as a key step. Witkos *et al.* (2011) had previously devised a strategy for miRNA target prediction in which the first step is to use programs considering conservation, particularly since these programs are associated with higher sensitivity and precision and essentially reduce the number of false positives. It is of the assumption that if a miRNA target is predicted by more than one program then it is more likely to be an appropriate target; and therefore only coinciding targets predicted across the three programs were considered valid here.

The sensitivity and precision scores for DIANA MicroTv3, TargetScan and PicTar clearly demonstrated superior performance to other programs (summarised below in Table 3.3) and based on these values the programs were selected for the study. A study by Baek *et al.*, 2008 tested the performance of several miRNA target prediction programs by comparing proteomic changes with quantitative mass-spectrometry using SILAC (stable isotope labelled amino acids in cell culture), after altering the level of miR-223 in mice neutrophils. The correlation of their results to the targets predicted by several programs demonstrated superior performance of TargetScan and PicTar. Furthermore, the context score provided for each prediction in TargetScan was strongly related to protein downregulation.

A similar correlation experiment was completed by Alexiou *et al.*, (2009), whereby a modified SILAC method coupled with mass-spectrometry was used to detect proteomic changes in response to increased expression of 5 miRNAs in HeLa cells. When assessing their results in relation to those received from target prediction programs, PicTar, TargetScan and DIANA-microT exhibited the highest levels of sensitivity (10-12%) and specificity (~50%).

A more recent study used benchmarked datasets to assess the performance of 38 available target prediction programs. Owing to the availability of more validated targets the levels of sensitivity and specificity have increased for all programs, but the performance of DIANA-microT was particularly distinguished compared to all other programs (Fan & Kurgan, 2014).

Table 3.3: miRNA target prediction program features and performance evaluations. *(*Adapted from Witkos *et al*., 2011)

Target Prediction Algorithm	Features		Experimental Evaluation Results							Program Assessment	
	Paremeters considered for the final score	Cross-species conservation	Sethupathy et al, 2006	Baek et al, 2008	Alexiou et al, 2009		Fan and Kurgan et al, 2014			PROs	CONs
			Senstivity	log2-fold change	Precision	Sensitivity	AUC	Sensitivity/ Specificity	Precision		
miRanda	complementarity and free energy binding	Conservation filter	**49%**	0.14	29%	**20%**	0.560	0.437 / 0.667	0.852	Benficial for sites that have imperfect binding within the seed region	Low precision, too many false positives
TargetScan	seed match, 3' complementary local AU content and position contribution	Scoring provided for each result	21%	**0.32**	**51%**	12%	**0.674**	0.823 / 0.389	0.855	Many parameters included in final target scoring, final score correlates with protein downregulation	Sites with poor seed pairing are omitted
TargetScanS	seed match type	only conserved sites are considered	**48%**	-	49%	8%	-	-	-	Simple tool to search for conserved sites with stringent seed pairing	Underestimates miRNAs with multiple target sites
PicTar	binding energy, complementarity and conservation	required pairing at conserved positions	**48%**	0.26	49%	10%	0.538	0.272 / 0.806	0.860	miRNAs with multiple alignments are favoured	Does not predict non-conserved sites
DIANA MicroT	free energy binding and complementarity	dataset of conserved UTRs among human and mouse is used	10%	-	48%	12%	**0.673**	**0.627 / 0.722**	**0.908**	SNR ratio and probability given for each target site, possibility og using own miRNA sequence as an input	Some miRNAs with multiple sites may be omitted
PITA	target site accessibility and energy	user-defined, cut off level	-	0.04	26%	6%	-	-	-	the secondary structure of the 3'UTR is considered for miRNA interaction	Low efficiency compared to other algorithms
Rna22	pattern recognition and folding energy	Not included	-	0.09	24%	6%	-	-	-	Allows to identify sites targeted by yet-undiscovered miRNAs	Low efficiency compared to other algorithms

**Bold text indicates superior performance*

3.4.2 Curating strategy to filter miRNA predicted targets

Under the second objective of developing a curating strategy to filter predicted targets for further functional analysis, the DIANA mirPATH v1 tool was used to effectively mine the large dataset of almost 3500 miRNA targets and to determine the pathways and physiologic processes that are potentially influenced by the combined expression of the miRNAs through their targets. According to initial assumptions, CRC and related pathways were significantly enriched by the combined targets of the miRNA-143, -145 and -133b (Figures 3.9 and 3.10). To infer that the miRNAs have a direct effect on the pathways listed would be precipitous at this stage because the targets used for the enrichment analysis have not all been validated as yet. The results do however provide suggestions for the potential mechanisms in which the miRNAs could contribute to CRC tumourigenesis.

MiR-143, -145 and 133b putative targets predicted through PicTar, TargetScan and DIANA-microT appear to be associated with KEGG pathways in four grouped categories. The first recognizable group involves several types of cancer; CML, CRC, Pancreatic Cancer, Melanoma, Glioma, Prostate Cancer and NSCLC. Further support for the relation of the three miRNAs to the cancers enriched through DIANA mirPATH v1 (pg 106) was obtained from the miRCancer database (http://mircancer.ecu.edu/), which is a collection of miRNA expression profiles in cancer types obtained from published literature *via* text mining in PubMed. Within the database there are 14 published articles on miR-143 downregulation in colon and CRC. In addition to the miRNAs involvement in several other cancers, evidence of miR-143 involvement in Glioma (1), malignant melanoma (1), Non-small cell lung cancer (2), pancreatic cancer (1) and prostate cancer (4) is available within the database. For miR-145, downregulation in colon/CRC (15), Glioma (2), Non-small cell lung cancer (7), Pancreatic Cancer (2) and Prostate Cancer (5), amongst a variety of other malignancies, has been published and is available in the miRCancer database. MiR-133b, despite being less frequently reported in cancer, is involved in CRC (2) and Prostate Cancer (1) amongst other cancers in the database. Note that the numbers in the brackets relate to the number of published articles available in

the miRCancer database. These associations relate consistently to the enriched KEGG pathways within the Cancer category as depicted in Figure 3.9, providing further support to the reliability of the miRNA predicted targets.

Several growth signalling pathways (Wnt, TGF-ß, MAPK and Notch signalling pathways) were also associated with the combined targets predicted for the three miRNAs. CRC has been linked with each enriched pathway providing further hints at the role of the miRNAs in CRC development (Bienz & Clevers, 2000; Xu & Pasche, 2007; Qiao & Wong, 2009; Grossi *et al*., 2014).

When assessing the miRNAs under study in relation to these pathways, a plethora of associations are discovered. In colorectal cell lines miR-145 prevents the translocation of ß-catenin and PAK-4 (serine/threonine p21 activating kinase) into the nucleus by directly targeting catenin δ -1, resulting in downregulation of c-Myc and Cyclin D through the canonical Wnt pathway (Yamada *et al.*, 2013). MiR-145 also acts to directly target PAK-4, eliciting downstream deregulation of the MAPK pathway *via* P-ERK (Wang *et al.*, 2012). Furthermore, miR-145 is responsible for the p-53 mediated repression of c-Myc, a proto-oncogene activated by the Wnt and MAPK pathway (Sachdeva *et al.*, 2009). EGF-R (epidermal growth factor receptor) initiated signalling also downregulates miR-145 *via* ERK1/2 in non-small cell lung cancer cells (Guo *et al.*, 2014). The upregulation of miR-145 by TGF-ß1 in mesenchymal stem cells and TGFBR2 targeting by miR-145 in vascular smooth muscle cells possibly indicates a negative feedback regulatory role of miR-145 in TGF-ß signalling (Mayorga & Penn, 2012; Zhao *et al.*, 2015).

MiR-143 is implicated in the MAPK and Wnt pathways, whereby ubiquitous expression of the miRNA in cooperation with miR-145 targeted the ERK5/c-myc pathway and also the p68/p72/ß-catenin pathway in intestinal tumours of $APC^{Min/+}$ mice (Takaoka *et al.*, 2012). Notably, miR-143 and miR-145 are bicistronic cluster miRNAs transcribed from the same gene and are commonly reported to cooperate in regulating their targets. Moreover, they are regulated similarly as they are derived from the same transcript. The miR-143/145 cluster has been found to be suppressed by RREB1 (Ras responsive element (RRE) protein), a downstream effector of KRAS

in the MAPK pathway (Kent *et al.*, 2013). Repression of the cluster miRNAs is dependent on the constitutively active form of KRAS found in CRC, therefore triggering all effectors in the signalling cascade. Interestingly, miR-145 and miR-143 in their individual mature form, target RREB1 and KRAS respectively, forming an auto-regulation loop of the KRAS signalling pathway in CRC (Kent *et al.*, 2010; Chen *et al.*, 2009). Reminiscent to the relationship of miR-145 with TGF-ß, miR-143 is also induced by TGF-ß in non-small cell lung cancer and is found to target Smad3 (Cheng *et al.*, 2014). Furthermore, the miR-143/145 cluster is induced by TFG-ß and BMP4 (Bone morphogenetic protein 4) in vascular smooth muscle cells (VSMC) (Davis-Dusenbery *et al.*, 2011). As a result of the induction of the miRNA cluster in VSMC, KLF4 is downregulated with miR-145 appearing to play a dominant role in targeting KLF4. KLF4 expression in turn however, negatively regulates the transcription of the miRNA cluster, substantiating an auto-regulation loop.

MiR-133b, despite being less reported in cancer in comparison to miR-143/145, is involved in repressing the MAPK and PI3K/Akt signalling pathways through directly targeting EGFR (Epidermal growth factor receptor) in ovarian cancer (Liu & Li, 2015). MiR-133b has been further implicated in the MAPK pathway whereby ERK1/2 phosphorylation was inhibited by the expression of the miRNA perturbing the signalling pathway. Furthermore, in this same study it was determined that downregulation of the ERK1/2 signalling cascade was also affected by miR-133b targeting of FGFR1 (Fibroblast growth factor receptor 1) and PPP2CA/B (Protein phosphatase 2A catalytic subunit) 3'UTRs. These two genes participate in the Ras-MAPK/ERK1/2 signalling cascade, with FGFR1 functioning as a ligand binding receptor and PPP2CA/B responsible for dephosphorylating molecules involved in critical cellular pathways (Feng *et al.*, 2013).

Despite the miRNAs being involved in distinct growth signalling cascades as described in the preceding paragraphs, their relation to other CRC pathways cannot be dismissed due to the evident cross talk between growth signalling pathways in CRC (Cheruku *et al.*, 2015).

Genes involved in cell to cell and cell to ECM (extracellular matrix) interactions were also shown to be potential targets of the combined expression of miR-143, -145 and 133b. This association is not surprising owing to the contribution of each miRNA to epithelial-mesynchymal transition, a vital step in the development of invasion and metastasis in cancer (Zhai *et al.*, 2015; Lin *et al.*, 2014; Hu *et al.*, 2012; Hu *et al.*, 2014; Ren *et al.*, 2014). Additionally, the significantly enriched pathways discussed above are also closely associated and interlinked in the regulation of EMT in cancer (Linsey & Langhans, 2014).

The last enriched category of miRNA targets relates to neuron signalling and neurodegenerative disorders. Although this association is not within the scope of this dissertation, it cannot be overlooked that EGFR, which is integral to the ErbB, MAPK and PI3K signalling pathways and a target of miR-133b, has been known to be implicated in neuron survival and neurodegenerative disorders (Wagner *et al.*, 2006; Bublil & Yarden, 2007). Furthermore, it has been reported that miRNA expression profiles in cancer have been found to be similar to the profiles in neurodegenerative disorders and the miRNAs are hypothesised to target pathways that are commonly deregulated between the two diseases, or alternatively by targeting gene subsets within each disease type (Du & Pertsemlidis, 2011; Saito & Saito, 2012). Although miR-133b has been reported to be downregulated in cancer, it has however also been reported to be repressed in mid-brain tissue in Parkinson's disease (PD) patients. This involvement in PD was further supported by the finding that a negative feedback regulation loop exists between mir-133b and PitX3, a transcription factor that is involved in the regulation of midbrain dopaminergic neurons (Kim *et al.*, 2007).

3.4.3 Selection of potential miRNA targets for functional analysis

Table 3.2 lists the shortlisted miRNA target genes that were curated and filtered according to the method described in Chapter 3.2. The top three ranked putative targets per miRNA are described below.

With regards to miR-143, there were only six shortlisted predictions according to the curating methodology used here (Table 3.2). Of the six predicted targets, the first

(KRAS) and the third (BCL2) ranked targets have already been experimentally validated. KRAS, which is associated with CRC and MAPK KEGG pathways and ranked first according to the filtering used in this study, has the strongest association with CRC as an established oncogene activating the MAPK pathway (Tan & Du, 2012). Between 35-45% of CRCs harbour KRAS mutations in codon 12 and 13 and therefore genotyping of KRAS in CRC patients has become a mandatory disease management tool due to the non-response to anti-EGFR antibody treatment in KRAS mutated CRC patients. KRAS has been determined to be a direct target for miR-143 in CRC (Chen *et al.*, 2009). In the study by Chen *et al.* (2009), the two conserved KRAS binding sites which have been predicted in the present study have been experimentally validated to bind to miR-143. The third non-conserved binding site demonstrated lower overall scoring compared to the conserved sites, but nevertheless cannot be dismissed as a putative binding site, as all three programs in this study were profoundly reliant on conservation and therefore bias in scoring may be an end result. While KRAS is already known to be a validated target of miR-143 in CRC, for the purpose of the inclusion of a positive control, the KRAS target was selected for functional analysis.

BCL2, an anti-apoptotic protein and ranked third in this study, is crucial in regulating cell death and is targeted by miR-143 in cervical cancer (Liu *et al.*, 2011). It is not certain whether BCL2 targeting by miR-143 occurs in CRC as there is a lack of evidence of the protein being overexpressed (Biden *et al.*, 1999; Ilyas *et al.*, 1998). An inverse correlation of the protein and miR-143 is necessary to infer potential miRNA targeting.

The second ranked putative target is PDGFRA (platelet derived growth factor receptor alpha polypeptide), a subunit of the PDGF receptor that is involved in activating growth signalling pathways such as Ras-MAPK and PI3K which are involved in several cancers, including CRC (Andrae *et al.*, 2008; Heldin *et al.*, 1998). In CRC, PDGFRA expression in association with PDGFRB is associated with lymph node metastasis and advanced disease and therefore increased expression in CRC would make the target attractive as a putative target of miR-143 (Wehler *et al.*, 2008).

MiR-145 is the most referenced miRNA hypothesised to be a tumour suppressor due to its widespread role in tumourigenesis. Of the 11 shortlisted potential targets for this miRNA, two have thus far been validated experimentally; SMAD3 and PPP3CA which are within the top three predicted targets in this study. SMAD3, the highest ranked putative target and a key player in the TGF-ß1 inflammatory pathway, is a direct target of miR-145 in nasopharyngeal cancer and in cystic fibrosis (Huang *et al.*, 2015; Megiorni *et al.*, 2013). In CRC, SMAD3 acts as a tumour suppressor, therefore an inverse correlation between miR-145 and the target cannot be determined (Fleming *et al.*, 2013).

FZD7 (Frizzled 7), a Wnt pathway receptor and the second highest ranked putative miR-145 target, was chosen as the potential target for further functional analysis. FZD7 has been dubbed as an emerging key player in Wnt pathway activation in several cancers (King *et al.*, 2012). Strong oncogenic potential of FZD7 in activating the canonical Wnt pathway in CRC has also been reported and therefore this protein's inverse correlation to miR-145 expression in CRC poses the gene as a reliable candidate for further functional analysis (Ueno *et al.*, 2008). Target prediction in the present study yielded a single 7mer-m8 target site containing the seed region at position 518-524 of the FZD7 3'UTR. The prediction of this individual site by all three target prediction programs using differing algorithms potentially determines the likelihood of the site being a true target. This however would need to be verified experimentally using luciferase reporter assays.

The third highest ranked potential target for miR-145 elucidated in this study is PPP3CA (protein phosphatase 3, catalytic subunit, alpha isozyme/Calcineurin alpha). PPP3CA also exhibits regulation by miR-145 in urothelial cancer cells (Ostenfeld *et al.*, 2010). A role of PPP3CA in CRC however has not been clarified despite its involvement in Wnt and MAPK KEGG pathways and therefore was not considered in this study for further functional analysis.

In considering miR-133b, a total of ten potential targets were shortlisted, of which four are experimentally validated targets (PPP2CA, PPP2CB, SP1 and FGFR1). PPP2CA and PPP2CB together form the protein phosphatase 2A catalytic subunit

PP2AC which is involved in the MAPK-ERK1/2 signalling cascade through dephosphorylating proteins within the signal pathway. Both individual genes have been found to be direct targets of miR-133b in myoblast cells together with FGFR1, a fibroblast growth factor receptor, which was also predicted here as a potential target for miR-133b, albeit only ranked at number 7 (Feng *et al.*, 2013). In CRC, PP2AC seems to function as a tumour suppressor, whereby PP2AC is commonly inactivated in CRC and growth is inhibited upon PP2AC activation (Cristobal *et al.*, 2014). Furthermore, this inactivity of PP2AC is attributed to hyper–phosphorylation of its sub-units and is associated with poor prognosis in CRC (Cristobal *et al.*, 2014). The expression profile of PP2AC in CRC makes it an unlikely target of miR-143 in CRC.

FBXW11 (F-box.WD repeat containing protein 11), also known as ßTrCP2 (beta-Transducin repeat-containing protein) or HOS, is the third ranked potential target for miR-133b. This protein is part of the F-box protein family, exhibiting a 40 residue structural motif known as the F-box, which forms part of an E3 ubiquitin ligase complex SCF (SKP1-Cullin 1–F-box proteins) and is responsible for recognizing substrates targeted for post-translational ubiquitination and proteasomal degradation (Bielskiene *et al.*, 2015). ßTrCP2 is involved in regulation of cell cycle checkpoints and several signal transduction pathways implicated in cancer (Fuchs *et al.*, 2004). An important feature in the context of this study is ßTrCP2 involvement in proteasomal degradation of phosphorylated ß-catenin and subsequent regulation of the Wnt pathway (Voutsadakis, 2008). In CRC, elevated levels ßTrCP mRNA and protein was recognised in colorectal tumours compared to normal tissue and this increase in expression was significantly associated with ß-catenin activation (Ougolkov *et al.*, 2004). Owing to the oncogenic potential of ßTrCP2/FBXW11 in CRC and particularly its involvement in the Wnt pathway, it was selected for further functional analysis.

There were a few noteworthy observations from the shortlisted predicted targets in Table 3.2. Gli3, a protein involved in the Hedgehog signalling pathway and found to be overexpressed in CRC (Kang *et al.*, 2012), was predicted as a potential target of miR-143 in this study. It has however been confirmed as a target of miR-133b in human Sertoli cells, promoting proliferation through the activation of Cyclin B1 and

Cyclin D1 in spermatogenesis regulation (Yoa *et al.*, 2016). Sp1, a transcription factor exhibiting widespread regulation of several biological processes and proven vital in tumourigenesis, is a validated target for miR-133b and miR-145 in gastric cancer cells, as reported by Qui *et al.*, 2014. However in this study, the Sp1 target has only been predicted as a potential target of miR-133b. Smad 3 is a downstream transcription factor of the TGF-ß signalling pathway and is phosphorylated by activated TGFBR1 to translocate into the nucleus to induce the expression of genes responsive to TGF-ß signalling (Xu & Pasche, 2007). Although SMAD3 was the highest ranked predicted target for miR-145 in this study, previous validation of SMAD3 targeting by miR-143 has recently been determined in non-small cell lung cancer (Cheng *et al.*, 2014). It may be possible that as a cluster, these two miRNAs both target SMAD3 in regulating TGF-ß signalling.

CSNK1G3, known as casein kinase 1, gamma 3, is responsible for phosphorylation of proteins involved in key CRC signal transduction pathways such as Wnt signalling (del Valle-Perez *et al.*, 2011), and has been predicted as a potential common target for miR-143 and miR-133b in the present study, thus posing CSNK1G3 as an interesting target for future evaluation.

3.4.4 Functional Analysis of selected potential miRNA targets

KRAS protein was assessed in HET 1A cells transfected with Anti-miR™ 143 and compared to untransfected cells and experimental controls. The increase in fluorescence in the anti-miR-143 transfected cells, when compared to the untransfected cells was an expected response owing to the previously established targeting of KRAS by miR-143 (Chen *et al.*, 2009). KRAS expression in the negative control and transfection control samples were comparable to the untransfected cells, indicating that the increase in KRAS expression in the cells transfected with anti-miR-143 was related to the inhibition of miR-143. The observed increase in regions of cytoplasmic fluorescence, together with staining of the nuclear periphery is consistent with a cytoplasmic inhibition of KRAS translation following knockdown of miR-143. Moreover, from these results it is suggested here that the trafficking of KRAS towards the cytosolic side of the cell membrane is also prevented. The

extension of KRAS from the nuclear periphery to the polar regions of cell is potentially indicative of KRAS transport to the plasma membrane. Transport of Ras proteins to the plasma membrane, reviewed by Hancock (2003), describes that KRAS is part of the RAS GTPase family of which cytosolic modification of a CAAX motif in the C-terminal of the protein is crucial in targeting of the plasma membrane. KRAS is post-translationally modified in the cytosol by prenylation which adds a farsenyl group to the cysteine residue within the CAAX motif at the carboxy terminal. On the cytosolic facing endoplasmic reticulum, the farsenylated C-terminal is then cleaved of the AAX from the CAAX motif by a protease known as *Rce*. Subsequently, the remaining cysteine residue containing a farsenyl group is methylated by the methyltransferase *Icmt*. The resulting C-terminal is hydrophobic, while the rest of the molecule is hydrophilic, making the KRAS protein amenable to plasma membrane integration. It has been determined however that not only is the post-translationally modified KRAS necessary for targeting the plasma-membrane but also for targeting of the endomembrane (Choy *et al.*, 1999). The endomembrane includes several membranous structures and organelles (nuclear membrane, endoplasmic reticulum, Golgi apparatus, lysosomes and vesicles) that function to transport lipids and proteins within the cell. The cytoplasmic pattern of KRAS expression observed here upon miR-143 inhibition is supportive of KRAS trafficking from the nucleus to the plasma membrane *via* the endomembrane.

Frizzled-7 (FZD7) protein expression was assessed by immunofluorescence after transfection of HET-1A cells with a miR-145 inhibitor. FZD7 was found here to be minimally expressed in untransfected HET-1A cells, this being consistent with the report by King *et al.* (2012) of limited FZD7 expression in normal cells. In contrast however, a marked expression of FZD7 protein was reported here in the Anti-miR-145 transfected cells. The increased fluorescence signal was particularly evident in the nucleus and nuclear periphery, potentially indicating an increase in FZD7 protein translation and processing at the endoplasmic reticulum, before being transported to the plasma membrane, where it functions as a seven-pass transmembrane receptor to strongly activate the Wnt pathway.

In this study an inverse correlation has been demonstrated between miR-145 and FZD7 through inhibition of miR-145 and consequent upregulation of FZD7 protein. This inverse correlation was similarly described in the ACHN renal cell carcinoma cell line, whereby transfection with a miR-145 precursor, which essentially induces cellular miR-145 overexpression, resulted in significant downregulation of FZD7 protein (Lu *et al.*, 2014). The inverse correlations with FZD7 protein noted upon inhibition and overexpression of miR-145 provides circumstantial evidence of direct targeting of FZD7 by miR-145. An earlier study by Zhang *et al.*, in 2011 had assessed direct targeting of miR-145 to a predicted binding site in FZD7 3'UTR (518-524) in 293T cells *via* luciferase reporter assay. The predicted binding site within FZD7 3'UTR was cloned into the Xba1 site of a pGL3 reporter vector downstream of the luciferase reporter gene and co-transfected into 293T cells with either a miR-145 precursor or anti-miR-145. Notably, the predicted binding site used in Zhang ***et al's*** (2008) study matched the site predicted in the present research, with the seed region being at position 518-524 of FZD7 3'UTR. However, luciferase activity was unchanged between the cells transfected with either the miR-145 inhibitor or the miR-145 precursor, rejecting the hypothesis of miR-145 targeting this particular seed region. An intriguing observation however is that despite FZD7 expression being limited and almost absent in normal cells (see King *et al.*, 2012), mRNA for the gene has been previously detected in human foetal kidney cells (Sagara *et al.*, 1998). It is plausible that the proteomic output of FZD7 in human embryonic 293T kidney cells is less dependent on miR-145 than in other cells such as CRC cells. This however would require validation with a luciferase reporter assay in a CRC cell line.

FBXW11/ß-TRCP2 expression was detected after anti-miR™ 133b transfection into HET-1A cells. Compared to the untransfected and control cells, FBXW11/ß-TRCP2 displayed clear upregulation, with concentrated nuclear and peri-nuclear expression, while retaining expression in the cytoplasmic region. In the control experiments FBXW11/ ß-TRCP2 was very weakly associated with the nucleus.

The inverse correlation recognised between miR-133b and FBXW11/ß-TRCP2 corroborates with a miRNA-target relationship. FBXW11/β-TrCP2 is known to

localise to both the cytosol and the cell nucleus, which is consistent with expression of FBXW11/ß-TRCP2 reported here with miR-133b inhibition. It is relevant to note here that there are two cellular splice variants of FBXW11/ß-TRCP2 that vary in subcellular localization, with the βTrCP2γ variant residing exclusively in the cytosol and βTrCP2β being solely detectable in the nucleus (Putters *et al.*, 2011). Interestingly, ß-TRCP has also been found to accumulate in the nuclei of cancer cells (Ougolkov *et al.*, 2004). It is plausible here that miR-133b targets the βTrCP2β variant and therefore upon downregulation of miR-133b, βTrCP2β variant protein expression could be induced in the nucleus. In the present study, since the antibody used could not discriminate between ß-TRCP2 splice variants, this will need further validation.

Notably, ß-catenin, a substrate of the E3 ubiquitin ligase containing ß-TRCP2, is commonly overexpressed in the nucleus of CRCcells (Brabletz *et al.*, 1998). It has also been shown that nuclear APC (adenomatous polyposis coli tumour-suppressor gene) and ß-TRCP bind to Wnt regulatory elements and regulate the transcriptional activity of ß-catenin in a cyclical manner, this by either inducing the transcription of Wnt responsive genes, acting to recruit ß-catenin transcriptional coactivators or by reducing transcription with the recruitment of co-repressors to the promoter regions of the Wnt responsive genes (Willert & Jones, 2006). The important role of ß-TRCP2 as a key regulator of ß-catenin stabilization and the expression of Wnt responsive genes makes the protein amenable to deregulation in CRC, and as supported by the immunofluorescence results reported on here, evidence of potential targeting by miR-133b.

Chapter 4: CONCLUSIONS AND FUTURE CONSIDERATIONS

4.1 Conclusions

CRC represents a large percentage of worldwide cancer incidence and mortality, therefore substantiating the importance of understanding the genetic and epigenetic mechanisms underlying tumourigenesis in these cells, which will ultimately allow for the design of innovative and effective diagnostic and therapeutic interventions to reduce the disease burden. Deregulation of miR-145, -143 and -133b in CRC indicates these small molecules as key drivers of tumourigenesis. Analysis of their regulation and biological targets will provide valuable information for CRC therapeutics. These miRNAs also have potential as predictive markers and therapeutic targets.

4.1.1 Epigenetic regulation of miRNAs and cross talk between epigenetic factors

The first part of this study aimed at identifying potential epigenetic regulation, by means of histone deacetylase inhibition and DNA demethylation, of these three putative suppressor miRNAs, in both early and late stage CRC cell lines originally derived from CRC patients. It was determined that all three putative tumour suppressor miRNAs are more susceptible to regulation by DNA demethylation in the late stage DLD1 (Dukes' stage C) CRC cells than the early stage SW1116 (Dukes' stage A) cells, these findings being consistent with published data suggesting that DNA hypermethylation is accumulated during CRC carcinogenesis process, with late Dukes' stages showing higher levels of DNA hypermethylation (Frigola *et al.*, 2005) Conversely, histone deacetylation would seem to play a minimal role in the regulation of miRNAs in the late stage DLD1 CRC cells, since the miRNAs were susceptible to histone deacetylation regulation only in early stage SW1116 cells. The non-response of miRNA-143, -145 and -133b to HDACi (TSA) treatment was an unexpected finding.

At the outset the focus in this study was to detect tumour stage-specific differences in epigenetic regulation of each miRNA. However the results were justified rather by the genotypic differences (MSI *vs* MSS/CIN) between the two cell lines than by their particular Dukes' stage. As the development of MSI and MSS/CIN tumours occur through separate carcinogenesis pathways wherein the accumulation of genetic and epigenetic alterations differ, it is expected that the miRNA levels differ between the two genotypes and are regulated through different mechanisms which ultimately will have an implication on the use of epigenetic therapy in CRC. Additional studies utilizing more MSI and MSS CRC cell lines will need to confirm the variances in epigenetic regulation of miR-143, -145 and 133b.

MiRNAs have also been found to be involved in epigenetic feedback loops with other epigenetic machinery and these miRNAs are referenced as epi-miRNAs. It is postulated that these double negative feedback loops that exist between epigenetic entities and miRNAs are key regulatory circuits in the cell which are crucial to cellular decision making (Osella *et al.*, 2014). Of particular interest in this study, miR-143 was reported to target DNMT3a, a DNA methyltransferase, directly in CRC (Ng *et al.*, 2009). It has thereafter been determined that miR-143 is hypermethylated by the increase in DNMT3 expression (Zhang *et al.*, 2016). Due to the polycistronic nature of the miR-143/145 cluster, it is not surprising that a feedback loop is also found between miR-145 and DNMT3b, wherein miR-145 directly targets DNMT3b by binding to its 3'UTR and in turn, DNMT3b is responsible for downregulation of miR-145 *via* CpG island promoter methylation (Xue *et al.*, 2015). An interesting finding in this particular study was that this double negative feedback loop between miR-145 and DNMT3b had sensitised prostate cancer cells to radiation therapy. With regards to histone acetylation, miR-145 mimics were shown to repress HDAC2 in hepatocellular carcinomas and has been validated as a direct target (Noh *et al.*, 2013). Class I HDACS (HDAC1, 2 and 3) are also upregulated CRC and have a prognostic value as their increased expression relates to poor survival outcomes (Weichert *et al.*, 2008). While these are only a few examples that are relevant to this present study, there is however growing numbers of examples of epi-miRNAs being

discovered which form double negative feedback loops with epigenetic machinery. A model of interplay between epigenetic regulators is depicted in Figure 4.1. In determining the mechanisms of regulation of miRNA, the existence of double negative feedback loops between the regulator and miRNA will be an important feature to consider.

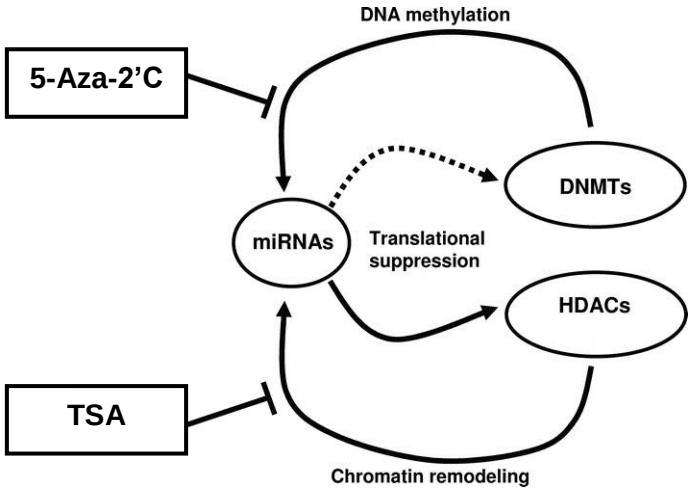

Figure 4.1: Interplay of epigenetic regulation. miRNAs commonly exist in double negative feedback loops with epigenetic machinery. miRNAs regulate the activity of DNMTs and HDACs and in turn the expression of miRNAs are regulated through DNA methylation and chromatin remodelling (Adapted from Chuang & Jones, 2007).

4.1.2 Computational target prediction as a catalyst in determining miRNA functions

The target genes of miRNA-145, -143 and -133b are putative oncogenes that could pose as therapeutic targets for CRC therapy. By using a strategic computational approach, this study aimed to identify the role of these miRNAs in colorectal carcinogenesis by analysing computationally predicted targets through TargetScan, PicTar and DIANA MicroT v3.0 algortihms.

Targets for miR-143, -145 and -133b predicted from all three bioinformatic tools were enriched for KEGG pathways using the DIANA mirPATH v1 algorithm with the combined targets falling into distinct categories; Cancer, Growth signalling pathways,

Cell-cell and cell-ECM interactions and Neuron signalling. The combined list of potential targets were used as it was hypothesised that if all three miRNAs are downregulated in CRC, that they would together affect CRC related pathways. References of each miRNA to these categories had provided initial confidence in the extensive list of targets received (described in Chapter 3.4.2). By selecting the KEGG pathways associated to CRC related pathways and only those targets that were commonly predicted by all three target prediction programs, the list was narrowed down significantly for each miRNA. The Wnt signalling KEGG pathway was found to be most enriched, followed by TGF-ß signalling pathway, “Colorectal cancer”, MAPK signalling pathway and Notch signalling pathway. Cross-talk between these pathways is characteristically associated with CRC carcinogenesis (Cheruku *et al.*, 2015). The ability of the bioinformatics tools selected in this study to accurately predict pathways of involvement in CRC demonstrated credibility of the methodology devised to filter the extensive list of predicted targets. Further confidence in this method was provided when it was determined that out of the six shortlisted targets for miR-143 there were two that have been previously validated experimentally. For miR-145, two out of ten have been validated and for miR-133b four out of the ten shortlisted targets have previously been proven as targets of the miRNA. Elected targets for further functional analysis were based on literature analysis of expression patterns in CRC. Inverse correlations between the miRNA and predicted target in CRC were determined for KRAS (miR-143), FZD7 (miR-145) and FBXW11/ß-TrCP2 (133b). Immunofluorescence staining with KRAS, FZD7 and FBXW11/ß-TrCP2 antibodies after transfection with anti-miR-143, -145 and -133b, respectively, demonstrated a positive corroboration of miRNA-target relationships for each pair and therefore potential therapeutic targets in CRC. Figure 4.2 illustrates the signalling pathways and their cross talk contributing to CRCmetastasis, highlighting in addition the miRNA targets assessed in this study.

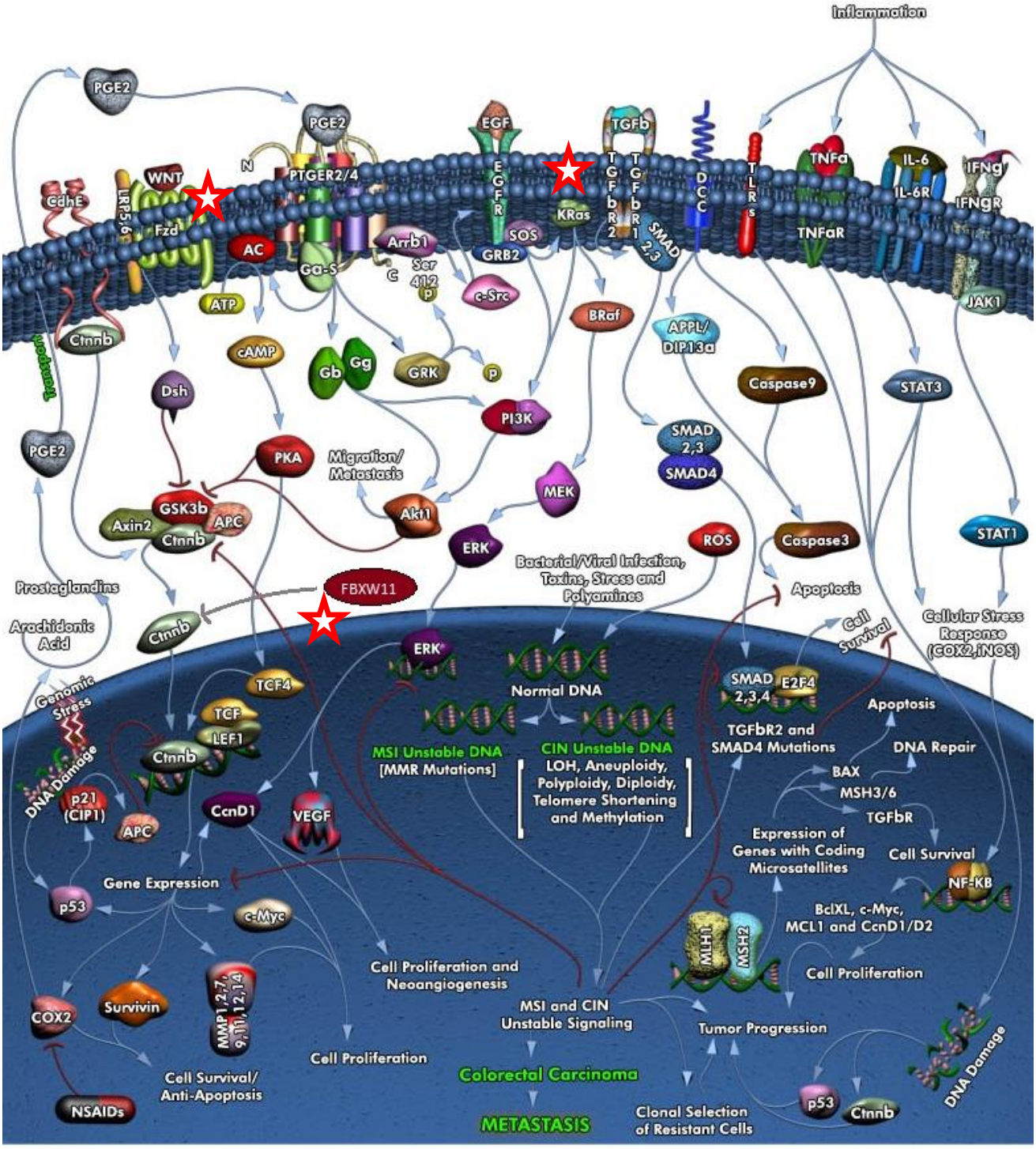

Figure 4.2: Colorectal cancer signalling pathways. Wnt, MAPK and TGF-beta signalling pathways are clear drivers of CRC tumourigenesis. The position of FZD7, KRAS and FBXW11 in the CRC metastatic pathway is indicted by red stars. Qiagen, 2013

The use of bioinformatics in the field of miRNA target prediction has exponentially increased over the last few years. The algorithms being developed now combine complex mathematical models to the principals already known regarding miRNA-target recognition and to expression data to provide reliable outputs (Banwait & Bastola, 2015). The majority of these new algorithms utilise machine learning, the science of allowing a computer to learn and perform functions without being explicitly programmed (Samuel *et al.*, 1959). Machine learning methods are an artificial intelligence-like approach to miRNA target prediction, which involves the development of complex algorithms using sets of validated target datasets and training data from microarrays as templates, in determining binding characteristics or statistically significant features. It then uses the learned characteristics or significant features to determine the maximum likelihood of a miRNA binding to a putative target region (Peterson *et al*., 2014). There are several machine learning applications used to develop algorithms for prediction of miRNAs; including for example, Support Vector Machines, NaÏve Bayes Classifier and Hidden Markov Models being the most commonly used in miRNA target prediction computational tools.

Machine learning methods are fast becoming a preferable method of prediction. Firstly, these supervised learning programs boast higher sensitivity and specificity when compared to programs that rely largely on sequence conservation, which was initially preferred as it reduced the number of false positives (Peterson *et al*., 2014). Programs that rely on conservation are not able to reliably predict non-conserved targets between species, which would result in a bias in the prediction results as would be the case in this study. In this case miRNA targets that have evolved through selection events would not be identified. Furthermore, as these models which are supervised learning systems requires training by experimentally validated datasets, the reliability of the program improves as more validated datasets are available. This essentially means that the predictive power of the programs will only increase as more targets are validated and as these data sets become available.

Despite miRNAs being discovered over two decades ago, identification of miRNA targets is still in an infant stage and therefore the establishment of more validated targets only enhances our ability to predict more targets in future. This clearly justifies the need to identify miRNA targets that are not currently validated and therefore provide us with a deeper understanding of the miRNA footprints in a cell.

4.2 Future Considerations

In this study, regulation patterns of miR-145, -143 and -133b in Dukes' stages A *versus* C and also MSI *versus* MSS genotypes of CRC have been established. These results however could not determine whether these changes in miRNA expression were due to the direct effect of CpG promoter hypermethylation or the presence of acetylated histones and therefore indirect effects on the miRNAs cannot be discounted. It will be of relevance to confirm the findings by performing bisulfite sequence analysis and qPCR to assess the existence of methylated CpG islands in promoter regions of the miRNAs. Additionally, to characterise the change in miRNA expression as a function of histone modification by acetylation, it will be necessary to perform chromatin immunoprecipitation (ChiP) assays.

Conducting the analysis in various MSI and MSS CRC cells will also prove valuable in determining the miRNA regulation mechanisms between both genotypes. Since these genotypes progress through separate carcinogenesis pathways, the differences in epigenetic regulation of miRNAs would affect the treatment optimisation strategies for each genotype.

5-Aza-2'-C and TSA were used as single agents in this study. However, there have been reports of synergistic activity between TSA and 5-Aza-2'-C in reactivating silenced genes and inhibiting cell proliferation (Chai *et al.*, 2008; Cecconi *et al.*, 2009). The influence of synergistic epigenetic treatment on the expression of miR-143, -145 and -133b in CRC could prove valuable as a potential therapeutic intervention.

MiRNA prediction methodology used in this study was successful in shortlisting candidate targets, some of which have already been validated as direct targets of the

miRNAs. However there were limitations in the methods, involving the use of older miRNA datasets through the use of PicTar, a potential conservation bias due to the use of programs that all are reliant upon mapping to orthologous sequences and the inability to detect synergistic target sites, due to the scoring of individual sites by the DIANA MicroT program. These would need to be considered in downstream functional analysis assays and alleviated through the use of new target prediction algorithms that consider updated miRNA-target information, the ability to detect non-conserved and synergistic sites.

KRAS, FZD7 and FBXW11/ß-TrCP2 proteomic expression as evaluated by microscopy increased upon miR-143, -145 and -133b inhibition, respectively. While this provides evidence of a miRNA-target relationship, it will be relevant to detect the mRNA expression of each gene using qPCR to confirm the absence of translational repression upon miRNA inhibition. Finally, to confirm the direct targeting of the miRNAs to each target, the 3'UTR of each gene containing the target sites predicted in the present study should be cloned into a reporter plasmid downstream of a luciferase or green fluorescent protein (GFP) open reading frame. Once the recombinant plasmid is transiently transfected into a neutral host cell together with the associated miRNA, the levels of fluorescence should be assessed to determine direct targeting of the predicted site by each miRNA. Alternatively, Western blotting could be utilised to detect changes in protein expression levels in nuclear and cytoplasmic compartments, respectively. Ultimately, detection of the target protein levels and the miRNAs in CRC and matched normal tissue samples may be of value.

References

Aguilera, O., Fraga, M.F., Ballestar, E., et al. (2006) Epigenetic inactivation of the Wnt antagonist DICKKOPF-1 (DKK-1) gene in human colorectal cancer. *Oncogene*. **25**, 4116–4121

Ahmed, D., Eide, P.W., Eilertsen, I.A., et al. (2013) Epigenetic and genetic features of 24 colon cancer cell lines. *Oncogenesis*. **2**: e71

Akao, Y., Nakagawa, Y., Kitade, Y., et al. (2007) Downregulation of microRNAs-143 and -145 in B-cell malignancies. *Cancer Sci*. **98(12)**: 1914-1920

Akao, Y., Nakagawa, Y., Naoe, T. (2006) MicroRNAs 143 and 145 are possible common onco-microRNAs in human cancers. *Oncol Rep*. **16(4)**: 845-850

Akcakaya, P., Ekelund, S., Kolosenko, I., et al. (2011) miR-185 and miR-133b deregulation is associated with overall survival and metastasis in colorectal cancer. *Int J Oncol*. **39**: 311-318

Alexiou, P., Maragkakis, M., Papadopoulos, G.L., et al. (2009) Lost in translation: an assessment and perspective for computational microRNA target identification. *Bioinformatics*. **25(23)**: 3049-3055

Allfrey, V.G., Faulkner, R., Mirsky, A.E. (1964) Acetylation and methylation of histones and their possible role in the regulation of RNA synthesis. *Proc Natl Acad Sci USA.* **51**: 786-794

American Cancer Society. 2015. *Colorectal Cancer*. [ONLINE] Available at:http://www.cancer.org/acs/groups/content/documents/document/acspc-042280.pdf. [Accessed 27 January 16].

Andrae, J., Gallini, R., Betsholtz, C. (2008) Role of platelet-derived growth factors in physiology and medicine. *Genes Dev*. **22**:1276–1312

Ardekani, A.M., Naeini, M.M. (2010) The Role of MicroRNAs in Human Diseases. *Avicenna J Med Biotechnol*. **2(4)**: 161-179

Ashktorab, H., Belgrave, K., Hosseinkhah, F., et al. (2009) Global Histone H4 Acetylation and HDAC2 Expression in Colon Adenoma and Carcinoma. *Dig Dis Sci.* **54(10)**: 2109-2117

Aukerman, M.J., Sakai, H. (2003) Regulation of flowering time and floral organ identity by a MicroRNA and its APETALA2-like target genes. *Plant Cell*. **15(11)**: 2730-2741

Baek, D., Villen, J., Shin, C., et al. (2008) The impact of microRNAs on protein output. *Nature*. **455(7209)**: 64-71

Balaguer, F., Moreira, L., Lozano, J.J., et al. (2011) Colorectal Cancers with Microsatellite Instability Display Unique miRNA Profiles. *Clin Cancer Res*. **17(19)**: 6239–6249

Bandres, E., Agirre, X., Ramirez, N., et al. (2007) MicroRNAs as cancer players: potential clinical and biological effects. *DNA Cell Biol*. **26(5)**: 273-282

Bandres, E., Cubedo, E., Agirre, X., et al. (2006) Identification by Real-time PCR of 13 mature microRNAs differentially expressed in colorectal cancer and non-tumoral tissues. *Molec Cancer*. **5**: 29 – 39

Banwait, J.K., Bastola D.R. (2015) Contribution of bioinformatics prediction in microRNA-based cancer therapeutics. *Adv Drug Deliv Rev*. **81**: 94-103

Barski, A., Caddapah, S., Cui, K., et al. (2007) High-resolution profiling of histone methylations in the human genome. *Cell*. **129(4)**: 823-837

Bartel, D.P. (2004) MicroRNAs: Genomics, Biogenesis, Mechanism, and Function. *Cell*. **116**: 281-297

Bartel, D.P. (2009) MicroRNAs: Target Recognition and Regulatory Functions. *Cell*. **136**: 215 - 233

Bauer, K.M., Hummon, A.B. (2012) Effects of the miR-143/-145 microRNA cluster on the colon cancer proteome and transcriptome. *J Proteome Res*. **11(9)**: 4744-4754

Ben-Ami, O., Pencovich, N., Lotem, J., et al. (2009) A regulatory interplay between miR-27a and Runx1 during megakaryopoiesis. *Proc Natl Acad Sci U S A*. **106(1)**: 238-243

Bender, C.M., Pao, M.M., Jones, P.A. (1998) Inhibition of DNA methylation by 5-aza-2'-deoxycytidine suppresses the growth of human tumor cell lines. *Cancer Res*. **58(1):** 95-101

Biden, K.G., Simms, L.A., Cummings, M., et al. (1999) Expression of Bcl-2 protein is decreased in colorectal adenocarcinomas with microsatellite instability. Oncogene. **18**: 1245-1249

Bielskiene, K., Bagdoniene, L., Mozuraitiene, J., et al. (2015) E3 ubiquitin ligases as drug targets and prognostic biomarkers in melanoma. *Medicina*. **51**: 1-9

Bienz, M., Clevers, H. (2000) Linking Colorectal Cancer to Wnt Signaling. *Cell*. **103**: 311–320

Bohnsack, M.T., Czaplinkski, K., Gorlich, D. (2004) Exportin 5 is a RanGTP-dependent dsRNA-binding protein that mediates nuclear export of pre-miRNAs. *RNA*. **10(185)**: 185-191

Bommer, G.T., Gerin, I., Feng, Y., et al. (2007) p53-mediated activation of miRNA34 candidate tumor-suppressor genes. *Curr Biol*. **17(15)**: 1298-1307

Borchert, G.M., Lanier, W., Davidson, B.L. (2006) RNA polymerase III transcribes human microRNAs. *Nat Struct Mol Biol*. **13(12)**: 1097-1101

Brabletz, T., Jung, A., Hermann, K., et al. (1998) Nuclear Overexpression of the Oncoprotein ß-Catenin in Colorectal Cancer is localized Predominantly at the Invasion Front. *Pathol. Res. Pract*. **194**: 701-704

Brennecke, J., Hipfner, D.R., Stark, A., et al. (2003) bantam encodes a developmentally regulated microRNA that controls cell proliferation and regulates the proapoptotic gene hid in Drosophila. *Cell*. **113(1)**: 25-36

Brennecke, J., Stark, A., Russell, R.B., et al. (2005) Principles of microRNA-target recognition. *PLoS Biol*. **3(3)**: e85

Bublil, E.M., Yarden, Y. (2007) The EGF receptor family: spearheading a merger of signalling and therapeutics. *Curr Opin Cell Biol*. **19**: 124–134

Cairns, B.R., Kim, Y.J, Sayre, M.H., et al. (1994) A multisubunit complex containing the SWI1/ADR6, SWI2/SNF2, SWI3, SNF5, and SNF6 gene products isolated from yeast. *Proc Natl Acad Sci USA*. **91**: 1950–1954.

Calin, G.A., Sevignani, C., Dumitru, C.D., et al. (2004) Human microRNA genes are frequently located at fragile sites and genomic regions involved in cancers. *Proc Natl Acad Sci U S A*. **101(9)**: 2999–3004

Camps, C., Buffa, F.M., Colella, S., et al. (2008) hsa-miR-210 Is induced by hypoxia and is an independent prognostic factor in breast cancer. *Clin Cancer Res*. **14(5)**: 1340-1348

CANSA. 2010. *National Cancer Registry*. [ONLINE] Available at:http://www.cansa.org.za/files/2015/10/NCR_Final_2010_tables1.pdf. [Accessed 27 January 16]

Cecconi, D., Donadelli., Pozza, E.D., et al. (2009) Synergistic effect of trichostatin A and 5aza2′ deoxycytidine on growth inhibition of pancreatic endocrine tumour cell lines: A proteomic study. *Proteomics.* **9(7)**: 1952-1966

Chai, G., Li, L., Zhou, W., et al. (2008) HDAC Inhibitors Act with 5-aza-2′-Deoxycytidine to Inhibit Cell Proliferation by Suppressing Removal of Incorporated Abases in Lung Cancer Cells. *PLoS ONE.* **3(6)**: e2445

Chang, T.C., Wentzel, E.A., Kent, O.A., et al. (2007) Transactivation of miR-34a by p53 broadly influences gene expression and promotes apoptosis. *Mol Cell*. **26(5)**: 745-752

Chang, T.C., Yu, D., Lee, Y.S., et al. (2008) Widespread microRNA repression by Myc contributes to tumorigenesis. *Nat Genet*. **40(1)**: 43-50

Chen, Y.X., Fang, J.Y., Lu, J., et al (2004) Regulation of histone acetylation on the expression of cell cycle-associated genes in human colon cancer cell lines. *Zhonghua Yi Xue Za Zhi.* **84(4)**: 312-317

Chen, X., Guo, X., Zhang, H., et al. (2009) Role of miR-143 targeting KRAS in colorectal tumorigenesis. *Oncogene*. **28**: 1385-1392

Chen, C., Ridzon, D.A., Broomer, A.J., et al. (2005) Real-time quantification of microRNAs by stem–loop RT–PCR. *Nuc Acids Res*. **33(20)**: e179

Chen, J., Wang, M.B. (2012) The roles of miRNA-143 in colon cancer and therapeutic Implications.*Transl Gastrointest Cancer*. **1(2)**: 160-174

Cheng, T., Hu, C., Yang, H., et al. (2014) Transforming growth factor-β-induced miR‑143 expression in regulation of non-small cell lung cancer cell viability and invasion capacity in vitro and in vivo. *Int J Oncol*. **45(5)**:1977-1988

Cheruku, H.R., Mohamedali, A., Cantor, D.I., et al. (2015) Transforming growth factor-β, MAPK and Wnt signaling interactions in colorectal cancer. *EuPA Open Proteomics*. **8**: 104-115

Chomczynski, P., Sacchi, N. (2006) The single-step method of RNA isolation by acid guanidinium thiocyanate-phenol-chloroform extraction: twenty-something years on. *Nat Protoc*. **1(2)**: 581-585

Choy, E., Chiu, V.K., Selletti, J., et al. (1999) Endomembrane Trafficking of Ras: The CAAX Motif Targets Proteins to the ER and Golgi. *Cell*. **98(1)**: 69-80

Christman, J.K. (2002) 5-Azacytidine and 5-aza-2'-deoxycytidine as inhibitors of DNA methylation: mechanistic studies and their implications for cancer therapy. *Oncogene.* **21**, 5483- 5495

Christobal, I., Manso, R., Rincon, R., et al. (2014) PP2A inhibition is a common event in colorectal cancer and its restoration using FTY720 shows promising therapeutic potential. *Mol Cancer Ther*. **13(4)**: 938-947

Chuang, J.C., Jones, P.A. (2007) Epigenetics and MicroRNAs. *Pediat Res*. **61(5)**: 24-29

Corcoran, D.L., Pandit, K.V., Gordon, B., et al. (2009) Features of Mammalian microRNA Promoters Emerge from Polymerase II Chromatin Immunoprecipitation Data. *PLoS ONE*. **4(4)**: e5279

Cornago, M., Garcia-Alberich, C., Blasco-Angulo, N., et al. (2014) Histone deacetylase inhibitors promote glioma cell death by G2 checkpoint abrogation leading to mitotic catastrophe. *Cell Death Dis*. **5**: e1435

Corney, D.C., Fleksen-Nikitin, A., Godwin, A.K., et al. (2007) MicroRNA-34b and MicroRNA-34c are targets of p53 and cooperate in control of cell proliferation and adhesion-independent growth. *Cancer Res*. **67(18)**: 8433-8438

Cummins, J.M., Velculescu, V.E. (2006) Implications of micro-RNA profiling for cancer diagnosis. *Oncogene*. **25**: 6220-6227

Davis-Dusenbery, B.N., Wu, C., Hata, A. (2011) Micro-managing Vascular Smooth Muscle Cell Differentiation and Phenotypic Modulation. *Arterioscler Thromb Vasc Biol*. **31(11)**: 2370–2377

Dedes, K.J., Dedes, I., Imesch, P., et al. (2009) Acquired vorinostat resistance shows partial cross-resistance to 'second-generation' HDAC inhibitors and correlates with loss of histone acetylation and apoptosis but not with altered HDAC and HAT activities*. Anti-Cancer Drugs*. **20(5)**: 321-333

Del Valle-Perez, B., Arques, O., Vinyoles, M., et al. (2011) Coordinated Action of CK1 Isoforms in Canonical Wnt Signaling. *Molec Cell Biol*. **31(14)**: 2877–2888

Diederichs, S., Haber, D.A. (2006) Sequence variations of microRNAs in human cancer: alterations in predicted secondary structure do not affect processing. *Cancer Res*. **66(12)**: 6097-6104

Ding, Y., Chan, C.Y., Lawrence, C.E. (2004) Sfold web server for statistical folding and rational design of nucleic acids. *Nucl Acids Res*. **32**: 135-141

Doench, J.G., Peterson, C.P., Sharp, P.A. (2003) siRNAs can function as miRNAs. *Genes Dev.* **17(4)**:438-42

Doench, J.G., Sharp, P.A. (2004) Specificity of microRNA target selection in translational repression. *Genes Dev.* **18(5)**: 504-511

Dokmanovic, M., Clarke, C., Marks, P.A. (2007) Histone Deacetylase Inhibitors: Overview and Perspectives. *Mol Cancer Res*. **5(10)**: 981-989

Dou, L., Zheng, D., Li, J., et al. (2012) Methylation-mediated repression of microRNA-143 enhances MLL-AF4 oncogene expression. *Oncogene*. **31(4)**: 507-517

Du, L., Pertsemlidis, A. (2011) Cancer and neurodegenerative disorders: pathogenic convergence through microRNA regulation*. J Molec Cell Biol*. **3**, 176–180

Duan, H., Heckman, C.A., Boxer, L.M. (2005) Histone deacetylase inhibitors down-regulate bcl-2 expression and induce apoptosis in t(14;18) lymphomas. *Mol Cell Biol*. **25(5)**: 1608-1619

Duan, F.T., Qian, F., Fang, K., et al. (2013) miR-133b, a muscle-specific microRNA, is a novel prognostic marker that participates in the progression of human colorectal cancer *via* regulation of CXCR4 expression. *Molec Cancer*., **12**: 164-176

Dukes, C.E. (1932) The classification of cancer of the rectum. *J Pathol Bacteriol*. **35 (3)**: 323-332

Eissenberg, J.C., Elgin, S.C.R. (2014) Heterochromatin and Euchromatin. *eLS*. 1-9

Ernst, C., McGowan, P.O., Deleva, V., et al. (2008) The effects of pH on DNA methylation state: In vitro and post-mortem brain studies. *J. Neurosci. Methods.* **174 (2008):** 123-125

Esau, C., Kang, X., Peralta, E., et al. (2004) MicroRNA-143 regulates adipocyte differentiation. *J Biol Chem*. **279(50)**: 52361-52365

Fan, X., Kurgan, L. (2014) Comprehensive overview and assessment of computational prediction of microRNA targets in animals. *Brief Bioinform*, **2014**, 1–15

Fearon, E.R., Vogelstein, B. (1990) A genetic model for colorectal tumorigenesis. *Cell*. **61**: 759-767

Fedier, A., Dedes, K.J., Imesch, P., et al. (2007) The histone deacetylase inhibitors suberoylanilide hydroxamic (Vorinostat) and valproic acid induce irreversible and MDR1-independent resistance in human colon cancer cells. *Int J Oncol*. **31**: 633-641

Feinberg, A.P., Tycko, B. (2004) The history of cancer epigenetics. *Nature Rev Cancer*. **4**: 143-153

Felsenfeld, G., Groudine, M. Epigenetic Mechanisms of Gene Regulation. *Nature*. **421**: 448-453

Fenaux, P. (2005) Inhibitors of DNA methylation: beyond myelodysplastic syndromes. *Nat Clin Prac Oncol*. **2**: S36-S44

Feng, Y., Niu, L.L., Wei, W., et al. (2013) A feedback circuit between miR-133 and the ERK1/2 pathway involving an exquisite mechanism for regulating myoblast proliferation and differentiation. *Cell Death Dis.* **4**, e934

Ferreira, D., Adega, F., Chaves, R. (2013) The Importance of Cancer Cell Lines as in vitro Models in Cancer Methylome Analysis and Anticancer Drugs Testing.

Oncogenomics and Cancer Proteomics - Novel Approaches in Biomarkers Discovery and Therapeutic Targets in Cancer. **Chapter 6**: DOI: 10.5772/53110

Fleming, N.I., Jorissen, R.N., Mouradov, D., et al. (2013) SMAD2, SMAD3 and SMAD4 Mutations in Colorectal Cancer. *Cancer Res*. **73(2)**: 725-735

Friedman, R.C., Farh, K.K., Burge, C.B. (2009) Most mammalian mRNAs are conserved targets of microRNAs. *Genome Res.* **19(1)**: 92-105

Frigola, J., Sole, X., Paz, M.F. (2005) Differential DNA hypermethylation and hypomethylation signatures in colorectal cancer. *Hum Mol Gen.* **14(2)**: 319-326

Fuchs, S.Y., Spiegelman, V.S., Kumar, K.G.S. (2004) The many faces of b-TrCP E3 ubiquitin ligases: reflections in the magic mirror of cancer. *Oncogene*. **23**, 2028–2036

Fukuhara, S., Chang, I., Mitsui, Y., et al. (2014) DNA mismatch repair gene MLH1 induces apoptosis in prostate cancer cells. *Oncotarget*. **5(22)**: 11297–11307

Giannakakis, A., Sandaltzopoulos, R., Greshock, J., et al. (2008) miR-210 links hypoxia with cell cycle regulation and is deleted in human epithelial ovarian cancer. *Cancer Biol Ther*. **7(2)**: 255-264

GLOBOCAN. 2012. *Colorectal Cancer Estimated Incidence, Mortality and Prevalence Worldwide in 2012*. [ONLINE] Available at: http://globocan.iarc.fr/Pages/fact_sheets_cancer.aspx. [Accessed 26 January 16].

Grimson, A., Farh, K.K., Johnston, W.K., et al. (2007) MicroRNA targeting specificity in mammals: determinants beyond seed pairing. *Mol Cell*. **27(1)**: 91-105

Grossi, V., Peserico, A., Tezil, T. (2014) p38α MAPK pathway: A key factor in colorectal cancer therapy and chemoresistance. *World J Gastroenterol*. **20(29)**: 9744–9758

Guenther, M.G., Levine, S.S., Boyer, L.A., et al. (2007) A chromatin landmark and transcription initiation at most promoters in human cells. *Cell*. **130(1)**: 77-88

Guo, Y.H., Zhang, C., Shi, J., et al. (2014) Abnormal activation of the EGFR signaling pathway mediates the downregulation of miR‑145 through the ERK1/2 in non-small cell lung cancer. *Oncol Rep*. **31(4)**: 1940-1946

Haggar, F.A., Boushey R.P. (2009) Colorectal cancer epidemiology: incidence, mortality, survival, and risk factors. *Clin Colon Rectal Surg*. **22(4)**: 191-197

Hammond, S.M. (2006) MicroRNA therapeutics: a new niche for antisense nucleic acids. *Trends Mol Med*. **12(3)**: 99-101

Han, J., Lee, Y., Yeom, K.H., et al. (2004) The Drosha–DGCR8 complex in primary microRNA processing. *Genes Dev*. **18**: 3016-3027

Hancock,F.H. (2003) Ras proteins: different signals from different locations. *Nature Rev Mol Cell Biol.* **4**: 373-385

Harada, K., Baba, Y., Ishimoto, T., et al. (2015) Suppressor microRNA-145 Is Epigenetically Regulated by Promoter Hypermethylation in Esophageal Squamous Cell Carcinoma. *Anticancer Res*. **35(9)**: 4617-4624

Hawkins, N., Norrie, M., Cheong, K., et al. (2002) CpG island methylation in sporadic colorectal cancers and its relationship to microsatellite instability. *Gastroenterol*. **122(5)**: 1376-1387

He, L., He, X., Lim, L.P., et al. (2007) A microRNA component of the p53 tumour suppressor network. *Nature*. **447(7148)**: 1130-1134

Hebbes, T.R., Thorne, A.W., Crane-Robinson, C. A direct link between core histone acetylation and transcriptionally active chromatin. *EMBO J*. **7(5)**: 1395-1402

Heldin, C.H., Östman, A., Rönnstrand, L. (1998) Signal transduction *via* platelet-derived growth factor receptors. *Biochim Biophys Acta*.**1378**: 79-113

Herman, J.G., Latif, F., Weng, Y. (1994) Silencing of the VHL tumor-suppressor gene by DNA methylation in renal carcinoma. *Proc Natl Acad Sci U S A*. **91(21)**: 9700-9704

Ho, Y.K., Xu, W.T., Too, H.P. (2013) Direct Quantification of mRNA and miRNA from Cell Lysates Using Reverse Transcription Real Time PCR: A Multidimensional Analysis of the Performance of Reagents and Workflows. *PLoS ONE*. **8(9)**: e72463.

Holliday, R. (1979) A new theory of carcinogenesis. *Br J Cancer*. **40(4)**: 513-522

Hopkins Colon Cancer Center. 2014. *TNM Staging*. [ONLINE] Available at:http://www.hopkinscoloncancercenter.org/CMS/CMS_Page.aspx?CurrentUDV=59

&CMS_Page_ID=EEA2CD91-3276-4123-BEEB-BAF1984D20C7. [Accessed 06 August 15].

Hrašovec, S., Glavač, D. (2012) MicroRNAs as novel biomarkers in colorectal cancer. *Front Genet.* **3(180**): 1-9

Hu, G., Chen, D., Li, X., et al. (2010) miR-133b regulates the MET proto-oncogene and inhibits the growth of colorectal cancer cells in vitro and in vivo. *Cancer Biol Ther*. **10(2)**:190-197

Hu, J., Guo, H., Li, I., et al. (2013) MiR-145 regulates epithelial to mesenchymal transition of breast cancer cells by targeting Oct4. *PLoS One*. **7(9)**: e45965

Hu, J., Qiu, M., Jiang, F., et al. (2014) MiR-145 regulates cancer stem-like properties and epithelial-to-mesenchymal transition in lung adenocarcinoma-initiating cells. *Tumour Biol*. **35(9)**: 8953-8961

Huang, H., Sun, P., Lei, Z., et al. (2015) miR145 inhibits invasion and metastasis by directly targeting Smad3 in nasopharyngeal cancer. *Tumor Biol*. **36(6)**:4123-4131

Hudson, R.S., Yi, M., Esposito, D., et al. (2011) MicroRNA-1 is a candidate tumor suppressor and prognostic marker in human prostate cancer. *Nucl Acids Res*. **2011**: 1-15

Iino, H., Simms, L., Young, J., et al. (2000) DNA microsatellite instability and mismatch repair protein loss in adenomas presenting in hereditary non-polyposis colorectal cancer. *Gut.* **47**: 37–42

Iio, A., Nakagawa, Y., Hirata, I., et al. (2010) Identification of non-coding RNAs embracing microRNA-143/145 cluster. *Molec Cancer*. **9**: 136-143

Ilyas, M., Hao, X-P., Wilkinson, K., et al. (1998) Loss of Bcl-2 expression correlates with tumour recurrence in colorectal cancer. *Gut*. **43**: 383-387

Imesch, P., Dedes, K.J., Furlato, M., et al. (2009) MLH1 protects from resistance acquisition by the histone deacetylase inhibitor trichostatin A in colon tumor cells. *Int J Oncol*. **35**: 631-640

Kang, H.N., Oh, S.C., Kim, J.S., et al. (2012) Abrogation of Gli3 expression suppresses the growth of colon cancer cells *via* activation of p53. *Exp Cell Res*. **318**: 539-549

Kantarijan, H.M., Cortes, J. (2006) New strategies in chronic myeloid leukemia. *Int J Hematol*. **83(4):** 289-293

Kao, J., Salari, K., Bocanegra, M., et al. (2009) Molecular profiling of breast cancer cell lines defines relevant tumor models and provides a resource for cancer gene discovery. *PLoS One*. **4(7)**: e6146

Kapuscinski, J. (1995) DAPI: a DNA-specific fluorescent probe. *Biotech Histochem*. **70(5)**: 220-233

Karczmarski, J., Rubel, T., Paziewska, A., et al. (2014) Histone H3 lysine 27 acetylation is altered in colon cancer. *Clin Proteomics*. **11**: 24-34

Kent, O.A., Chivukula, R.R., Mellendore, M. (2010) Repression of the miR-143/145 cluster by oncogenic Ras initiates a tumor-promoting feed-forward pathway. *Genes Dev*. **24(24)**: 2754-2759

Kent, O.A., Fox-Talbot, K., Halushka, M.K. (2013) RREB1 repressed miR-143/145 modulates KRAS signaling through downregulation of multiple targets. *Oncogene*. **32(20)**: 2576-2585

Kertesz, M., Iovino, N., Unnerstall, U., et al. (2007) The role of site accessibility in microRNA target recognition. *Nat Genet*. **39(10)**: 1278-1284

Kessler, Y., Helfer-Hungerbuehler, A.K., Cattori, V., et al. (2009) Quantitative TaqMan® real-time PCR assays for gene expression normalisation in feline tissues. *BMC Mol Biol*. **10(106)**: 1-14

Kim, J., Inoue, K., Ishii, J., et al. (2007) A microRNA feedback circuit in midbrain dopamine neurons. *Science*. **317(5842)**: 1220-1224

Kim, H.R., Kim, E.J., Yang, S.H., et al. (2006) Trichostatin A induces apoptosis in lung cancer cells *via* simultaneous activation of the death receptor-mediated and mitochondrial pathway? *Exp Mol Med*. **38(6)**: 616-624

Kim, V.N., Nam, J.W. (2006) Genomics of microRNA. *Trends Genet.* **22(3)**: 165-173

King, T.D., Zhang, W., Suto, M.J., et al. (2012) Frizzled7 as an emerging target for cancer therapy. *Cell Signal*. **24(4)**: 846–851

Kinzler, K.W., Vogelstein, B. (1996) Lessons from hereditary colorectal cancer. *Cell.* **87(2)**: 159-170

Kiriakidou, M., Nelson, P.T., Kouranov, A., et al. (2004) A combined computational-experimental approach predicts human microRNA targets. *Genes Dev*. **18**:1165–1178

Kouzarides, T. (2007) Chromatin modifications and their function. *Cell.* **128(4)**: 693-705

Krek, A., Grün, D., Poy, M.N., et al. (2005) Combinatorial microRNA target predictions. *Nat Genet*. 3**7(5)**:495-500

Kuhn, D.E., Martin, M.M., Feldman, D.S., et al. (2008) Experimental Validation of miRNA Targets. *Methods*. **44(1)**: 47–54

Kulis, M., Esteller, M. (2010) DNA methylation and cancer. *Adv Genet*. **70**: 27-56

Lalkhen, A.G., McCluskey, A. (2008) Clinical tests: sensitivity and specificity. *Continuing Education in Anaesthesia, Critical Care & Pain*. **8(6)**: 221-223

Lall, S., Grün, D., Krek, A., et al. (2006) A genome-wide map of conserved microRNA targets in C. elegans. *Curr Biol*. **16(5)**:460-471

Lanza, G., Ferracin, M., Gafa, R., et al. (2007) mRNA/microRNA gene expression profile in microsatellite unstable colorectal cancer*. Mol Cancer.* **6(54)**: 1-11

Lee, C.R., Risom, T., Strauss, W.M. (2007) Evolutionary conservation of microRNA regulatory circuits: an examination of microRNA gene complexity and conserved microRNA-target interactions through metazoan phylogeny. *DNA Cell Biol*. **26(4)**: 209-218

Lee, R.C., Ambros, V. (2001) An extensive class of small RNAs in Caenorhabditis elegans. Science. **294(5543)**:862-864

Lee, R.C., Feinbaum, R.L., Ambros, V. (1993) The C. elegans heterochronic gene lin-4 encodes small RNAs with antisense complementarity to lin-14. *Cell*. **75(5)**: 843-854

Lee, Y., Jeon, K., Lee, J.T., et al (2002) MicroRNA maturation: stepwise processing and subcellular localization. *EMBO J*. **21(17)**: 4663–4670

Lee, Y., Kim, M., Han, J., et al. (2004) MicroRNA genes are transcribed by RNA polymerase II. *EMBO J*. **23(20)**: 4051-4060

Lengauer, C., Kinzler, K.W., Vogelstein, B. (1998) Genetic instabilities in human cancers. *Nature.* **396**: 643-649

Leslie, A., Carey, F.A., Pratt, N.R., et al (2002) The colorectal adenoma-carcinoma sequence*. Br J Surg*. **89(7)**: 845-860

Lewis, B.P., Burge, C.B., Bartel, D.P. (2005) Conserved Seed Pairing, Often Flanked by Adenosines, Indicates that Thousands of Human Genes are MicroRNA Targets. *Cell*. **120(1)**: 15-20

Lewis, B.P., Shih, I.H., Jones-Rhoades, M.W., et al. (2003) Prediction of mammalian microRNA targets. *Cell*. **115(7)**: 787-798

Li, E., Bestor, T.H., Jaenisch, R. (1992) Targeted mutation of the DNA methyltransferase gene results in embryonic lethality. *Cell*. **69(6)**: 915-926

Liggett, W.H.Jr., Sidransky, D. (1998) Role of the p16 tumor suppressor gene in cancer*. J Clin Oncol*. **16(3)**: 1197-1206

Lin, C.W., Kao, S.H., Yang, P.C. (2014) The miRNAs and epithelial-mesenchymal transition in cancers. *Curr Pharm Des*.**20(33)**: 5309-5318

Lin, C.W., Li, X.R., Zhang, Y., et al. TAp63 suppress metastasis *via* miR-133b in colon cancer cells. *Br J Cancer*. **110**: 2310-2320

Lindsey, S., Langhans, S.A. (2012) Crosstalk of Oncogenic Signaling Pathways during Epithelial-Mesenchymal Transition. *Front Oncol*.**4**(358): 1-10

Liu, Y., He, G., Wang, Y., et al. (2013) MCM-2 is a therapeutic target of Trichostatin A in colon cancer cells. *Toxicol Lett*. **221(1):** 23-30

Liu, C.L., Kaplan, T., Kim, M., et al. (2005) Single-Nucleosome Mapping of Histone Modifications in S. Cerevisiae. *PloS Biology*. **3(10)**: e328

Liu, X., Li, G. (2015) MicroRNA-133b inhibits proliferation and invasion of ovarian cancer cells through Akt and Erk1/2 inactivation by targeting epidermal growth factor receptor. *Int J Clin Exp Pathol.* **8(9)**: 10605–10614

Liu, L., Yu, X., Guo, X., et al. (2012) miR-143 is downregulated in cervical cancer and promotes apoptosis and inhibits tumor formation by targeting Bcl-2. *Mol Med Rep*. **5**: 753-760

Livak, K.J., Schmittgen, T.D. (2001) Analysis of Relative Gene Expression Data Using Real-Time Quantitative PCR and the 22DDCT Method. *Methods*. **25**, 402–408

Lorenz, R., Bernhart, S.H., Siederdissen, C.H., et al. (2011) ViennaRNA Package 2.0. *Algorithm Mol Biol*. **6**: 26-40

Lu, R., Ji, Z., Li, X., et al. (2014) miR‑145 functions as tumor suppressor and targets two oncogenes, ANGPT2 and NEDD9, in renal cell carcinoma. *Cancer Res Clin Oncol.***140**:387–397

Lujambio, A., Calin, G.A., Villanueva, A., et al. (2008) A microRNA DNA methylation signature for human cancer metastasis. *Proc Natl Acad Sci U S A*. **105(36)**: 13556-13561

Lujambio, A., Esteller, M. (2009) How epigenetics can explain human metastasis: a new role for microRNAs. *Cell Cycle*. **8(3)**: 377-382

Lujambio, A., Ropero, A., Ballestar, E., et al. (2007) Genetic Unmasking of an Epigenetically Silenced microRNA in Human Cancer Cells. *Cancer Res*. **67(4)**: 1424 – 1429

Lv, L., Zhou, J., Lin, C., et al. (2015). DNA methylation is involved in the aberrant expression of miR-133b in colorectal cancer cells. *Oncol Lett*. **10**: 907-912

Macleod, K.F., Sherry, N., Hannon, G., et al. (1995) p53-dependent and independent expression of p21 during cell growth, differentiation and DNA damage. *Genes Dev*. **9**: 935-944

Maeda, K., Kawakami, K., Ishida, Y., et al. (2003) Hypermethylation of the CDKN2A gene in colorectal cancer is associated with shorter survival. *Oncol Rep*.**10**: 935-938

Margolis, D. (2005) Depletion of Latent HIV Infection In Vivo: Moving Towards Eradication of HIV Infection. *The PRN Notebook.* **10(4)**: 7-10

Marina, O., Trujillo, A., Sanders, C., et al. (2010) The Effects of Acetic Acid on Mammalian Cells. *Biomedical Optics and 3-D Imaging*. **OSA Technical Digest (CD) (Optical Society of America, 2010)**: paper BSuD74

Marson, A., Levine, S.S., Cole, M.F., et al. (2008) Connecting microRNA genes to the core transcriptional regulatory circuitry of embryonic stem cells. *Cell*. **134(3)**: 521-533

Mayorga, M.E., Penn, M.S. (2012) miR-145 is differentially regulated by TGF-β1 and ischaemia and targets Disabled-2 expression and wnt/β-catenin activity. *J Cell Mol Med*. **16(5)**: 1106-1113

Megiorni, F., Cialfi, S., Cimino, G.,et al. Elevated levels of miR-145 correlate with SMAD3 down-regulation in Cystic Fibrosis patients. *J Cys Fibros*.**12**: 797–802

Meng, J., Zhang, H.H., Zhou, C.X., et al. (2012) The histone deacetylase inhibitor trichostatin A induces cell cycle arrest and apoptosis in colorectal cancer cells *via* p53-dependent and -independent pathways. *Oncol Rep*. **28(1):** 384-388

Merlo, A., Herman, J.G., Mao, L. (1995) 5' CpG island methylation is associated with transcriptional silencing of the tumour suppressor p16/CDKN2/MTS1 in human cancers. *Nat Med*. **1(7)**: 686-692

Michael, M.Z., O'Connor, S.M., van Holst Pellekaan, N.G., et al. Reduced accumulation of specific microRNAs in colorectal neoplasia. *Mol Cancer Res*. **1(12)**: 882-891

Miriadson, J.M. (2008) Class I Histone Deacetylase Expression Has Independent Prognostic Impact in Human Colorectal Cancer: Specific Role of Class I Histone Deacetylases In vitro and In vivo. *Epigenetics*. **3(1)**: 28-37

Moore, P.S., Barbi, S., Donadelli, M., et al. (2004) Gene expression profiling after treatment with the histone deacetylase inhibitor trichostatin A reveals altered expression of both pro- and anti-apoptotic genes in pancreatic adenocarcinoma cells. *Biochim Biophys Acta*. **1693(3)**: 167-176

Nakazawa, T., Kondo, T., Ma, D., et al. (2012) Global histone modification of histone H3 in colorectal cancer and its precursor lesions. *Hum Pathol*. **43**: 834-842

Nasser, M.W., Datta, J., Nuovo, G., et al. (2008) Down-regulation of micro-RNA-1 (miR-1) in lung cancer. Suppression of tumorigenic property of lung cancer cells and

their sensitization to doxorubicin-induced apoptosis by miR-1. *J Biol Chem*. **283(48)**: 33394-33405

Ng, E.K.O., Tsang, W. P., Ng, S.S.M., et al. (2009) MicroRNA-143 targets DNA methyltransferases 3A in colorectal cancer. *Br J Cancer*. **101**: 699 – 706

Nielsen, C.B., Shomron, N., Sandberg, R., et al. (2007) Determinants of targeting by endogenous and exogenous microRNAs and siRNAs. *RNA*. **11**: 1894-1910

Noh, J. H., Chang, Y. G., Kim, M.G., et al. (2013) MiR-145 functions as a tumor suppressor by directly targeting histone deacetylase 2 in liver cancer. *Cancer Lett.* **335**: 455-462

O'Donnell, K.A., Wentzel, E.A., Zeller, K.I., et al. (2005) c-Myc-regulated microRNAs modulate E2F1 expression. *Nature*. **435(7043)**: 839-843

O'Hara, S.P., Mott, J.L., Splinter, P.L., et al. (2009) MicroRNAs: key modulators of posttranscriptional gene expression. *Gastroenterol*. **136(1)**: 17-25

Okano, M., Bell, D.W., Haber, D.A., et al. (1999) DNA Methyltransferases Dnmt3a and Dnmt3b Are Essential for De Novo Methylation and Mammalian Development. *Cell*. **99**: 247-257

Osella, M., Riba, A., Testori, A., et al. (2014) Interplay of microRNA and epigenetic regulation in the human regulatory network. *Front Genet*. **5(345)**: 1-10

Ostenfeld, M.S., Bramsen, J.B., Lamy, P., et al (2010) miR-145 induces caspase-dependent and -independent cell death in urothelial cancer cell lines with targeting of an expression signature present in Ta bladder tumors. *Oncogene*. **29**, 1073–1084

Oudet, P., Gross-Bellard, M., Chambon, P. (1975) Electron microscopic and biochemical evidence that chromatin structure is a repeating unit. *Cell.* **4**: 281–300

Ougolkov, A., Zhang., Yamashita., et al. (2004) Associations Among ß-TrCP, an E3 Ubiquitin Ligase Receptor, ß-Catenin, and NF-κB in Colorectal Cancer. *J Nat Cancer Inst*. **96(15)**: 1161-1170

Ozsolak, F., Poling, L.L., Wang, Z., et al. (2008) Chromatin structure analyses identify miRNA promoters. *Genes Dev*. **22**: 3172-3183

Pagliuca, A., Valvo, C., Fabrizi, E., et al. (2012) Analysis of the combined action of miR-143 and miR-145 on oncogenic pathways in colorectal cancer cells reveals a coordinate program of gene repression. *Oncogene*. 1-8

Pal, R., Mamidi, M.K., Das, A.K., et al. (2012) Diverse effects of dimethyl sulfoxide (DMSO) on the differentiation potential of human embryonic stem cells. *Arch Toxicol*. **86(4)**: 651-661

Palii, S.S., van Emburgh, B.O., Sankpal, U.T., et al. (2008) DNA Methylation Inhibitor 5-Aza-2'- Deoxycytidine Induces Reversible Genome-Wide DNA Damage That Is Distinctly Influenced by DNA Methyltransferases 1 and 3B. *Mol Cell Biol*. **28(2)**: 752–771

Peltomaki, P. (2001) Deficient DNA mismatch repair: a common etiologic factor for colon cancer. *Hum Mol Gen*. **10 (7)**: 735-740

Peterson, S.M., Thompson, J.A., Ufkin, M.L., et al. (2014) Common features of microRNA target prediction tools. *Front Genet*. **5(23)**: 1-10

Phillips, T., Shaw, K. (2008) Chromatin Remodeling in Eukaryotes. *Nature Education.* **1(1)**: 209-216

Pliml, J., Sorm, F. (1964) Synthesis of 2`-deoxy-D-ribofuranosyl-5-azacytosine. *Coll Czech Chem Commun.* **29**:2576–2577.

Plumb, J.A., Strathdee, G., Sludden J., et al. (2000) Reversal of drug resistance in human tumor xenografts by 2'-deoxy-5-azacytidine-induced demethylation of the hMLH1 gene promoter. *Cancer Res*. **60(21)**: 6039-6044

Powell, S.M., Zilz, N., Beazer-Barclay, Y., et al (1992) APC mutations occur early during colorectal tumorigenesis. *Nature.* **359 (6392)**: 235-237

Pradhan, S., Bacolla, A., Wells, R.D., et al. (1999) Recombinant Human DNA (Cytosine-5) Methyltransferase. *J Biol Chem*. **274(46)**: 33002-33010

Putters, J., Slotman, J.A., Gerlach, J.P., et al. (2011) Specificity, location and function of βTrCP isoforms and their splice variants. *Cell Signalling*. **23**: 641-647

Qiagen. 2013. *Colorectal Cancer Metastasis*. [ONLINE] Available at: https://www.qiagen.com/be/shop/genes-and-pathways/pathway-details/?pwid=121. [Accessed 05 February 16].

Qian, X., Yu, J., Yin, Yu., et al. (2013) MicroRNA-143 inhibits tumor growth and angiogenesis and sensitizes chemosensitivity to oxaliplatin in colorectal cancers. *Cell Cycle*. **12(9)**: 1385–1394

Qiao, L., Wong, B. C.Y. (2009) Role of Notch signaling in colorectal cancer. *Carcinogenesis.* **30(12)**: 1979–1986

Qin, T., Jelinek, J., Si, J., et al. (2009) Mechanisms of resistance to 5-aza-2′-deoxycytidine in human cancer cell lines. *Blood*. **113(3)**: 659–667

Qiu, T., Zhou, J., Wang, J., et al. (2014) MiR-145, miR-133a and miR-133b inhibit proliferation, migration, invasion and cell cycle progression *via* targeting transcription factor Sp1 in gastric cancer. *FEBS Lett*. **588(7)**: 1168-1177

Raver-Shapira, N., Marciano, E., Meiri, E., et al. (2007) Transcriptional activation of miR-34a contributes to p53-mediated apoptosis. *Mol Cell*. **26(5)**: 731-743

Ren, D., Wang, M., Guo, W., et al. (2014) Double-negative feedback loop between ZEB2 and miR-145 regulates epithelial-mesenchymal transition and stem cell properties in prostate cancer cells. *Cell Tissue Res.* **358(3)**: 763-778

Rhodes, L.V., Nitschke, A.M., Segar, H.C., et al. (2012) The histone deacetylase inhibitor trichostatin A alters microRNA expression profiles in apoptosis-resistant breast cancer cells. *Oncol Rep*. **27(1)**: 10–16

Richon, V.M., Sandhoff, T.W., Rifkind, R.A., et al. (2000) Histone deacetylase inhibitor selectively induces p21WAF1 expression and gene-associated histone acetylation. *Proc Natl Acad Sci U S A*. **97(18)**: 10014-10019

Riggs, A.D., Porter, T.N. (1996) Overview of Epigenetic Mechanisms. *Epigenetic Mechanisms of Gene Regulation*. **32**: 29-45

Rikiishi, H. (2011) Autophagic and apoptotic effects of HDAC inhibitors on cancer cells. *J Biomed Biotechnol*. **2011(830260)**: 1-9

Rodriguez, A., Griffiths-Jones, S., Ashurst, J.L., et al. (2004) Identification of Mammalian microRNA Host Genes and Transcription Units. *Genome Res*. **14(10a)**: 1902-1910

Sachdeva, M., Zhu, S., Wu, F., et al. (2009) p53 represses c-Myc through induction of the tumor suppressor miR-145. *Proc Natl Acad Sci USA*. **106(9)**: 3207-3212

Saetrom, P., Heale, B.S., Snove, O Jr., et al. (2007) Distance constraints between microRNA target sites dictate efficacy and cooperativity. *Nucl Acids Res*. **35(7)**: 2333-2342

Sagara, N., Toda, G., Hirai, M., et al. (1998) Molecular Cloning, Differential Expression, and Chromosomal Localization of Human Frizzled-1, Frizzled-2, and Frizzled-7. *Biochem Biophys Res Com.* **252**: 117–122

Saini, H.K., Griffiths-Jones, S., Enright, A.J. (2007) Genomic analysis of human microRNA transcripts. *Proc Natl Acad Sci*. **104(45)**: 17719-17724

Saito, Y., Jones, P.A. (2006) Epigenetic activation of tumor suppressor microRNAs in human cancer cells. *Cell Cycle*. **5(19)**: 2220-2222

Saito, Y., Saito, H. (2012) MicroRNAs in cancers and neurodegenerative disorders. *Front Genet*. **3(194)**: 1-5

Samuel, A.L. (1959) Some studies in machine learning using the game of checkers. *IBM J Res Dev*. **3(3)**: 210-229

Santos, N.C., Figuera-Coelho, J., Martins-Silva, J., et al. (2003) Multidisciplinary utilization of dimethyl sulfoxide:pharmacological, cellular, and molecular aspects. *Biochem Pharmacol*. **65**: 1035-1041

Schmittgen, T.D., Lee, E.J., Jiang, J., et al. (2008) Real-time PCR quantification of precursor and mature microRNA. *Methods*. **44(1)**: 31–38

Schwartz, B., Avivi-Greem, C., Polak-Charcon, S. (1998) Sodium butyrate induces restinoblastoma protein dephosphorylation, p16 expression and growth arrest of colon cancer cells. *Mol Cell Biochem*. **188**: 21-30

Scott, G.K., Mattie, M.D., Berger, C.E., et al. Rapid alteration of microRNA levels by histone deacetylase inhibition. *Cancer Res*. **66(3)**: 1277-1281

Sealy, L., Chalkley, R. (1978) The effect of sodium butyrate on histone modification. *Cell.* **14(1)**: 115-121

Sethupathy, P., Megraw, M., Hatzigeorgiou, H.G. (2006) A guide through present computational approached for the identification of mammalian targets. *Nat Methods*. **3**: 881-886

Shalgi, R., Lieber, D., Oren, M., et al. (2007) Global and local architecture of the mammalian microRNA-transcription factor regulatory network. *PLoS Comput Biol*. **3(7)**: e131

Shannon, B.A., Iacopetta, B.J. (2001) Methylation of the hMLH1, p16, and MDR1 genes in colorectal carcinoma: associations with clinicopathological features. *Cancer Lett*. **167(1)**: 91-97

Shi, B., Sepp-Lorenzino, L., Prisco, M., et al. (2007) Micro RNA 145 targets the insulin receptor substrate-1 and inhibits the growth of colon cancer cells. *J Biol Chem*. **282(45)**: 32582-325890

Sigma-Aldrich, (2014), *miRNA Pathway* [ONLINE]. Available at: http://www.sigmaaldrich.com/life-science/functional-genomics-and-rnai/mirna/learning-center/mirna-introduction.html [Accessed 28 January 16].

Slaby, O., Svoboda, M., Fabian, P., et al. (2007) Altered Expression of miR-21, miR-31, miR-143 and miR-145 Is Related to Clinicopathologic Features of Colorectal Cancer. *Oncol*. **72**: 397-402

Smalheiser, N.R. (2003) EST analyses predict the existence of a population of chimeric microRNA precursor-mRNA transcripts expressed in normal human and mouse tissues. *Genome Biol.* **4(7)**: 403

Smith, C. L., Peterson, C. L. (2005) ATP-dependent chromatin remodeling. *Curr Top Dev Biol.* **65**: 115–148

Sorm, F., Vesely, J. (1968) Effect of 5-aza-2'-deoxycytidine against leukemic and hemopoietic tissues in AKR mice. *Neoplasma*. **15(4)**: 339-343

Spizzo, R., Nicoloso, M.S., Lupini, L., et al. (2010) miR-145 participates with TP53 in a death-promoting regulatory loop and targets estrogen receptor-alpha in human breast cancer cells. *Cell Death Differ*. **17(2)**: 246-254

Stark, A., Brennecke, J., Russell, R.B., et al (2003) Identification of Drosophila MicroRNA Targets. *PLoS Biol.* **1(3)**: e60

Sucharov, C., Bristow, M.R., Port, J.D. (2009) miRNA Expression in the Failing Human Heart: Functional Correlates. *J Mol Cell Cardiol*. **45(2)**: 185-192

Suh, S.O., Chen, Y., Zaman, M.S., et al. (2011) MicroRNA-145 is regulated by DNA methylation and p53 gene mutation in prostate cancer. *Carcinogenesis*. **32(5)**: 772-778

Suzuki, H.I., Yamagata, K., Sugimoto, K., et al. (2009) Modulation of microRNA processing by p53. *Nature*. **460(7254)**: 529-533

Takaoka, Y., Shimizu, Y., Hasegawa, H., et al. (2012) Forced Expression of miR-143 Represses ERK5/c-Myc and p68/p72 Signaling in Concert with miR-145 in Gut Tumors of Apc^{Min} Mice. *PLoS ONE.* **7(8)**: e42137

Tamaru, H., Selker, E.U. (2001) A histone H3 methyltransferase controls DNA methylation in Neurospora crassa. *Nature.* **414:** 277-283

Tan, C., Du, X. (2012) KRAS mutation testing in metastatic colorectal cancer. World *J Gastroenterol*.**18(37)**: 5171-5180

Tan, S.C., Yiap, B.C. (2009) DNA, RNA, and protein extraction: the past and the present. *J Biomed Biotechnol*. **2009(574398)**: 1-10

Tang, L., Nogales, E., Ciferri, C. (2010) Structure and Function of SWI/SNF Chromatin Remodeling Complexes and Mechanistic Implications for Transcription. *Prog Biophys Mol Biol*. **102(2-3)**: 122–128

Tarasov, V., Jung, P., Verdoodt, B., et al. (2007) Differential regulation of microRNAs by p53 revealed by massively parallel sequencing: miR-34a is a p53 target that induces apoptosis and G1-arrest. *Cell Cycle*. **6(13)**: 1586-1593

Thomson, D.W., Bracken, C.P., Goodall, G.J. (2011) Experimental strategies for microRNA target Identification. *Nucleic Acids Res*. **39(16)**: 6845–6853

Tsai, H.C., Li, H., Van Neste, L., et al. (2012) Transient Low Doses of DNA Demethylating Agents Exert Durable Anti-tumor Effects on Hematological and Epithelial Tumor Cells. *Cancer Cell*. **21(3)**: 430–446

Tsuji, N., Kobayashi, M., Nagashima., et al. (1975) A new antifungal antibiotic, trichostatin. *J Antibiot*. **XXIX (1)**: 1-6

Ueno, K., Hiura, M., Suehiro, Y., et al. (2008) Frizzled-7 as a Potential Therapeutic Target in Colorectal Cancer. *Neoplasia*. **10**, 697–705

Understedt, J.S., Sowa, Y., Xu, W.S., et al. (2004) Role of thioredoxin in the response of normal and transformed cells to histone deacetylase inhibitors. *Proc Natl Acad Sci*. **102(3)**: 673–678

Van Holde, K. E. (1988) Chromatin*. Springer Series in Molecular Biology* (New York, Springer-Verlag)

Vargas, J.E., Filippi-Chiela, E.C., Suhre, T., et al. (2014) Inhibition of HDAC increases the senescence induced by natural polyphenols in glioma cells. *Biochem Cell Biol*. **92(4)**: 297-304

Vidali, G., Boffa, l.C., Bradbury, E.M., et al. (1978) Butyrate suppression of histone deacetylation leads to accumulation of multiacetylated forms of histones H3 and H4 and increased DNase I sensitivity of the associated DNA sequences. *Proc Natl Acad Sci USA.* **75(5):** 2239-2243

Vignali, M., Hassan, A.H., Neely, K.E., et al. (2000) ATP-dependent chromatin-remodeling complexes. *Mol Cell Biol*. **20**:1899–1910

Vogelstein, B., Fearon, E.R., Hamilton. S.R., et al. (1988) Genetic alterations during colorectal-tumor development. *N Engl J Med*. **319(9)**: 525-532

Voinnet, O. (2009) Origin, biogenesis, and activity of plant microRNAs. *Cell*. **136(4)**: 669-687

Voutsadakis, I.A. (2008) The ubiquitin-proteasome system in colorectal cancer. *Biochim Biophys Acta*.**1782**: 800–808

Waddington, C.H. (1942) Canalization of development and the inheritance of acquired characters. *Nature.* **150:** 563-565

Wagner, B., Natarajan, A., Grunaug, S., et al. (2006) Neuronal survival depends on EGFR signalling in cortical but not midbrain astrocytes. *EMBO J*. **25**: 752–762

Walther, A., Houslton, R., Tomlinson, I. (2008) Association between chromosomal instability and prognosis in colorectal cancer: a meta-analysis. *Gut.* **57(7**): 941-950

Wang, Z., Zhang, X., Yang, Z., et al. (2012) MiR-145 regulates PAK4 *via* the MAPK pathway and exhibits an antitumor effect in human colon cells. *Biochem Biophys Res Commun*. **427(3)**: 444-449

Watanabe, T., Kobunai, T., Yamamoto, Y., et al. (2012) Chromosomal instability (CIN) phenotype, CIN high or CIN low, predicts survival for colorectal cancer. *J Clin Oncol*. **30(18)**: 2256-2264

Wehler, T.C., Frerichs, K., Graf, C., et al. (2008) PDGFRα/ß expression correlates with the metastatic behavior of human colorectal cancer: A possible rationale for a molecular targeting strategy. *Oncol Rep*. **19**: 697-704

Weichert, W., Röske, A., Niesporek, S., et al. (2008) Class I Histone Deacetylase Expression Has Independent Prognostic Impact in Human Colorectal Cancer: Specific Role of Class I Histone Deacetylases In vitro and In vivo. *Clin Cancer Res*. **14(6)**: 1669-1677

Wiemer, E.A.A. (2007) The role of microRNAs in cancer: No small matter. *Eur J Cancer*. **43**: 1529-1544

Wightman, B., Ha, I., Ruvkun, G. (1993) Posttranscriptional regulation of the heterochronic gene lin-14 by lin-4 mediates temporal pattern formation in C. elegans. *Cell*. **75(5)**: 855-862

Wijermans, P.W., Krulder, J.W., Huijgens, P.C., et al. (1997) Continuous infusion of low-dose 5Aza2' deoxycytidine in elderly patients with high-risk myelodysplastic syndrome. *Leukemia*. **11(1)**: 1-5

Wijermans, P.W., Lubbert, M., Verhoef, G., et al. (2000) Low-dose 5aza2' deoxycytidine, a DNA hypomethylating agent, for the treatment of high-risk myelodysplastic syndrome: a multicenter phase II study in elderly patients. *J Clin Oncol*. **18(5)**: 956-962.

Willert, K., Jones, K.A. (2006) Wnt signaling: is the party in the nucleus?. *Genes Dev*. **20**:1394–1404

Witkos, T.M., Koscianska, E., Krzyzosiak, W.J. (2011) Practical Aspects of microRNA Target Prediction. *Curr Mol Med*. **11(2)**: 93-109

Witt, O., Deubzer, H.E., Milde, T., et al. (2008) HDAC family: What are the cancer relevant targets? *Cancer Lett*. **277(1)**: 8-21

Worthley, D.L., Leggett, B.A. (2010) Colorectal Cancer: Molecular Features and Clinical Opportunities. *Clin Biochem Rev.* **31**: 31-38

Xiang, K.M., Li, X.R. (2014) MiR-133b Acts as a Tumor Suppressor and Negatively Regulates TBPL1 in Colorectal Cancer Cells. *Asian Pac J Cancer Prev*. **15**: 3767-3772

Xiong, Y., Zhang, H., Beach, D. (1992) D type cyclins associate with multiple protein kinases and the DNA replication and repair factor PCNA. *Cell*. **71(3)**:505-514

Xu, W.S., Parmigiani, R.B., Marks, P.A. (2007) Histone deacetylase inhibitors: molecular mechanisms of action. *Oncogene*. **26**: 5541–5552

Xu, Y., Pasche, B. (2007) TGF-b signaling alterations and susceptibility to colorectal cancer. *Hum Mol Genet*. **16(1)**: 14–20

Xue, G., Ren, Z., Chen, Y., et al. (2015) A feedback regulation between miR145 and DNA methyltransferase 3b in prostate cancer cell and their responses to irradiation. *Cancer Lett*. **361(1)**: 121-127

Yamada, N., Noguchi, S., Mori, T., et al. (2013) Tumor-suppressive microRNA-145 targets catenin δ-1 to regulate Wnt/β-catenin signaling in human colon cancer cells. *Cancer Lett*. **335(2)**: 332-342

Yanaihara, N., Caplen, N., Bowman, E., et al. (2006) Unique microRNA molecular profiles in lung cancer diagnosis and prognosis. *Cancer Cell*. **9(3)**: 189-198

Yi, J., Wang, Z.W., Cang, H., et al. (2001) p16 gene methylation in colorectal cancers associated with Duke′s staging. *World J Gastroenterol*. **7(5)**: 722–725

Yoa, C., Sun, M., Yuan, Q., et al. (2016) MiRNA-133b promotes the proliferation of human Sertoli cells through targeting GLI3. *Oncotarget*. **7(3)**: 2201-2219

Yoshida, M., Beppu, T. (1988) Reversible arrest of proliferation of rat 3Y1 fibroblasts in both the G1 and G2 phases by trichostatin A. *Exp Cell Res*. **177(1):** 122-31

Yuan, G.V., Liu, Y.J., Dion, M.F., et al. (2005) Genome-scale identification of nucleosome positions in S. cerevisiae. *Science*. **309(5734)**: 626-630

Zakhari, S. (2013) Alcohol Metabolism and Epigenetics Changes. *Alcohol Res: Curr Rev*. **35(1)**:616

Zaman, M.S., Chen, Y., Deng, G., et al. (2010) The functional significance of microRNA-145 in prostate cancer. *Br J Cancer*. **103**: 256-264

Zauber, A.G, (2015) The Impact of Screening on Colorectal Cancer Mortality and Incidence: Has It Really Made a Difference? *Dig Dis Sci*. **60 (3)**: 681-691

Zhai, L., Ma, C., Li, W., et al. (2015) miR-143 suppresses epithelial–mesenchymal transition and inhibits tumor growth of breast cancer through down-regulation of ERK5. *Molec Carcinog*. doi:10.1002/mc.22445

Zhang, J., Guo, H., Zhang, H., et al. (2011) Putative tumor suppressor miR-145 inhibits colon cancer cell growth by targeting oncogene Friend leukemia virus integration1. *Cancer*. **117(1)**: 86–95

Zhang, H., Kolb, F.A., Brondani, V., et al. (2002) Human Dicer preferentially cleaves dsRNAs at their termini without a requirement for ATP. *EMBO J*. **21(21)**: 5875-5885

Zhang, H.P., Wang, Y.H., Cao, C.J., et al. (2016) A regulatory circuit involving miR-143 and DNMT3a mediates vascular smooth muscle cell proliferation induced by homocysteine. *Mol Med Reports*. **13(1)**: 483-490

Zhao, H., Kalota, A., Jin, S., et al. (2009) The c-myb proto-oncogene and microRNA-15a comprise an active autoregulatory feedback loop in human hematopoietic cells. *Blood.* **113(3)**: 505-516

Zhao, N., Koenig, S.N., Trask, A.J., et al. (2015) MicroRNA miR145 regulates TGFBR2 expression and matrix synthesis in vascular smooth muscle cells. *Circ Res.* **116(1)**: 23-34

Zhou, H., Xia, X.G., Xu, Z. (2005) An RNA polymerase II construct synthesizes short-hairpin RNA with a quantitative indicator and mediates highly efficient RNAi. *Nucl Acids Res*. **33(6)**: e62

Zuker, M. (2003) Mfold web server for nucleic acid folding and hybridization prediction. *Nucl Acids Res.* **31(13)**: 3406–3415

Appendix A – Ethics Waiver

University
of the Witwatersrand,
Johannesburg

Human Research Ethics Committee (Medical)
(formerly Committee for Research on Human Subjects (Medical)

Secretariat: Research Office, Room SH10005, 10th floor, Senate House • Telephone: +27 11 717-1234 • Fax: +27 11 339-5708
Private Bag 3, Wits 2050, South Africa

Ref: W-CJ-090317-4
17/03/2009

TO WHOM IT MAY CONCERN:

Waiver: This certifies that the following research does not require clearance from the Human Research Ethics Committee (Medical).

Investigator: **Ms D Govan and Dr C B Penny**

Project title: **Detecting epigenetic silencing of selected microRNA's at different stages of colon cancer.**

Reason: This is a wholly laboratory study using commercial cell lines from the American Culture Type Collection. There are no humans involved.

UNIVERSITY OF THE WITWATERSRAND
PROF PE CLEATON - JONES
HREC (MEDICAL)
2009 -03- 17
JOHANNESBURG

Professor Peter Cleaton-Jones
Chair: Human Research Ethics Committee (Medical)

copy: Anisa Keshav, Research Office, Senate House, Wits

Appendix B – Reagent Constituents

10%v/v FBS/DMEM:F12

5mL fetal bovine serum (Invitrogen)

45mL DMEM:F12 (Invitrogen)

100µL 10000U penicillin/mL/10 000ugstreptomycin/mL (Lonza)

2%v/v FBS/DMEM:F12

1mL fetal bovine serum (Invitrogen)

49mL DMEM:F12 (Invitrogen)

100µL 10000U penicillin/mL/10 000ugstreptomycin/mL (Lonza)

BEBM (Bronchial Epithelial Basal Medium)

50mL of BEBM (Lonza)

200µL Bovine Pituitary Extract,

50µL Insulin,

50µL hydrocortisone,

50µL GA-1000 (Gentamycin – Amphotericin),

50µL Retinoic Acid,

50µL Epinephrine,

50µL Transferrin,

50µL Triiodothyronine and

50µL human EGF (epidermal growth factor).

200mL PBS

1X PBS tablet (Sigma-Aldrich)

200mL dH2O

3%v/v Formaldehyde

48.5mL PBS (Sigma-Aldrich)

1.5mL Formaldehyde (Univar)

0.5%w/v BSA/PBS

0.5g bovine serum albumin (Sigma-Aldrich)

100mL PBS (Sigma-Aldrich)

0.5%v/v BSA/PBS/Triton X

25mL 0.5%v/v BSA/PBS (Sigma-Aldrich)

125µL Triton X (Lonza)

Primary antibody 1:100

1µL primary antibody (KRAS, FZD7 and ß-TrCP2)

99µL 0.5%v/v BSA/PBS

- KRAS (F234) Mouse monoclonal IgG 200ug/mL Santa Cruz Biotechnologies Cat. no. sc-30
- FZD7 (F-13) Goat polyclonal IgG 200ug/mL Santa Cruz Biotechnologies Cat. no. sc-31063
- ß-TrCP (E-20) Goat polyclonal IgG 200ug/mL Santa Cruz Biotechnologies Cat. no. sc-9599

Secondary antibody 1:200

1µL secondary antibody (Santa-Cruz)

199µL 0.5%v/v BSA/PBS

- Alexa Fluor® 568 conjugated donkey anti goat 0.5mL, Life Technologies
- Alexa Fluor® 568 conjugated donkey anti mouse 0.5mL, Life Technologies

DAPI 1:10 000

1µL DAPI (Boehringer Mannheim)

9 999µL/~10mL PBS

Microscope and software details

- Olympus IX71- inverted microscope with epifluorescence
    - Software: analySIS FIVE, Olympus Soft Imaging
    - Systems, Germany

- Zeiss Laser Scanning Microscope
    - LSM 780, ZEN Software (2011)

Appendix C - The $2^{-\Delta\Delta Ct}$ method

The $2^{-\Delta\Delta Ct}$ method was used to assess relative gene expression in this study (Livak and Schmittgen, 2001). The Ct of the target gene was first normalised to that of the reference gene (in this case 18S rRNA) for both test and control samples following equations:

$\Delta Ct(miR) = Ct\ (miR - treated) - C(18s\ rRNA - treated)$

$\Delta Ct(control) = Ct\ (miR - control) - Ct\ (18s\ rRNA - control)$

The CT of the miR sample was then normalised to the CT of the control as seen below:

$\Delta\Delta Ct = \Delta Ct(miR) - \Delta C(control)$

As a result, the ratio of the target gene in the test sample to the calibrator sample is found, which is normalised to the reference gene. All treated sample results are relative to the untreated samples. The expression ratio can be calculated as below:

Normalised target gene expression = $2^{(-\Delta\Delta Ct)}$

Appendix D – KEGG pathway enrichment per miRNA target prediction program

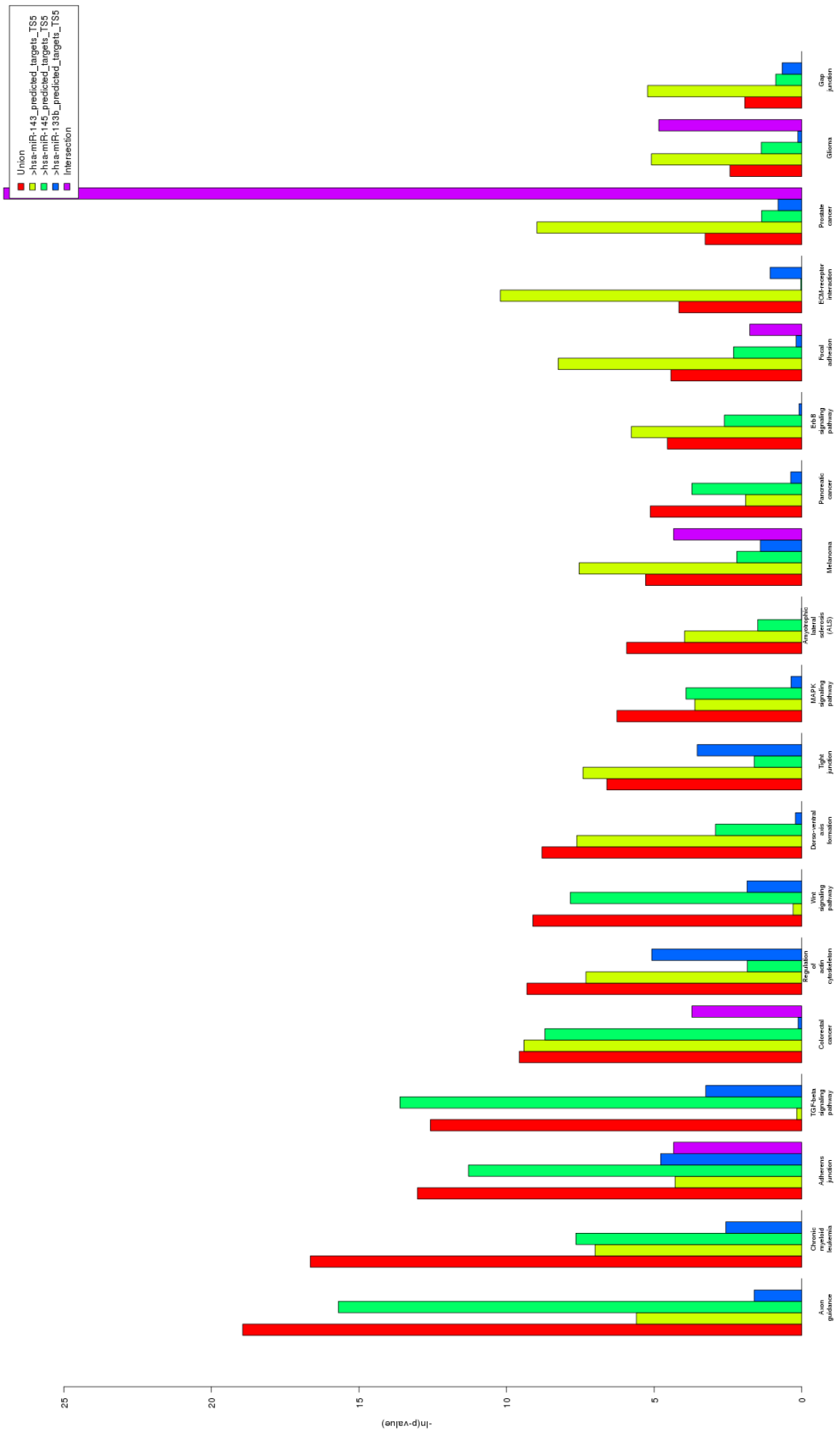

Figure A1: DIANA mirPATH v1.0 enrichment for miR-143, -145, -133b targets predicted by TargetScan 5.1

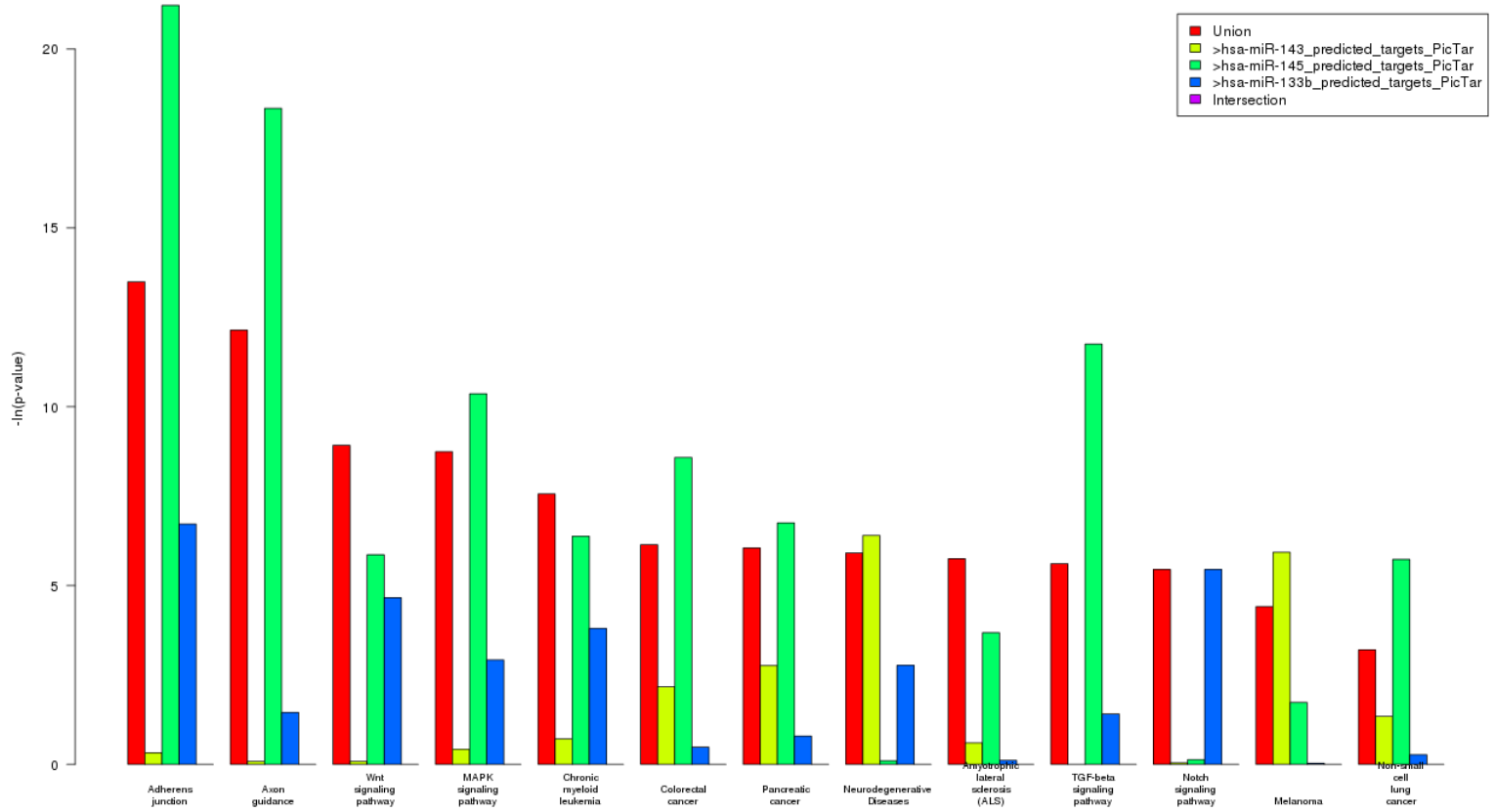

Figure A2: DIANA mirPATH v1.0 enrichment for miR-143, -145, -133b targets predicted by PicTar

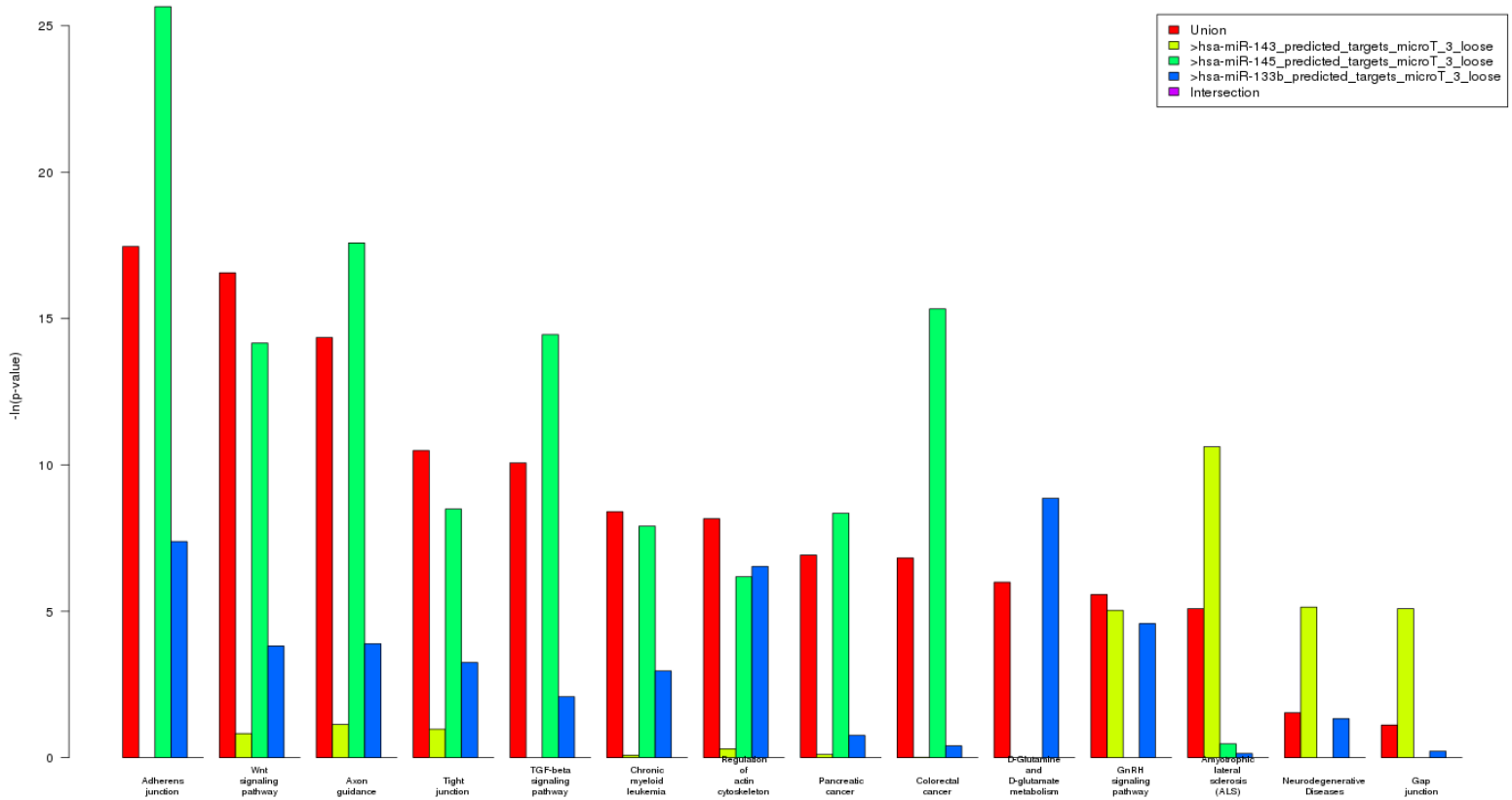

Figure A3: DIANA mirPATH v1.0 enrichment for miR-143, -145, -133b targets predicted by DIANA microT v3.0

Appendix E – Conservation of miRNA target sites

miR-143

Figure A4: Conservation of miR-143 binding site in KRAS across 15 species. (TargetScan 5.1)

miR-145

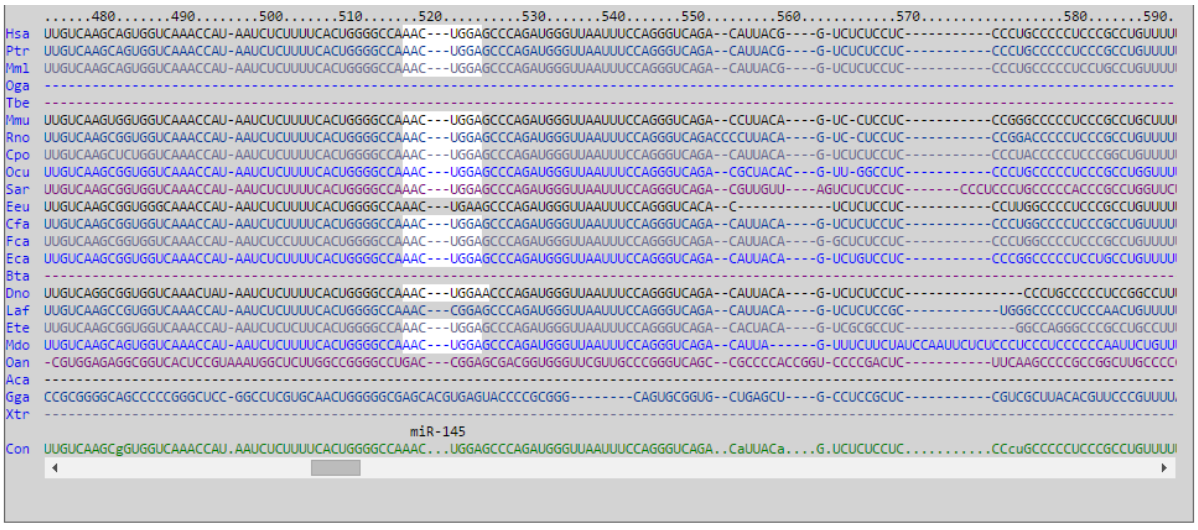

Figure A5: Conservation of miR-145 binding site in FZD7 across 14 species. (TargetScan 5.1)

miR-133b

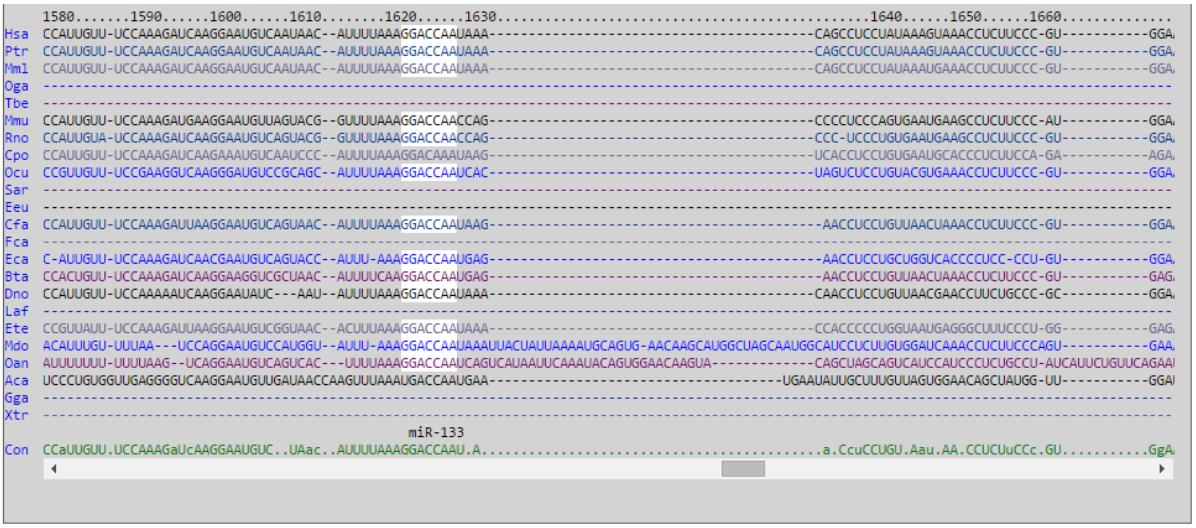

Figure A6: Conservation of miR-133b binding site in FBXW11 across 13 species. (TargetScan 5.1)

Appendix F – Turnitin Report